UDK 621.3:(53+54+621+66)(05)(497.1)=00 ISSN 0352-9045

INFORMACIJE MIDEM 2 ◦ 1996

Strokovno društvo za mikroelektroniko elektronske sestavne dele in materiale

Časopis za mikroelektroniko, elektronske sestavne dele in materiale
Časopis za mikroelektroniku, elektronske sastavne dijelove i materijale
Journal of Microelectronics, Electronic Components and Materials

INFORMACIJE MIDEM, LETNIK 26, ŠT. 2(78), LJUBLJANA, junij 1996

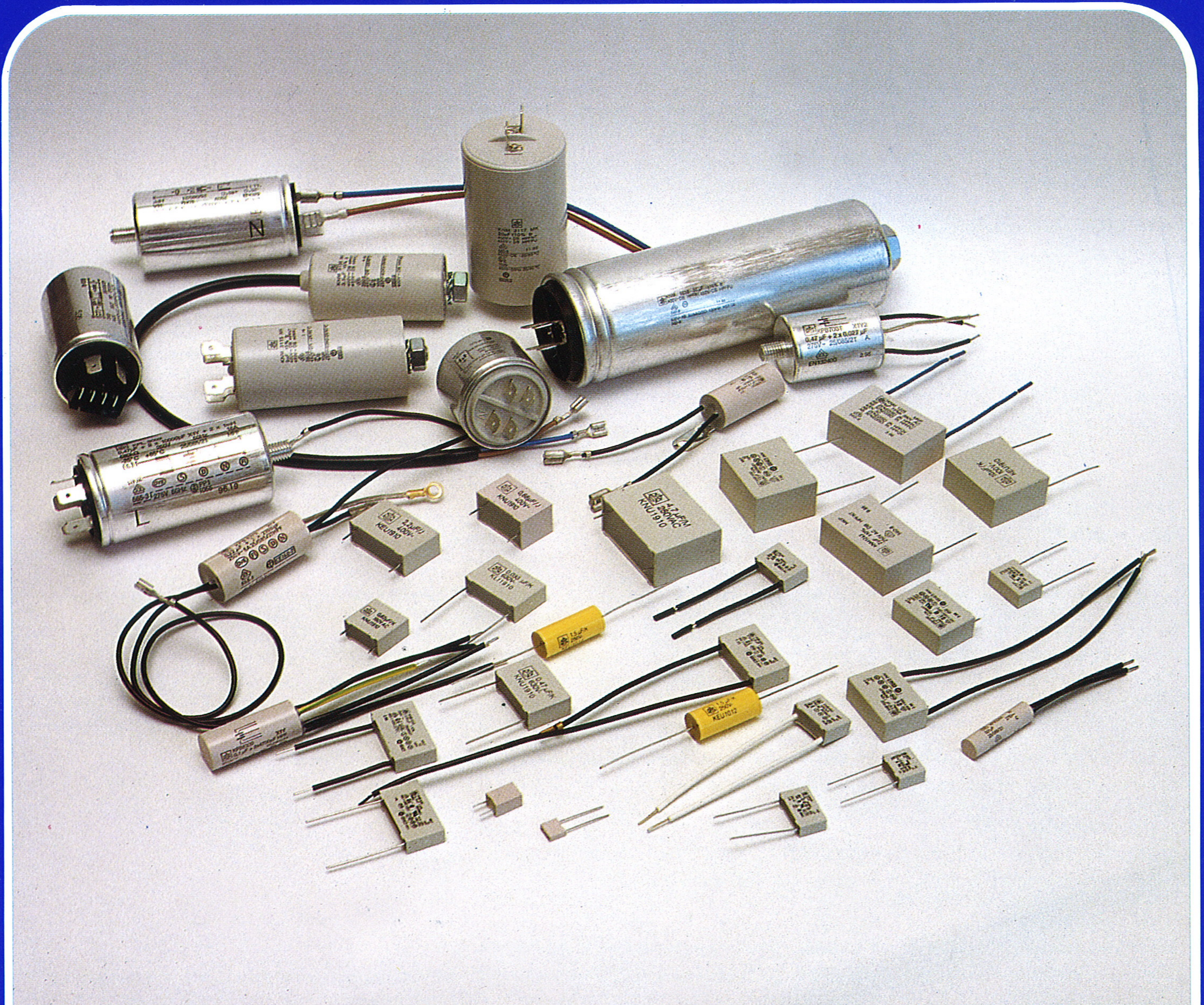

ISKRA KONDENZATORJI SEMIČ
1951 - 1996

INFORMACIJE MIDEM 2 ° 1996

INFORMACIJE MIDEM	LETNIK 26, ŠT. 2(78), LJUBLJANA,	JUNIJ 1996
INFORMACIJE MIDEM	GODINA 26, BR. 2(78), LJUBLJANA,	JUN 1996
INFORMACIJE MIDEM	VOLUME 26, NO. 2(78), LJUBLJANA,	JUNE 1996

Izdaja trimesečno (marec, junij, september, december) Strokovno društvo za mikroelektroniko, elektronske sestavne dele in materiale.
Izdaja tromjesečno (mart, jun, septembar, decembar) Stručno društvo za mikroelektroniku, elektronske sastavne dijelove i materiale.
Published quarterly (march, june, september, december) by Society for Microelectronics, Electronic Components and Materials - MIDEM.

Glavni in odgovorni urednik
Glavni i odgovorni urednik
Editor in Chief
Mag. Iztok Šorli, dipl.ing.,
MIKROIKS d.o.o., Ljubljana

Tehnični urednik
Tehnički urednik
Executive Editor
Mag. Iztok Šorli, dipl. ing.

Uredniški odbor
Redakcioni odbor
Executive Editorial Board
Doc. dr. Rudi Babič, dipl.ing., Fakulteta za elektrotehniko, računalništvo in informatiko Maribor
Dr.Rudi Ročak, dipl.ing., MIKROIKS d.o.o., Ljubljana
mag.Milan Slokan, dipl.ing., MIDEM, Ljubljana
Zlatko Bele, dipl.ing., MIKROIKS d.o.o., Ljubljana
Dr. Wolfgang Pribyl, SIEMENS EZM, Villach, Austria
mag. Meta Limpel, dipl.ing., MIDEM, Ljubljana
Miloš Kogovšek, dipl.ing., Iskra INDOK d.o.o., Ljubljana
Dr. Marija Kosec, dipl. ing., Inštitut Jožef Štefan, Ljubljana

Časopisni svet
Izdavački savet
International Advisory Board
Prof. dr. Slavko Amon, dipl.ing., Fakulteta za elektrotehniko, Ljubljana, PREDSEDNIK - PRESIDENT
Prof. dr. Cor Claeys, IMEC, Leuven
Dr. Jean-Marie Haussonne, C.N.E.T. Centre LAB, Lannion
Dr. Marko Hrovat, dipl.ing., Inštitut Jožef Stefan, Ljubljana
Prof. dr. Zvonko Fazarinc, dipl.ing., CIS, Stanford University, Stanford, USA
Prof.dr.Drago Kolar, dipl.ing., Inštitut Jožef Stefan, Ljubljana
† RNDr. DrSc. Radomir Kužel, Charles University, Prague
Dr. Giorgio Randone, ITALTEL S.I.T. spa, Milano
Prof.dr. Stane Pejovnik, dipl.ing., Kemijski inštitut Boris Kidrič, Ljubljana
Prof. dr. Giovanni Soncini, University of Trento, Trento
Prof.dr. Janez Trontelj, dipl.ing., Fakulteta za elektrotehniko, Ljubljana
Dr. Anton Zalar, dipl.ing., ITPO, Ljubljana
Dr. Peter Weissglas, Swedish Institute of Microelectronics, Stockholm

Naslov uredništva
Adresa redakcije
Headquarters
Uredništvo Informacije MIDEM
Elektrotehniška zveza Slovenije
Dunajska 10, 1000 Ljubljana, Slovenija
(0)61 - 316 886

Letna naročnina znaša 12.000,00 SIT, cena posamezne številke je 3000,00 SIT. Člani in sponzorji MIDEM prejemajo Informacije MIDEM brezplačno.
Godišnja pretplata iznosi 12.000,00 SIT, cijena pojedinog broja je 3000,00 SIT. Članovi i sponzori MIDEM primaju Informacije MIDEM besplatno.
Annual subscription rate is DEM 200, separate issue is DEM 50. MIDEM members and Society sponsors receive Informacije MIDEM for free.

Znanstveni svet za tehnične vede I je podal pozitivno mnenje o časopisu kot znanstveno strokovni reviji za mikroelektroniko, elektronske sestavne dele in materiale. Izdajo revije sofinanci rajo Ministrstvo za znanost in tehnologijo in sponzorji društva.
Scientific Council for Technical Sciences of Slovene Ministry of Science and Technology has recognized Informacije MIDEM as scientific Journal for microelectronics, electronic components and materials.
Publishing of the Journal is financed by Slovene Ministry of Science and Technology and by Society sponsors.

Znanstveno strokovne prispevke objavljene v Informacijah MIDEM zajemamo v:
* domačo bazo podatkov ISKRA SAIDC-el, kakor tudi
* v tujo bazo podatkov INSPEC

Prispevke iz revije zajema ISI® v naslednje svoje produkte: Sci Search®, Research Alert® in Materials Science Citation Index™

Scientific and professional papers published in Informacije MIDEM are assessed into:
* domestic data base ISKRA SAIDC-el and
* foreign data base INSPEC

The Journal is indexed by ISI® for Sci Search®, Research Alert® and Material Science Citation Index™

Po mnenju Ministrstva za informiranje št.23/300-92 šteje glasilo Informacije MIDEM med proizvode informativnega značaja, za katere se plačuje davek od prometa proizvodov po stopnji 5 %.

Grafična priprava in tisk
Grafička priprema i štampa
Printed by
BIRO M, Ljubljana

Naklada
Tiraž
Circulation
1000 izvodov
1000 primjeraka
1000 issues

UDK621.3:(53+54+621+66), ISSN0352-9045 | Informacije MIDEM 26(1996)2,Ljubljana

VSEBINA		CONTENT
Uvodnik nove predsednice društva	78	New MIDEM President Editorial
ZNANSTVENO STROKOVNI PRISPEVKI		PROFESSIONAL SCIENTIFIC PAPERS
A. Macher, K. Reichmann, O. Fruhwirth, K. Gatterer, G.W. Herzog: Primerjava NTC materialov s perovskitno strukturo z NTC materiali s spinelno strukturo za uporabo pri povišanih temperaturah	79	A. Macher, K. Reichmann, O. Fruhwirth, K. Gatterer, G.W. Herzog: Perovskite Versus Spinel Type NTC Materials for Application at Elevated Temperatures
J. Maček, M. Marinšek: Priprava disperzij nikelj/cirkonijev dioksid z gel-precipitacijo nikljovega hidroksida in hidratiziranega cirkonijevega oksida: vpliv reakcijskih pogojev na karakteristike	86	J. Maček, M. Marinšek: The Preparation of Nickel/Zirconia Dispersions from Nickel Hydroxide/Hydrous Zirconium Oxide Gel-Precipitate Precursors: Influence of the Reaction Conditions on the Characteristics
B. Saje, B. Reinsch, S. Kobe-Beseničar, D. Kolar, I.R. Harris: Nitriranje Sm_2Fe_{17} zlitine z dodatkom tantala	94	B. Saje, B. Reinsch, S. Kobe-Beseničar, D. Kolar, I.R. Harris: Nitrogenation of Sm_2Fe_{17} Alloy with Ta Addition
B.Cvikl: O nizkofrekvenčni C-U odvisnosti Ag/n-Si(111) Schottky-jevih diod, nanešenih po metodi curka ioniziranih skupkov, CIS	97	B.Cvikl: On Low Frequency C-U Relationship of the Ionized Cluster Beam, ICB, Deposited Ag/n-Si(111) Schottky Diodes
K. Korošec, A. Vesenjak, B. Jarc, M. Solar, R. Babič: Izvedba nerekurzivnega digitalnega sita s standardnimi integriranimi komponentami v modoficirani obliki porazdeljene aritmetike	107	K. Korošec, A. Vesenjak, B. Jarc, M. Solar, R. Babič: The FIR Digital Filter Realization with Standard Integrated Circuits in the Modified Distributed Arithmetic Structure
UPORABA PLAZME V ELEKTRONIKI		APPLICATION OF PLASMA IN ELECTRONICS
I. Šorli, W. Petasch, B. Kegel, H. Schmid, G. Liebel, W. Ries: Procesi v plazmi. II. del: Uporaba v elektroniki	113	I. Šorli, W. Petasch, B. Kegel, H. Schmid, G. Liebel, W. Ries: Plasma Processes. Part II.: Applications in Electronics
PREDSTAVLJAMO PODJETJE Z NASLOVNICE		REPRESENT OF COMPANY FROM FRONT PAGE
Iskra tovarna kondenzatorjev in opreme Semič, Slovenija	121	Iskra Capacitor Factory, Semič, Slovenia
MIDEM IN NJEGOVI ČLANI		MIDEM SOCIETY AND ITS MEMBERS
Občni zbor društva MIDEM	122	General Assembly of MIDEM Society
A. Zalar: Ustanovitev novega instituta	126	A. Zalar: Foundation of a new Institute
KONFERENCE, POSVETOVANJA, SEMINARJI, POROČILA		CONFERENCES, COLLOQUYUMS, SEMINARS, REPORTS
D. Belavič: Delavnica ISHM/NATO 1996	127	D. Belavič: ISHM/NATO Workshop 1996
M. Kosec: Delavnica COST 514: Feroelektrične tanke plasti	128	M. Kosec: Workshop COST 514: Ferroelectric Thin Films
S. Novak: Poročilo s simpozija	129	S. Novak: Report from Symposium
D. Križaj: Poročilo s konference ISPSD'96	130	D. Križaj: ISPSD'96 Conference Report
VESTI	131	NEWS
KOLEDAR PRIREDITEV	135	CALENDAR OF EVENTS
MIDEM prijavnica	137	MIDEM Registration Form
Slika na naslovnici: Proizvodi Iskre Kondenzatorji Semič		Frontpage: Products of Iskra Capacitor Factory Semič

VSEBINA **CONTENT**

Spoštovane članice, spoštovani člani društva MIDEM

Hvala za zaupanje, ker ste me izvolili za predsednico. Zavedam se, da obdržati to, kar društvo MIDEM je, ne bo lahko. Društvo izdaja revijo zavidljive kvalitete. Koliko pa je revij v Sloveniji, iz katerih ISI zajema članke za baze podatkov? Podobno velja za letno strokovno konferenco MIEL-SD. Letos je slaba polovica prijavljenih referatov iz tujine. Med avtorji so zelo ugledna imena. Visok strokovni nivo revije in konference je potrebno obdržati, verjamem pa, da ga je mogoče tudi zvišati. Računam na vas, na vašo strokovno moč in temu ustrezne prispevke. Dovolite mi, da k sodelovanju posebej povabim članice in člane iz gospodarstva. Poleg strokovnih člankov ste dobrodošli z novicami iz razvoja in proizvodnje, z vašimi uspehi in problemi.

Ob koncu mi ne zamerite še dveh trivialnih vprašanj. Smo kot del tehnične inteligence zadovoljni s svojo vlogo v družbi? Nas je kdo, kdaj, kot skupino strokovnjakov vprašal za kakšno mnenje v zvezi z razvojnimi in drugimi gospodarskimi odločitvami? Če nas že ne sprašujejo, pa se sami kdaj oglasimo v javnosti.

"MIDEM je trdno društvo" je dejal dosedanji predsednik dr. Rudi Ročak ob koncu svojega mandata. Ostanimo to še naprej. Rudiju pa hvala, ker je veliko pripomogel k tej trdnosti.

Predsednica društva MIDEM
dr. Marija Kosec, dipl.ing.

PEROVSKITE VERSUS SPINEL TYPE NTC MATERIALS FOR APPLICATION AT ELEVATED TEMPERATURES

A. Macher, K. Reichmann, O. Fruhwirth, K. Gatterer*, G.W. Herzog
Institut für chemische Technologie anorganischer Stoffe,
*Institut für Physikalische und Theoretische Chemie,
Technische Universität Graz, Österreich

Key words: NTC, Negative Temperature Coefficients, spinel type materials, perovskite type materials, material conductivity, polarons, impendance spectroscopy, impedance spectra, relaxation phenomena, polaron jump frequency, probability of polaron hopping

Abstract: Commercial NTC´s made of spinel type $NiMn_2O_4$ materials cannot be used at elevated temperatures because of different reasons, e.g. too low resistivity and activation energy, poor thermal stability. Searching for proper materials we investigated Al and Ti doped $LaCoO_3$ with the composition $LaMe_xCo_{1-x}O_3$ ranging from x = 0,1 to 0,7. In contrast to $NiMn_2O_4$ the DC conductivity of the perovskite type material can be tuned by Ti doping within a wide range of applicability. The conduction mechanism was studied with impedance spectroscopy and leads to the conclusion, that both kinds of materials conduct via small polaron hopping. Relaxation phenomena are observed in the frequency range 1 to 1000 kHz and interpreted with theories of Holstein, Sewell and Appel. To explain the difference of the DC response upon doping of spinel and perovskite type materials the conventional probability factor had to be modified.

Perovskitni in spinelni NTC za uporabo pri visokih temperaturah

Ključne besede: NTC koeficienti temperaturni negativni, materiali tipa spinel, materiali tipa perovskite, provodnost materiala, polaroni, spektroskopija impedančna, spektri impedančni, pojav relaksacije, frekvenca preskoka polarona, verjetnost preskoka polarona

Povzetek: Komercialni NTC upori na osnovi spinela $NiMn_2O_4$ iz več razlogov niso uporabni pri visokih temperaturah. Imajo prenizko upornost, previsoko aktivacijsko energijo in so toplotno slabo obstojni. Z namenom dobiti primernejše materiale smo raziskovali prevodnost perovskitov na osnovi $LaCoO_3$ s sestavo $LaMe_xCo_{1-x}O_3$, kjer je Me: Ti, Al in $0.1 \leq x \leq 0.7$. V nasprotju s spinelnimi materiali na osnovi $NiMn_2O_4$ se da z dodatkom Ti prevodnost perovskitov na osnovi $LaCoO_3$ spreminjati v širokem območju.

Mehanizem prevajanja, ki smo ga študirali z impedančno spektroskopijo, se da pri obeh tipih materialov pojasniti s takoimenovanim "small polaron hopping". Relaksacijske pojave v frekvenčnem območju 1 do 1000 kHz smo razložili s Holstein, Sewell, Appel teorijo. Pri razlagi razlike v prevajanju dopiranih spinelov in perovskitov je bilo potrebno sprementi standardni faktor verjetnosti.

INTRODUCTION

NTC materials are usually based on inverse spinels of the type $Ni_{1-x}Mn_{2+x}O_4$. In air they are thermally stable only in the range x = - 0,2 to 1 above 700°C /1/. Therefore, conventionally sintered materials are always composed of quenched high temperature phases reflecting consequently the technology of processing.

The temperature dependent inversion between cations on tetrahedral and octrahedral sites is said to be connected with a disproportion of Mn^{3+} ions, and leads to rather complicated cation distributions /2, 3, 4/. The inversion phenomenon is also a main reason for aging problems, which can be overcome by stabilizing bivalent ions on tetrahedral sites. For instance, a sufficient improvement can be obtained by substitution with Zn^{2+} ions /5, 6, 7/.

The application of sintered materials demands a stable DC conductivity with respect to temperature changes. In many cases, at high enough temperatures the DC conductivity displays an exponential temperature dependence, which can be fitted well by

$$\sigma = \sigma_0 \exp\left[\frac{-E_A}{kT}\right] \quad (1)$$

- σ specific conductivity
- σ_0 preexponential factor
- E_A activation energy
- k Boltzmann´s constant
- T absolute temperature

However, at lower temperatures the DC conductivity deviates from this exponential behaviour in a rather intrinsic manner, i.e. different processing steps or even doping are not very effective. Up to now little attention has been paid to this low temperature deviations, although they are already observable in the undoped materials like $NiMn_2O_4$ and $CoMn_2O_4$ /8, 9/.

In general, manganite materials cannot be used for applications at elevated temperatures because of too low resistivity, too small activation energy and poor

thermal stability. Aiming at proper materials, we investigated the perovskite system $LaMe_xCo_{1-x}O_3$ by substituting Al^{3+} and Ti^{4+} for Co^{3+} ions. Ti and Mg doping was first studied by Ramadass et al. /10/. They reported, that in contrast to the above mentioned manganites, the DC conductivity of the perovskite $LaCoO_3$ can be modified within a wide range. In this work we compare DC and AC conductivities of spinel and perovskite type materials and apply small polaron models for their interpretation. We anticipated, that both types of materials conduct via a similar process of small polaron hopping.

EXPERIMENTAL

Powders of different spinel and perovskite type materials were produced by coprecipitation of hydroxides from chloride solutions at about pH 11 and calcination at 900°C for 30 minutes. They were pressed into pellets and sintered between 1100 and 1200°C in air for several hours. Electrical contacts were made with a silver paste (E 4031 Demetron) fired at 750°C. Characterization of powders and pellets were made by XRD, REM and titration of the Co^{3+} content. Experimental details are described elsewhere /5,6/.

DC measurements within the temperature range -30 to +400°C were carried out potentiostatically using platinum clamps. For AC measurements we used the HP impedance analyser 4192A, operative in the frequency range 5 Hz to 13 MHZ.

DC CONDUCTIVITY

Typical examples of DC conductivities for both kinds of materials are shown in figs.1 to 3. Whereas Zn doping of $NiMn_2O_4$ has rather little influence on the conductivity, Ti and Al doping of $LaCoO_3$ leads to a dramatic decrease of conductivity at x >0,1. The effect is unexpectedly high (fig. 4) and demands for a reasonable explanation. Many conductivity curves deviate at low temperatures from the exponential dependence.

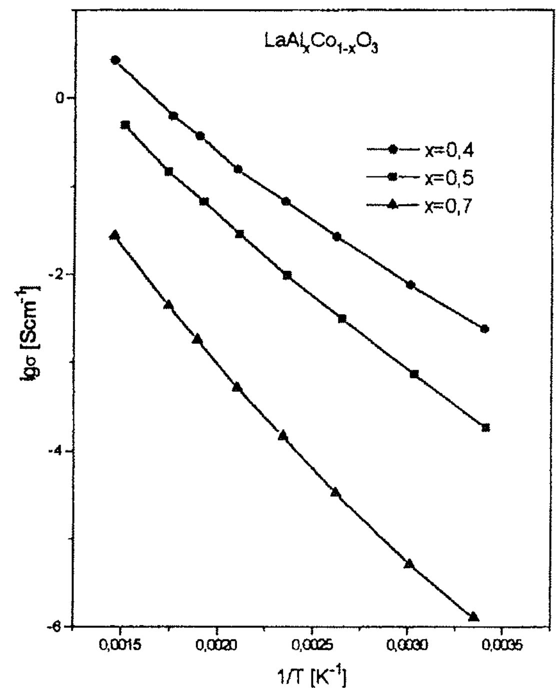

Fig. 2: DC conductivity of Al doped cobaltites

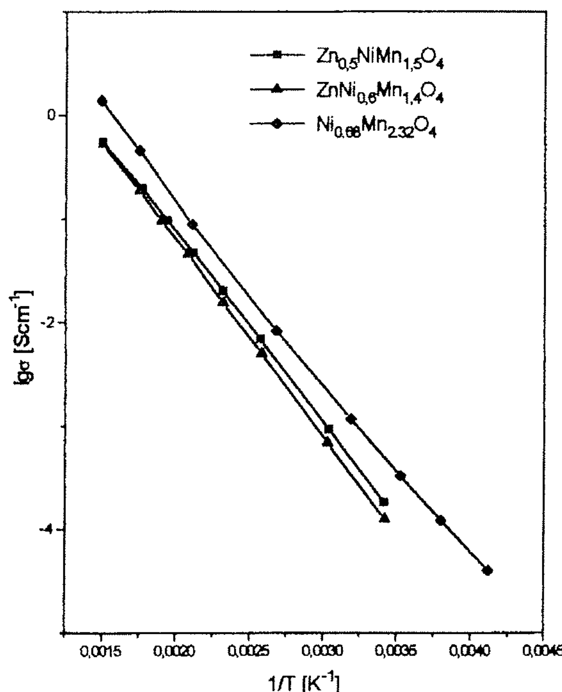

Fig. 1: DC conductivity of Zn doped manganites

The simplest explanation for the observed exponential conductivity is based on the idea, that charges are hopping over an energy barrier (activation energy) located between neighbouring cations of different valency, similar to the activated motion of ions in solids (jump model, /11/). A theory developed by Holstein /12/ describes the charge transfer as a phonon assisted hopping of (localized) electrons i.e. polarons, leading to deviations from pure exponential behaviour below the Debye temperature. For the diffusion coefficient of activated electrons in a linear chain Holstein obtains two solutions, one due to the diffusion of localized states at higher temperatures (D_{loc} with NTC character), and one due to the motion in a band at very low temperatures (D_{band} with PTC character):

$$D_{loc} = a^2 2\pi v_0 \left(\frac{J^2}{h^2 v_0^2}\right) \sqrt{\frac{2\pi}{2Y \operatorname{csch}(hv_0/2kT)}} \exp\left[-2Y \tanh\left(\frac{hv_0}{4kT}\right)\right] \qquad (2)$$

$$D_{band} = a^2 2\pi\nu_0 \sqrt{\frac{2Y\,\mathrm{csch}(h\nu_0/2kT)}{\pi}} \qquad (3)$$

$$\exp\left[-2Y\,\mathrm{csch}\left(\frac{h\nu_0}{4kT}\right)\right]$$

ν_0 vibrational frequency
$Y = E_b/h\nu_0$
a jump distance
E_b polaron binding energy
J overlap integral
$h\nu_0$ vibrational energy

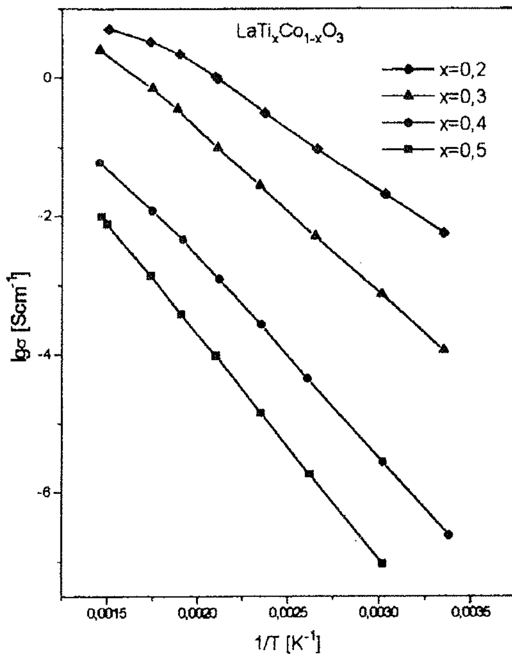

Fig. 3: DC conductivity of Ti doped cobaltites

In the high temperature case with $h\nu_0 << kT$ the exponent $\tanh(h\nu_0/4kT)$ can be replaced by its argument. With n for the polaron density, $E_A = E_b/2$ for the activation energy, $J = h\nu_0$ and the Nernst relation $\sigma = (ne^2/kT)D$ one obtains for the DC conductivity

$$\sigma_{loc} = \frac{ne^2a^2}{kT} P\nu_0 \exp\left[\frac{-E_A}{4kT}\right] \qquad (4)$$

The factor P contains all preexponential D_{loc} terms except $a^2\nu_0$. In the classical adiabatic limit of hopping P equals 1. Assuming that n is approximately given by c(1-c)N ion pairs of different valency (N density of cations, c fraction of donor ions, 1-c fraction of acceptor ions) one obtains

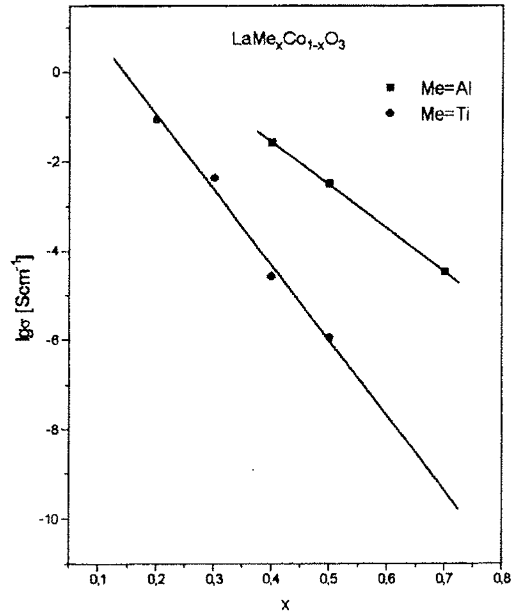

Fig. 4: Composition dependence of DC conductivity at 400 K

$$\sigma_{loc} = \frac{ne^2a^2}{kT} c(1-c)\nu_0 \exp\left[\frac{-E_A}{kT}\right] \qquad (5)$$

At this stage one can roughly estimate the DC conductivity of manganites and compare it with the experimental value. Use of the data $\nu_0 = 10^{13}$ Hz, $N = 2{,}7\times10^{28}$ m^{-3}, $c = 0{,}5$, $a = 3$Å, $E_A = 0{,}35$ eV, e= electron charge and T = 300 K gives $s = 4{,}9\times10^{-4}$ Scm^{-1}. The measured value is about $5{,}4\times10^{-4}$ Scm^{-1}.

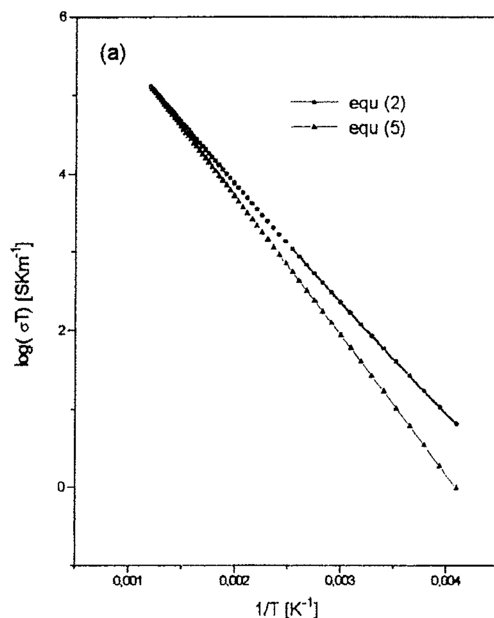

Fig. 5a: Schematic representation of Holstein formulae (2) and (5)

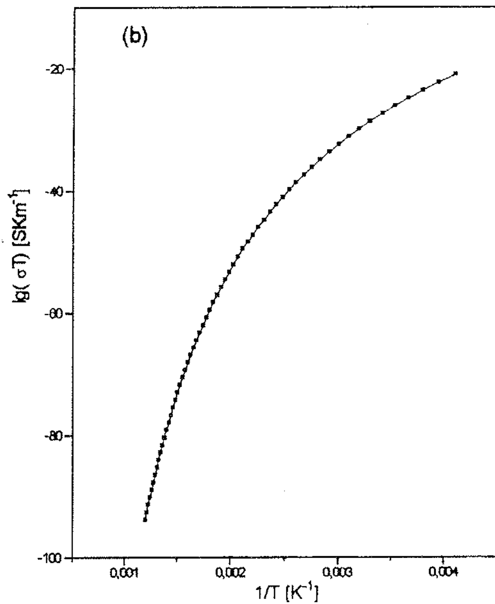

Fig. 5b: Holstein formula (3) on the basis of manganite data

As shown in fig. 5a the Holstein formulae (2) and (5) seem to be a good approach for explaining not only the intrinsic low- but also the exponential high-temperature regimes.

IMPEDANCE SPECTRA

To prove the overall applicability of the small polaron model, we searched for a possibility to measure independently the polaron jump frequency. From impedance spectra we found relaxation phenomena between 1 kHz and 1 MHz. As can be seen from the dispersion curves in figs. 6 and 7 the relaxation effects of both perovskite and spinel type materials are quite similar. In the region around 1 MHz an electrical dispersion is observed, which is caused by the common oxide properties.

The relaxation effects can be simulated electrically by Randles´ equivalent circuits, which are sometimes used in electrochemistry. The circuits consist of a series combination of a resistor (R_1) and a parallel condensor (C_1) - resistor (R_2):

$$G_p = \frac{1/(R_1+R_2)+(1/R_1)(\omega t)^2}{1+(\omega t)^2}$$

$$t = \frac{R_1}{R_1+R_2} R_2 C_1 \qquad (6)$$

Although such equivalent circuits yield a good data fit for the complex properties, it is not possible to assign the circuit elements to conductive and capacitive regions within the ceramic material. Thus we tried to find an atomistic interpretation.

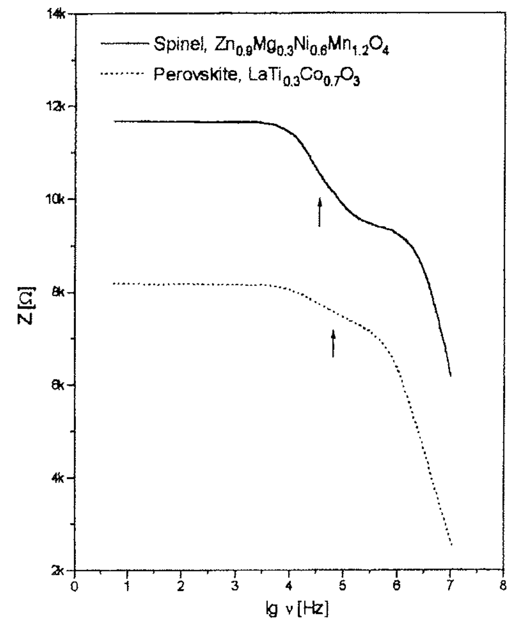

Fig. 6: Comparison of impedance spectra of spinel and perovskite type material

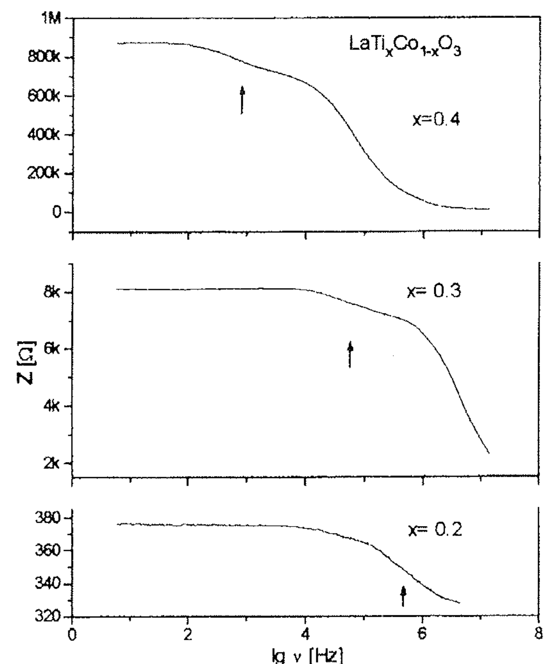

Fig. 7: Impedance spectra of Ti doped cobaltites

Sewell /13/ calculated the complex conductivity of small polarons from first basic principles. In a Debye-like way Appel /14/ applied the two-site model for hopping charges (equivalent to a dipolar flip-flop process) and obtained a frequency dependence, which equals Sewell´s and Randles´formulae:

$$Re(\sigma) \equiv G_p = \frac{ne^2a^2}{kT}\frac{1}{\tau}\frac{\omega^2\tau^2}{1+\omega^2\tau^2} + \sigma_0 \qquad (7)$$

Thus from the inflection point of G_p or Z dispersion curves (indicated by arrows in figs. 6 and 7) the relaxation time $\tau = 1/\omega$ can be obtained and interpreted as the reciprocal mean jump frequency given by $c(1-c)\nu$. The temperature dependence of the DC conductivity and of the mean jump frequency are equal:

$$\frac{1}{\tau} = \frac{1}{\tau_0}\exp\left[\frac{-E_A}{kT}\right] \qquad (8)$$

The independently measured data are compared in fig. 8. $1/\tau_0$ ranges from 10^{12} to 10^{13} Hz and has the expected order of magnitude.

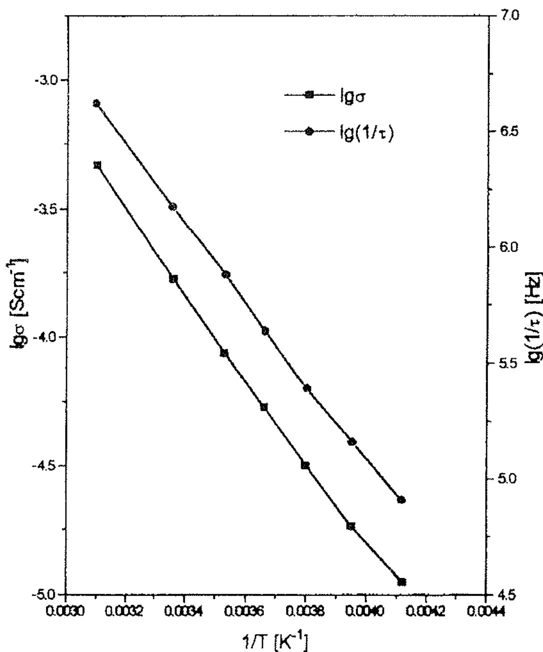

FIG. 8: Comparison of temperature dependence of DC conductivity and mean jump frequency of Zn doped manganite

Besides the temperature shift of the impedance dispersion curves a similar shift with composition x is observed, that is also directly connected with DC conductivities (fig. 9). Both shifts give strong evidence, that relaxation sets in when the AC frequency ν exceeds the mean jump frequency $1/\tau$.

From the experimental results of DC and AC conductivities and the applied dynamic models a phenomenological picture of hopping charges in NTC materials can be drawn. They conduct via polarons, that are able to diffuse through the lattice. At low enough frequencies the real part is given by independently diffusing charges. At frequencies higher than the mean jump frequency the dipoles cause an additive part to the conductivity by localized relaxation. The dispersion curves are broader by about 25% than predicted by the applied formulas, probably due to the strong coupling of hopping charges to the ionic environment, i.e. during the hopping process neighbouring ions are rearranging almost immediately. Observed and expected mean jump frequencies agree satisfactorily.

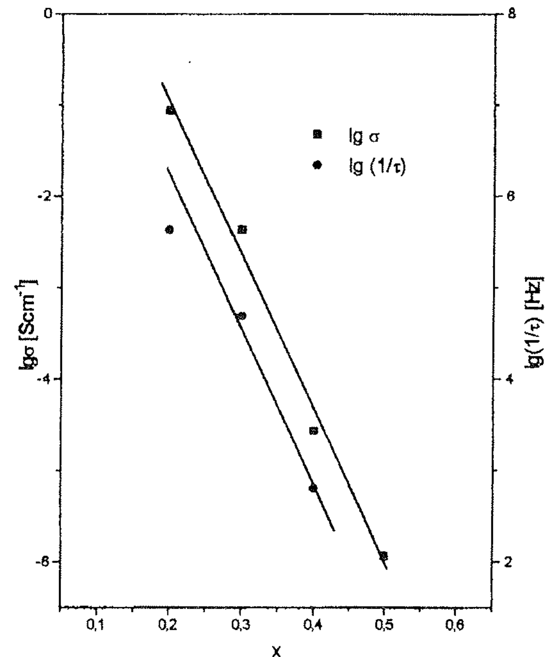

Fig. 9: Composition dependence of mean jumping frequency compared with composition dependence of the conductivity σ of $LaTi_xCo_{1-x}O_3$

HOPPING IN SPINELS

A more detailed interpretation taking into account the different atomistic structure of the materials with regard to application still remains to be discussed. Because of the inverse spinel structure of $NiMn_2O_4$ (degree of inversion 70-90% /2/) in connection with disproportion, the octahedral cation chains contain Mn^{3+} in a matrix of Mn^{4+} ions, corresponding to an electron majority. Undoped $NiMn_2O_4$ shows a negative Seebeck coefficient /15/.

However, the Seebeck coefficient does not depend exclusively on the excess charge density but also on the relative mobilities of the hopping charges. So for undoped stochiometric materials with equal positive and negative charge densities, the sign of the Seebeck coefficient is determined by the ratio of mobilities. This seems to be the case with undoped $LaCoO_3$ /16/.

To understand the different conductivity response upon doping we start the discussion from a more or less

hypothetical intrinsic situation. In this situation the densities are given by the equilibrium of disproportion, the corresponding energies we estimate to be about 1 eV. Now, doping of spinels in the range $0,1 < x < 0,5$ causes no appreciable change as observed e.g. in $ZnNiMnO_4$ or $Cu_xNi_{1-x}Mn_2O_4$ or even in the non-stoichiometric compound $Ni_xMn_{2-x}O_4$ /17, 18, 19/.

The reason, why spinels doping in the range $x = 0$ to about 0,5 is not very effective seems to be simply given by the native high degree of polaronic disorder provoked by inversion. Observed conductivity changes range within one order of magnitude, the activation energies remain approximately constant. The weak density dependence of conductivity is usually approximated by the jump probability product c(1-c).

HOPPING IN PEROVSKITES

A quite different situation of polaronic disorder is found in perovskites. Doping with donors or acceptors below $x = 0,1$ causes a quite normal i.e. linear conductivity increase with x (see Th^{4+} and Sr^{2+} doping in $LaCoO_3$, /16/). The same holds for Ti^{4+} doping, but above the limit $x = 0,1$ there is an exponential-like decrease with increasing x.

To explain the crucial exponential-like decrease (fig.4) we assume, that the probability factor c(1-c) is inadequate and has to be improved by statistical methods. There are two statistical approaches, a random liquid model leading to a probability given by cexp(-c) /20, 21/ and a solid state model leading to a binominal distribution probability /22, 23/, which itself is the precursor of the Gaussian function $\exp(-c^2)$. For small c values the first model would give on expansion the product c(1-c).

According to the binominal distribution, the probability of finding no or one acceptor ion in the second nearest shell around a donor ion or vice versa, is given in table 1. For high x values a pronounced decrease of donor-acceptor pairs (conducting polarons) is calculated.

Table 1: Composition of second shell

x	no acceptor [%]	one acceptor [%]
0.01	88.64	10.74
0.05	54.04	34.13
0.10	28.24	37.66
0.20	6.87	20.62
0.30	1.38	7.12
0.40	0.22	1.74
0.50	0.02	0.29

Both models supply probability functions with an initial increase and a following exponential-like decrease of conducting Co^{3+}/Co^{2+} or blocking Ti^{4+}/Co^{2+} and Al^{3+}/Co^{3+} pairs. As no irregularities in the susceptibility behaviour are observed /10/, we exclude super-exchange hopping via oxygen ions to one of the 6 nearest neighbours. Hence a hopping process to one of the 12 second nearest neighbours over a distance of about 6 Å remains to be operative. This is in contrast to hopping in spinels over distances of about 3 Å to one of the 4 octahedral neighbours.

CONCLUSIONS

Comparing the electrical properties of doped manganites and cobaltites, one can state that small polaron hopping is operative in both kinds of materials. However, there are essential differences upon doping concentration, arising from the different structures. In the perovskite case there is no inversion provoking high native disorder, so that doping is much more effective than in the spinel case. Hence for a quantitative description of the hopping probability one needs a better statistical approach. Because of the exponential decrease of DC conductivity with increasing Ti doping, the higher activation energies and the much better thermal stability, perovskites could be used for NTC applications up to 500°C. Al doped cobaltites do not meet all of these requirements.

LITERATURE

/1/ Y.V. Golikov, S. Tubin, D. Bamburov, V. Balakirew, "High Tech Ceramics", ed.by P. Vincenzini, Elsevier Sci. Publ., Amsterdam (1987) 237

/2/ B. Boucher, R. Buhl, M. Perrin, Acta Cryst., B25 (1969) 2326

/3/ E.G. Larson, R.J. Arnott, D.G. Wickham, J. Phys. Chem. Solids, 23 (1962)1771

/4/ V. Brabers, J. Terhell, Phys. Stat. Sol., 69 (1982) 325

/5/ O. Fruhwirth, A. Macher, K. Reichmann, H.G. Schuster, Third Euro-Ceramics Vol.2, ed. by P. Duran, J.F. Fernandez, Faenza, (1993) 395

/6/ A. Macher, Thesis, Technische Universität Graz (1994)

/7/ A. Feltz, A. Seidel, Z. Anorg. Allg. Chem. 608 (1992) 166

/8/ K.V. Reichmann, G.W. Herzog, Ceramica acta, 5-6 (1992) 85

/9/ K.V. Reichmann, Thesis, Technische Universität Graz (1992)

/10/ N. Ramadass, J. Gopalakrishnan, M.V.C. Sastri, J. Less-Common Metals 65 (1979) 129

/11/ I. Bunget, M. Popescu, Physics of Solid Dielectrics in Mat. Sci. Monographs, Elsevier, Amsterdam (1984)

/12/ T. Holstein, Annals of Physics, 8 (1959) 343

/13/ G.L. Sewell, Phys. Rev., 129 2 (1963) 597

/14/ J. Appel, Solid State Phys., 21 (1968) 193

/15/ K.V. Reichmann, Diploma Thesis, Technische Universität Graz (1991)

/16/ P. Gerthsen, K.H. Härdtl, Z. Naturf., 17a (1969) 514

/17/ J. Töpfer, A. Feltz, Solid State Ionics, 59 (1993) 249

/18/ B. Gillot, R. Legros, R. Metz, A. Rousset, Solid State Ionics, 51 (1992) 7

/19/ S.T. Kshirsagar, J. Soc. Jap. 27 (1969) 1164

/20/ I. Fritsch-Faules, L.R. Faulkner, J. Electroanal. Chem., 263 (1989) 237

/21/ M. Inokuti, F. Hirayama, J.Chem.Phys. 43 (1965) 1978

/22/ T. Luxbacher, H.P. Fritzer, K. Gatterer, C.D. Flint, J. Appl. Spectr., 62 (1995) 26

/23/ T. Luxbacher, H.P. Fritzer, R. Sabry-Grant, C.D. Flint, Chem. Phys. Lett., 241 (1995) 103

ACKNOWLEDGEMENT

The authors are indebted to SIEMENS+MATSUSHITA COMPONENTS, Deutschlandsberg, especially to H.G. Schuster for the preparation of some materials, and the FORSCHUNGSFÖRDERUNGSFONDS DER GEWERBLICHEN WIRTSCHAFT, Austria, for stimulation and financial support of this work.

A. Macher,
K. Reichmann,
O. Fruhwirth,
G.W. Herzog
Institut für chemische Technologie anorganischer Stoffe,
Technische Universität Graz, Österreich
K. Gatterer,
Institut für Physikalische und Theoretische Chemie,
Technische Universität Graz, Österreich
Stremayrgasse 16/III
A-8010 Graz, Austria
tel. +43 316 873 82 85
fax +43 316 837 619

Prispelo (Arrived): 10.5.1996 *Sprejeto (Accepted): 18.6.1996*

THE PREPARATION OF NICKEL/ZIRCONIA DISPERSIONS FROM NICKEL HYDROXIDE/HYDROUS ZIRCONIUM OXIDE GEL-PRECIPITATE PRECURSORS: INFLUENCE OF THE REACTION CONDITIONS ON THE CHARACTERISTICS

Jadran Maček and Marjan Marinšek
Faculty of Chemistry and Chemical Technology
University of Ljubljana, Ljubljana, Slovenia

Key words: composite materials, microstructure properties, Zr Zirconia gels, hydrolysis, solvent influences, crystallization, thermal analysis, dispersions of nickel, Zr Zirconium oxide, SOFC, Solid Oxide Fuel Cells, TPR, Temperature Programmed Reduction

Abstract: Dispersions of nickel in a zirconia ceramic matrix were prepared by the gel-precipitation method from a methanol solution and subsequent thermal treatment (drying, calcination and TPR). Substituting methanol for water and using gaseous ammonia for initiation of gelation provides a reaction medium in which the system of hydrolysis reactions and above all condensation reactions can be controlled to a large degree. A study is made of the influence of the reaction conditions, temperature and final pH of the reaction mixture on the composition and characteristics of the composite materials. Well defined dispersions of nickel in zirconia matrix could be obtained in this way.

Priprava disperzij nikelj/cirkonijev dioksid z gel-precipitacijo nikljevega hidroksida in hidratiziranega cirkonijevega oksida: vpliv reakcijskih pogojev na karakteristike

Ključne besede: materiali sestavljeni, lastnosti mikrostrukturne, Zr geli cirkonijevi, hidroliza, vplivi topil, kristalizacija, analize termične, Ni disperzija niklja, Zr dioksid cirkonijev, SOFC celice izgorevalne za okside trdne, TPR redukcija temperaturna programirana

Povzetek: Disperzije niklja v keramični matrici cirkonijevega dioksida so bile pripravljene z uporabo gel-precipitacijske metode iz metanolnih raztopin in kasnejše termične obdelave (sušenje, kalcinacija in TPR). Zamenjava vode z metanolom kot reakcijskim medijem in uporaba plinastega amoniaka za sprožtev hidroliznih in kondenzacijskih reakcij zagotovi reakcijski medij, v katerem lahko v večji meri kontroliramo potek hidroliznih in predvsem kondenzacijskih reakcij. Namen prispevka je študij vpliva reakcijskih pogojev (temperature in končne pH vrednosti reakcijske mešanice) na karakteristike končnih kompozitnih materialov. Z uporabo gel-precipitacijske metode lahko pripravimo homogene disperzije niklja v matrici cirkonijevega dioksida.

Introduction

The reaction medium has a significant effect on the course of the gel-precipitation and the properties of the end product. Although accepted as a standard reaction medium, water restricts the reaction conditions to its physico-chemical properties. Solvation reactions can be modified substantially if water is replaced by other in particular organic media such as methanol. This alcohol has a lower dielectric constant and dipole moment than water ($\varepsilon_{MeOH}^{25°C}$ = 32.6, $\varepsilon_{H2O}^{25°C}$ = 78.5, μ_{MeOH} = 1.70, μ_{H2O} = 1.84), so that the influence of the electrostatic potential in methanol is consequently greater /1,2/. The dipole moment of the solvent or reaction medium determines the range of the influence of the individual sol particles on the neighboring particles. In this way the electrostatic double layer of the sol and so the sol coagulation process are affected. One of the major problems concerning the sol-gel processes is the reproduction and the reliability of the results obtained. Thus, the study of hydrolysis and condensation reactions can be very helpful to set-up the appropriate reaction conditions in preparing composite materials with well defined final microstructural and morphological properties.

Zirconium oxide and its solid solutions are materials of current scientific and technological interest. They find application in various fields of materials science such as high technology ceramics and ionic conductors /3/. Recently it became clear that non-equilibrium and metastable phases, prepared by decomposing hydrous zirconium oxide at temperatures below 1000 K, might also be of great interest, for instance, to find new func-

tional materials in heterogeneous catalysis /4/. A composite such as nickel - zirconia can be prepared in several ways. The most used and reported process for the preparation of nickel dispersion in zirconia matrix is the subsequent deposition of nickel on the already formed zirconia /5-7/. The degree of homogeneity of such composites can be enhanced by the simultaneous gel precipitation of both precursors needed for composite formation /8/. Suitability of such processes for the preparation of nickel dispersions in zirconia matrix was the objective of our work. We also investigated the effect of the Ni^{2+} ions on some solid-state properties of zirconia, such as crystallization and thermal behavior. These materials could be used for further preparation of solid oxide fuel cell (SOFC) anodes.

Experimental

By the gel-coprecipitation method zirconium and nickel were precipitated from the water or methanol solutions. The starting solutions of the metal chlorides were prepared by dissolving 38 g of $NiCl_2{\cdot}6H_2O$ tetrachloride (Kemika Zagreb, p.a.) and the corresponding amount of $ZrCl_4$ (Fluka, assay >98%) in 400 ml of water or methanol, to which a twofold stoichiometric excess of water necessary for the reaction was added. A hydrolysis reaction was initiated by the introduction of gaseous ammonia (flow rate 3.88 lh^{-1}) through a glass frite into the solution of metal chlorides. This solution was vigorously agitated by a pitched-blade turbine (≈ 2000 $revsmin^{-1}$).

The introduction of ammonia initiates hydrolysis of the reaction mixture and precipitation of the hydrated zirconia and nickel hydroxide. The product was filtered and washed with distilled water until no reaction on chloride ions was observed ($AgNO_3$ test). In cases of a final pH of 7, the chloride ions cannot be washed out completely. The precipitate was dried for six hours at 120°C. The dried sample was milled in a ball mill and calcined for two hours at 500°C in air flow (18 lh^{-1}). After calcination, temperature programmed reduction (TPR) in a dynamic atmosphere of 4 vol% hydrogen and 96 vol% argon with a flow rate of 18 lh-1 was used for the reduction of nickel. A tube furnace, a heating rate of 5 Kmin-1, a final temperature of 500°C and thermostating for two hours at this temperature were used. The samples were cooled down in the same atmosphere.

The amount of nickel in the samples was determined by the volumetric method and by atomic absorption spectroscopy using a Perkin Elmer Zeeman 5100 apparatus. The particle size distribution of the precipitates was determined by laser beam diffraction on a Fritsch Analysette 22 apparatus. Auger Electron Spectroscopy (AES) depth profiling was performed on a PHI SAM 545 A analyser using electron static beam of primary electrons (3 keV, 0.5 mA and 40 μm in diameter). The sample was etched with Ar+ ions at an incident angle of 47° and etching rate of 2 nmmin-1. The thermal properties of the samples and the temperature of the crystal structure transformations were determined using a Netsch 409 STA thermoanalyser. Scanning electron microscopy (Jeol T-300 microscope) and specific surface area determination by the BET method and Ströhlein area meter were used for further characterization of the samples.

The thermally treated samples were also characterized by X-ray powder diffraction using a Philips PW-1710 instrument (30 mA, 40 kV in Cu-Kα radiation) and a Guinier de Wolff camera. The PDF CD-ROM database, sets 1-42, was used for the identification of samples.

Results and Discussion

Nickel dispersions in a ceramic matrix can be prepared either by separate formation of nickel and ceramic powders and their subsequent homogenization, by impregnation of zirconia powder by nickel, or by coprecipita- tion of nickel and ceramic precursors followed by appropriate thermal treatment and reduction. Our research was focused on the formation of nickel dispersions in a zirconia matrix by gel-coprecipitation. This method is attractive inasmuch as it reduces the number of operations required and yields a product with a high degree of homogeneity. A nonaqueous solvent, namely methanol, was used for the experiments besides water, in order to control the precipitation and gel formation reactions better.

A major difficulty in coprecipitation reactions of binary cation systems is the difference in precipitation rates of precipitation of both cations especially when they differ appreciably, as is the case of nickel and zirconium cations. In addition to the discrepancy in hydrolysis rates, the polymerization reactions of the two species also differ.

The course of coprecipitation of nickel hydroxide and hydrated zirconium oxide was followed by atomic absorption spectroscopy (AAS). The results of progress of hydrolysis reaction followed by AAS are summarised in Table 1. Precipitation of nickel hydroxide slightly lags behind that of hydrated zirconium oxide. The pH of the suspension rises very rapidly within the range of pH values at which precipitation of both gels is most intense, so that the two gel-precipitates overlap in their formation. Although, by terminating the flow of ammonia into the reaction mixture the reactions did not stop completely but nevertheless the results of AAS measurements show that precipitation of zirconia overtakes the precipitation of nickel hydroxide. The concentrations of the two cations change very little up to pH value 3. Between pH 3 and 4, condensation reactions take place and formation of the gel-precipitate of hydrated zirconium oxide occurs, /9,11,13,14,17/ while polymerization should be complete at pH 9 /16/. Nickel precipitates at pH>7 as $Ni(OH)_2$. With an excess of the precipitating reagent a soluble hexaamino complex of nickel is formed($[Ni(NH_3)_6]Cl_2$), which lowers the nickel content in the product /12/. In all cases the highest nickel content in the ceramic matrix was obtained at pH 8.

At higher pH values the results obtained in methanol differ greatly from those obtained in water. The solubility of the nickel hexaamino complex is appreciably lower

in this reaction medium than in water, so that at higher pH values the nickel concentration in the reaction medium decreases further and the nickel content of the product correspondingly increases. Washing the product in water can redissolve part of the nickel thus precipitated.

It was expected from the start of experimentation that completely homogenous products could not be obtained by coprecipitation processes. The precipitation of hydrated zirconia begins at lower pH values and furthermore takes place at different rates as the precipitation of nickel hydroxide. In these precipitation experiments hydrated zirconium oxide and nickel hydroxide are obtained. Because the zirconium precipitation begins earlier, the nuclei and also the centers of the precipitated particles should be composed to a larger extend of hydrated zirconium oxide and the outer layers of nickel hydroxide. Between these two extremes a zone of intermediate composition should exist. However, the inhomogeneity of dominance of zirconium or nickel phase are limited to the microscopic level as it was confirmed by the Auger and SEM analysis (Figures 1 and 2).

Table 1: Results of precipitation reactions as followed by AAS

Sample	pH	Zr^{4+} [gl-1]	Ni^{2+} [gl-1]
A1	1.0	12.50	17.41
A2	4.0	10.50	17.21
A3	5.0	<100 ppm	17.20
A4	6.0	<100 ppm	16.09
A5	8.0	<100 ppm	11.55
A6	10.0	<100 ppm	13.94
B1	1.0	12.50	17.63
B2	3.0	12.25	17.61
B3	4.0	<100 ppm	17.58
B4	6.0	<100 ppm	15.26
B5	7.0	<100 ppm	8.07
B6	8.0	<100 ppm	0.45
B7	10.0	<100 ppm	<100 ppm

* A samples were prepared from aqueous solution
* B samples were prepared from methanol solution with an addition of twofold stoichiometric amount of water needed for the hydrolysis reaction

The etching of the pressed tablets of the coprecipitated product during the Auger analysis reveals rather uniform composition in both cations although the etching depth was 120 nm that is deeper than the average particle diameter. The deviation from the average con-

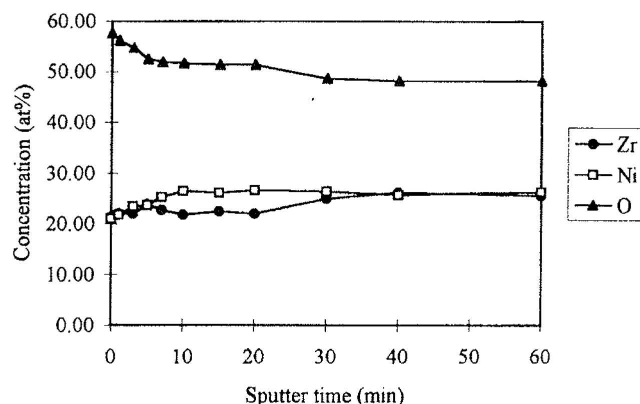

Fig. 1: AES composition - depth profile of C10ZrN83.16 sample (36.68 wt% of Ni and 63.32 wt% of zirconia)

centration is for zirconium and nickel at most 2,36 at. %. The reason for mentioned results could be, that in gel precipitation reactions we should not adhere to the standard theories of precipitate formation. The gel of hydrated zirconia is a very voluminous 3D network with ample space inside the structure for the remaining reaction mixture. Nickel hydroxide precipitates inside this 3D framework as well as on the already formed surface area of the hydrated zirconia giving spatially very uniform dispersions. Upon syneresis and drying of the gel this fine dispersion of nickel is preserved.

SEM micrographs of the C10ZrN88.44 sample with 40.18 vol% nickel in ZrO_2 matrix after heat treatment,

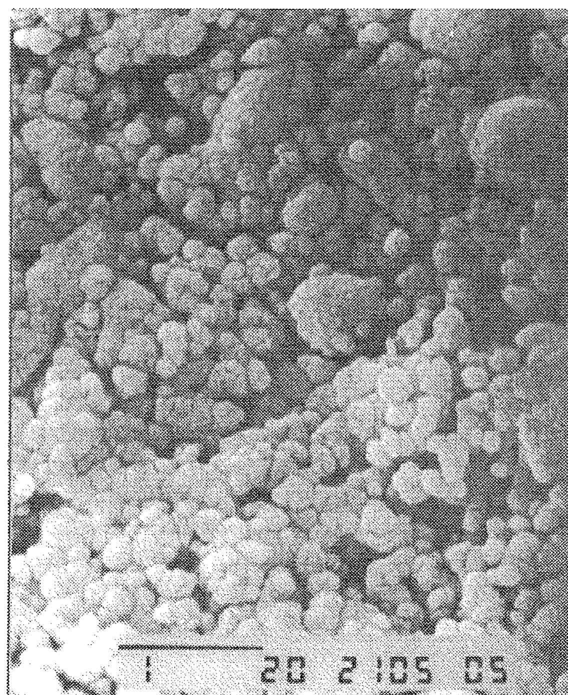

Fig. 2a: SEM surface of C10ZrN88.44 sample (40.18% of Ni)

reduction and sintering show the homogeneity or heterogeneity of nickel dispersion in Ni-ZrO_2 composite materials at the microscopic level. Figure 2 shows a fracture in the $C10ZrN8_{8.44}$ sample tablet (Fig. 2a) and a fracture in the etched sample (Fig. 2b). Both images show the nickel dispersion in the ceramic matrix to be relatively homogeneous, although there are microscopic areas where one or the other phase is dominant.

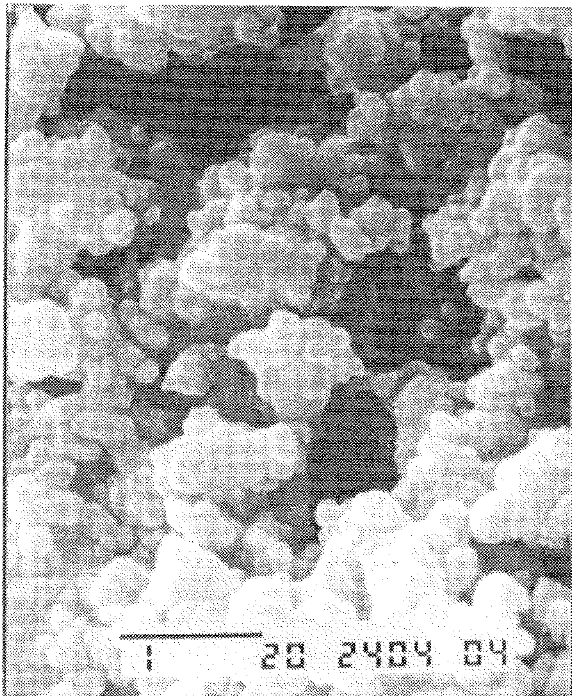

Fig. 2b: Surface of $C10ZrN8_{8.44}$ sample after etching with HCl

The particle size and distribution affect the possible application of these cermets since they influence also the specific surface, porosity, density, etc. of the fired products. The characteristics of the intermediate gel-precipitate can be changed to a degree by the reaction conditions and therefore the influence of reaction conditions, i.e. pH and temperature and the mixing rate, on the size of the precipitates was studied (Table 2). The mixing rate was throughout all experiments kept constant in order to minimise its influence on the particle size by breaking the gel into smaller particles. Higher pH values of the reaction mixture and higher temperatures lead to precipitates of lower mean particle size.

The pH of the reaction medium can influence the reaction and the product through changes in reaction kinetics and by changing the charge of the particles in the solution. Up to pH 7 the reactions proceed in a similar way in all cases. Hydrolysis that is highly sensitive to the pH of the reaction medium is assumed to be completed before this pH value is attained. The stages subsequent to the hydrolysis reaction, i.e. gelation, aging and possibly agglomeration of the precipitate, influence particle size even more strongly. Being faster in alkaline media, the aging process in particular favors smaller agglomerate sizes that agrees with the results. Like the mean particle size, the standard deviation falls as temperature and pH increase, leading to a narrower distribution of particle sizes.

Table 2: Nickel content, mean agglomerate size and standard deviation, as a function of temperature and pH of the reaction mixture

Sample	Gel-precipitation		Composite		
	Temperature (°C)	Final pH	Ni content (wt%)	d (μm)	σ (μm)
A10ZrN7	10	7	9.71	27.99	14.68
A10ZrN8	10	8	27.57	23.71	12.80
A10ZrN9	10	9	24.94	20.44	12.45
A10ZrN10	10	10	18.58	17.10	9.43
A20ZrN7	20	7	9.51	22.98	12.03
A20ZrN8	20	8	26.84	18.10	9.59
A20ZrN9	20	9	24.22	16.25	8.42
A20ZrN10	20	10	18.30	13.16	7.64
A30ZrN7	30	7	9.09	20.66	10.30
A30ZrN8	30	8	23.38	16.48	8.92
A30ZrN9	30	9	20.67	11.99	7.47
A30ZrN10	30	10	16.93	9.21	6.58
B10ZrN7	10	7	24.34	23.38	10.56
B10ZrN7.7	10	7.5	25.29	19.52	9.71
B10ZrN8	10	8	31.52	17.74	8.54
B10ZrN8.5	10	8.5	30.63	16.71	9.32
B10ZrN9	10	9	29.55	16.11	9.13
B10ZrN10	10	10	28.00	12.16	6.87

* A series samples were prepared from aqueous solution
* B series samples were prepared from methanol solution with an addition of twofold stoichiometric amount of water needed for the hydrolysis reaction

The mean agglomerate size of the gel-precipitation obtained in methanol is greater than in an aqueous medium under the same conditions. This accords with the mentioned interaction of the charged sol species in the solvent with a lower dielectric constant and smaller dipole moment. Since the gelation-precipitation system is bimodal, not only the major constituent, i.e. the zirconia precursors, but also the presence of nickel hydroxide in the product has a large influence on the

course of the reaction (table 3). A higher initial Ni^{2+}/Zr^{4+} ratio influences the amount of nickel in the precipitate as well as the mean particle size, which diminishes with higher initial ratio of metals.

Table 3: Nickel content in the ceramic matrix, mean particle size of the precipitate, standard deviation and specific surface area as a function of the initial Ni^{2+}/Zr^{4+} molar ratio

Sample	Initial		Composite		
	Ni^{2}/Zr^{4+} ratio	Ni (wt%)	d (μm)	σ (μm)	Spec. surf. area (m^2g^{-1})
$C10ZrN8_0$	0	0	19.69	8.79	71
B10ZrN8	2.04	31.52	17.74	8.54	55
$C10ZrN8_{3.16}$	3.16	36.68	17.20	8.40	51
$C10ZrN8_{4.94}$	4.94	41.82	15.71	9.32	48
$C10ZrN8_{8.44}$	8.44	50.76	12.23	5.07	47
$C10ZrN8_{27.22}$	27.22	75.98	10.26	7.11	33
$C10ZrN8_\infty$	∞	99.13	3.48	1.46	19

* all samples were prepared from methanol solutions at 10°C with an addition of twofold stehiometric amount of water, final pH value of 8 and calcination in air at 500°C for two hours followed by TPR to 500°C

The relation between various parameters of the system under observation is given in Figures 3 and 4 according to mathematical correlation of the results. Correlation equations were derived for the samples obtained from methanol solutions at a constant pH value of 8 or at a constant initial Ni^{2+}/Zr^{4+} molar ratio of 2.04.

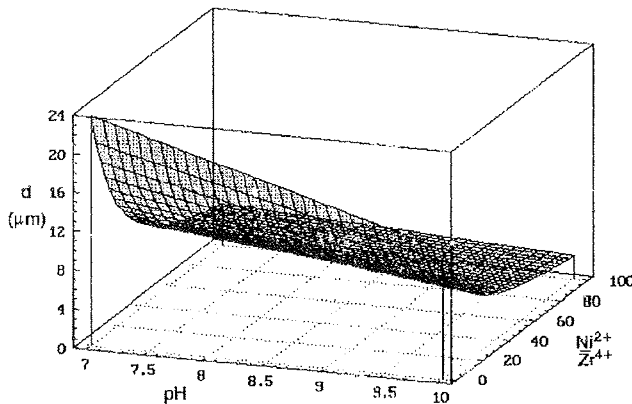

Fig. 3: Average particle size profile of precipitated composites as a function of final pH in the reaction mixture and initial molar ratio Ni^{2+}/Zr^{4+}

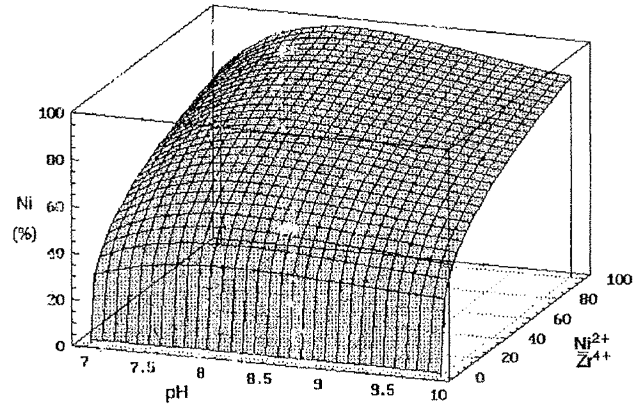

Fig. 4: Chemical composition of finally prepared composites as a function of final pH in the reaction mixture and initial molar ratio Ni^{2+}/Zr^{4+}

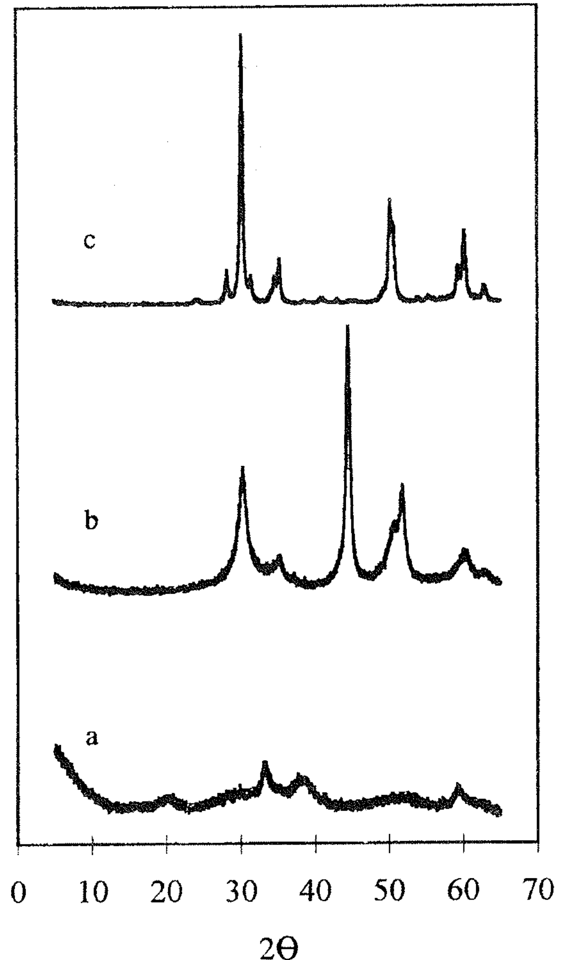

Fig. 5: X-ray diffractions of samples;
a) dry $C10ZrN8_{8.44}$,
b) thernally treated $C10ZrN8_{8.44}$ and
c) thernally treated $C10ZrN8_0$

The structure of the components was determined from the X-ray powder diffraction data (Figure 5). The dried samples appeared to be amorphous to X-ray. Their diffraction patterns exhibited only a broad band, around $2\Theta = 30.5°$ characteristic for amorphous ZrO_2 and the reflections characteristic for NiO. After thermal treatment (calcination and TPR at 500°C) the undoped ZrO_2 (C10ZrN8_0 sample) reveals both, the formation of monoclinic and tetragonal modifications. The formation of a thermodynamically metastable tetragonal structure has been reported in the calcination of amorphous hydrated zirconium gels /10,18-20/. Dollimore /21/ has suggested a scheme for the transformation from the amorphous to the crystalline phase over an intermediate metastable tetragonal phase which at increasing temperatures slowly changes into a stable monoclinic modification. The formation of the intermediate structure is a consequence of the stabilization of the metastable structure in the first phase of crystallization by lower surface energy /15,16,23,24/. X-ray difractograms of the C10ZrN$8_{8.44}$ sample indicate the course of crystallization of the gel-precipitate of hydrated zirconium oxide and nickel hydroxide. Gel dried at 120°C does not display the orderly structure of ZrO_2. The position of the diffraction lines corresponds to nickel hydroxide, but the high background and broad peaks indicate that this hydroxide is not well crystallized. After calcination and TPR the structure of the sample is rearranged. The addition of nickel strongly affected the relative amount of monoclinic and tetragonal zirconia, causing a sharp increase in the tetragonal fraction and a decrease in the monoclinic fraction. The most intense monoclinic line ($d=3.16$ Å, $2\Theta=28.24°$) is no longer visible. According to M. Valigi et.all /5/ the increasement of methastable tetragonal fraction is the consequence of an interaction of a limited fraction of nickel with the hydrous zirconia surface during the experimental set-up. The diffraction lines at 2.034 and 1.762 respectively correspond to the face centered metal nickel (FCC) formed by TPR. However, more detailed descriptions of the crystalline phase formation during thermal treatment of mixed nickel-zirconium gels prepared by the gel-precipitation method can be found elsewhere /22/.

The processes occurring during thermal treatment of the samples were monitored by TG/DTA analysis. The TG/DTA curves of the pure $Ni(OH)_2$ (C10ZrN8_∞), C10ZrN$8_{8.44}$ sample (50 wt% Ni and 50 wt% ZrO_2 in the end product) and the pure zirconium gel (C10ZrN8_0 sample) are shown in Figure 6.

The DTA curve of the C10ZrN8_∞ sample (pure nickel hydroxide precipitate) displays two endothermic peaks at temperatures of 120.1°C and 279°C respectively. The first endothermic peak, which is accompanied by a considerable mass loss, is the result of the removal of physically bonded water, while the endothermic peak at 279°C results from the dehydration of the nickel (II) hydroxide into amorphous nickel (II) oxide. Similar results have been reported by Godall and Livingston /25/. According to the literature the NiO structure develops gradually in the temperature region between 250°C and 815°C /25,26/, which could be assigned to the unpronounced broad exothermic peak that follows dehydration of the nickel hydroxide.

In the DTA experiments for nickel free hydrous zirconium oxide (C10ZrN80 sample) two thermal effects were detected: i) a broad endothermic effect in the range approximately 50-300°C (peak temperature 147°C), due to to the evaporation of methanol and water from the surface of gels, and the elimination of physically bonded water trapped in pores of partially dried gel, and ii) a very sharp exothermic peak at approximately 444°C due to the transition from an amorphous to the crystalline structure (the so-called "glow phenomenon" /19/). More detailed dehydration studies of zirconia gels prepared by the gel-precipitation method and the influence of water partial pressure in the drying atmosphere can be found elsewhere /27/.

The TG/DTA analysis of the zirconium and nickel gel-precipitate mixture (the C10ZrN$8_{8.44}$ sample) shows that the TG and DTA curves are not simple combinations of the hydrated zirconium oxide and nickel hydroxide curves. The drying process proceeds over a broad temperature interval, as in the case of the C10ZrN8_∞ sample. Two endothermic effects, attributed to the elimination of physically bonded water and the dehydration of $Ni(OH)_2$, and a broad unpronounced exothermic effect of zirconia crystallization and NiO structure formation were detected. Likewise, the endothermic peak of the dehydration of the nickel

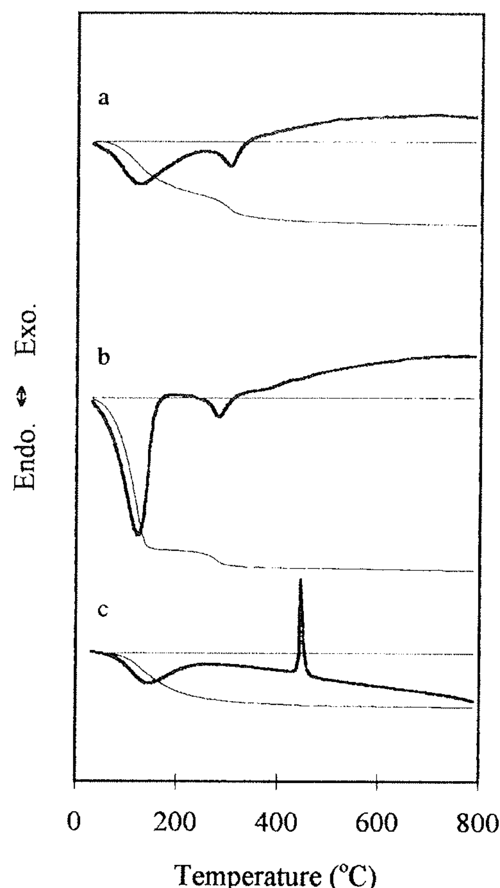

Fig. 6: TG (—), DTA (—) analysis of samples:
a) C10ZrN$8_{8.44}$,
b) C10ZrN8_∞ and
c) C10ZrN8_0

hydroxide occurs at 300°C rather than at 279°C there is no clear exothermic peak of the zirconium oxide crystalline arrangement at 444°C, which may be attributable to the masking of this process by that of the formation of nickel oxide in the same temperature region (Figure 6). The exothermic peak was affected by the presence of nickel and was shifted to higher temperature and broadened as the nickel content increased. Similar results were reported by M. Valigi et. all /5/ who attributed such a behavior of the drying gel to the nickel interaction with hydrous zirconia matrix. He suggested, that because of the nickel interaction a fraction of the zirconia may not be able to crystallize or its crystallization rate is too slow that the process escapes detection.

Conclusions

Processes for preparation of nickel dispersions in zirconia matrix by the gel coprecipitation method were studied in nonaqueous media. The use of methanol as a solvent facilitated a controlled and stepwise hydrolysis of zirconium tetrachloride precursor that cannot be otherwise obtained in aqueous medium. The improvement to the so far described processes is the substitution of aqueous ammonia solution, used for the pH correction, for the gaseous ammonia. Thus the water needed for the hydrolysis and ammonia are introduced separately that enables a wider choice of experimental conditions and due to the lower volume concentration of gaseous ammonia and its better dispersion in the reaction mixture also less pronounced local supersaturations. Although the stability of zirconium and nickel cations in the methanol solution toward pH of the medium and the rates of depletion of the reaction mixture on these cations differ the products show rather high degree of homogeneity. In order to solve the problems concerning the reliability of the results obtained the relation between various parameters of the system was proposed. The addition of nickel to the composite strongly affect the course of crystallization of the composite. Higher imputes of nickel cause a sharp increase in the tetragonal fraction and a decrease in the monoclinic fraction. The crystallization of the composites is attributed by the exothermic effect detectable by DTA analysis. The exothermic peak of crystallization was shifted to higher temperature and broadened as the nickel content increased.

Literature

/1/ R.D. Nelson, Handbook of Powder Technology, Vol. 7, Dispersing Powders in Liquids, Ed. J.C. Williams, T. Allen, Elsevier Science Publishers, Amsterdam, 1988, pp. 137-150.

/2/ C.J. Brinker, G.W. Sherer, Sol-Gel Processing, Academic Press, Inc., San Diego, 1990, pp. 36-37 and 127-130.

/3/ C.H. Steele, in High Conductivity Solid Ionic Conductors, Recent Trends and Application, Ed. T. Takahashi, World Scientific, Singapore, 1989, p. 402.

/4/ A. Cimino, D. Cordischi, S. De Rossi, G. Ferraris, D. Gazzoli, V. Indovina, G. Minelli, M. Occhiuzzi and M. Valigi, Studies on Chromia/Zirconia Catalysts I. Preparation and Characterization of the System, J. Catal., 127, 1991, p. 774.

/5/ M. Valigi, D. Gazzoli, R. Dragone, M. Gherardi and G. Minelli, Nickel Oxide-Zirconium Oxide: Ni^{2+} Incorporation and its Influence on the Phase Transition and Sintering of Zirconia, J. Mater. Sci., 5 (1), 1995, pp. 183-89.

/6/ J. Großmann, K. Rose and D. Sporn, Processing and Physical Properties of Sol-Gel Derived Nanostructured Ni-ZrO_2 Cermets, in Proc. of the 4th International Conference on Electronic Ceramics & Applications, Electroceramics IV, (R. Waser, S. Hoffmann, D. Bonnenberg, Ch. Hoffmann), Augustinus Buchhandlung, Aachen, Germany, 1994, pp. 1319-22.

/7/ Z. Ogumi, T. Ioroi, Y. Uchimoto, Z. Takehara, T. Ogawa and K. Toyama, Novel Method for Preparing Nickel/YSZ Cermet by a Vapour-Phase Process, J. Am. Ceram. Soc., 78 (3), 1995, pp. 593-98.

/8/ P. Cousin and R.A. Ross, Preparation of Mixed Oxides: a Review, Materials Science and Engineering, A130, 1990, pp. 119-125.

/9/ J. Livage, M. Henry, C. Sanchez, Sol-Gel Processing of Transition Metal Oxides, Prog. Solid. St. Chem., 18, 1988, pp. 259-286.

/10/ H.Th. Rijnten, Physical and Chemical Aspects of Adsorbents and Catalysts, Ed. B.G. Linsen, Academic Press, London, 1970, pp. 315-372.

/11/ F.G.R. Gimblett, Inorganic Polymer Chemistry, Butterworths & Co., London, 1963, pp. 106-108, 291.

/12/ D. Nicholls, Pergamon Texts in Inorganic Chemistry, The Chemistry of Iron, Cobalt and Nickel, 24, Ed. I.C. Bailar Jr., Pergamon Press, Oxford, 1975, pp. 1109-1161.

/13/ W.L. Jolly, The Synthesis and Characterisation of Inorganic Compounds, Prentice-Hall, Inc., London, 1970, p. 69.

/14/ L.M. Zaitsev, and G.S. Bochkarev, Formation of O Bridges in Zr Compounds, Russ. J. Inorg. Chem. (English Trans.), 7, 1962, p. 409.

/15/ F.A. Cotton and G. Wilkinson, Advanced Inorganic Chemistry, 5th Ed., John Willey & Sons, New York, 1988, pp. 744,779-780.

/16/ A.F. Wells, Structural Inorganic Chemistry, Fourth Edition, Clarendon Press, Oxford, 1975, pp. 448-9.

/17/ A.N. Ermakov, I.N. Marov and V.K. Balyaeva, Preparation of Aqueous Solutions of Zr Oxychloride, Russ. J. Inorg. Chem. (English Transl.), 8, 1963, p. 845.

/18/ J. Livage, K. Doi and C. Mazieres, Nature and Thermal Evolution of Amorphous Hydrated Zirconium Oxide, J. Am. Ceram. Soc., 51 (6), 1968, pp. 349-353.

/19/ A.A. Rahman, Applications of Thermal Analysis in Surface Chemical Investigations of Zirconia Gels, Thermochim. Acta, 85, 1985, pp. 3-13.

/20/ A. Clearfield, Crystalline Hydrous ZrO2, Inorg. Chem., 3,1964, p. 146.

/21/ D. Dollimore, A. Dyer, G.A. Galmen and C.A.C. Kang, Proc. 2nd European Symp. Thermal. Anal., ed. D. Dollimate, Heyden 1981, p. 387.

/22/ J. Maček and M. Marinšek, A Study of Nickel Zirconia Composite Materials Prepared by Gel-Precipitation Method in Nonaqueous Media, Fizika A, 4 (2), Zagreb 1995, pp. 413-22.

/23/ R.C. Garvie, High Temperature Oxides, Ed. M.A. Alper, Academic Press, N. Y., 1970, pp. 118-164.

/24/ T.A. Wheat, Preparation and Characterization of Lime-Stabilized Zirconia, J. Can. Ceram. Soc., 42, 1973, pp. 11-18.

/25/ A.M. Godalla and T.W. Livingston, Thermal Behavior of Oxides and Hydroxides of Iron and Nickel, Thermochim. Acta, 145, 1989, pp. 1-9.

26/ C. Duval, Inorganic Thermogravimetric Analysis, Elsevier Publishing Company, Amsterdam, 1953, p. 224.

/27/ M. Marinšek, B. Novosel and J. Maček, Dehydration of Zirconia-Gels Followed by Thermal Analysis, Proc. 23rd International Conference on Microelectronics, MIEL'95 and 31st Symposium on Devices and Materials, SD'95 (I. Šorli, B. Kren, M. Limpel), Terme Čatež, Slovenia, 1995, pp. 289-94.

prof. dr.Jadran Maček
Marjan Marinšek, dipl. ing.
Fakulteta za kemijo in kemijsko tehnologijo,
Katedra za anorgansko kemijsko tehnologijo,
Aškerčeva 5, 1000 Ljubljana, Slovenija
Tel.: +386 61 176 05 19
Fax: +386 61 125 82 20

Prispelo (Arrived): 02.04.96 ***Sprejeto (Accepted): 07.05.96***

UDK 621.3:(53+54+621+66), ISSN0352-9045

NITROGENATION OF Sm_2Fe_{17} ALLOY WITH Ta ADDITION

B. Saje[a,b], B. Reinsch[c], S. Kobe-Beseničar[b], D. Kolar[b], I.R. Harris[d]
[a] Magneti Ljubljana d.d., Ljubljana, Slovenia
[b] Jožef Stefan Institute, Ljubljana, Slovenia
[c] Max Planck Institute for Metals Research, PML, Stuttgart, Germany*,
[d] School of Metallurgy and Materials, University of Birmingham, United Kingdom

Key words: permanent magnets, nitrogenation, nitrides, Ta, Tantalum, Sm-Fe-Ta alloys, Sm-Fe-Ta powders, TPA ThermoPiezic Analyzers, SEM, Scanning Electron Microscopy, XRD, X-Ray Diffraction, TMA, Thermomagnetic Analysis

Abstract: The nitrogenation behaviour of a Sm-Fe-Ta based alloy which can be used for the preparation of Sm-Fe-N based permanent magnets has been described. Diffusion experiments on thin polished plates provided the nitrogenation processing parameters. Thermomagnetic analysis of partially and fully nitrided powders showed that the required nitrogenation times are somewhat lower than the calculated values which was attributed to the powder condition.

Nitriranje Sm_2Fe_{17} zlitine z dodatkom tantala

Ključne besede: magneti trajni, nitriranje, nitridi, Ta tantal, Sm-Fe-Ta zlitine, Sm-Fe-Ta prahovi, TPA analizatorji termopiezo, SEM mikroskopija elektronska skenirna, XRD uklon Rentgen žarkov, TMA analiza termomagnetna

Povzetek: Opisan je postopek nitriranja zlitine Sm_2Fe_{17} z dodatkom tantala, ki je primerna za izdelavo trajnih magnetov na osnovi Sm-Fe-N. Procesne parametre smo določili s pomočjo difuzijskih eksperimentov. Za te eksperimente smo uporabili tanke polirane ploščice.

Termomagnetna analiza delno in v celoti nitriranih prahov je pokazala, da so časi potrebni za nitriranje nekoliko krajši od izračunanih. To pripisujemo morfologiji prahov.

Introduction and experimental work

Permanent magnets based on the $Sm_2Fe_{17}N_{3-\delta}$ (δ=0.3) interstitial ternary phase are considered to be an attractive proposition for bonded magnets /1/. Unfortunately the binary Sm_2Fe_{17} phase is formed through a peritectic reaction between primarily crystallised iron and Sm-rich liquid. Free iron especially, unless removed by a subsequent isothermal homogenisation treatment, reduces the coercivity of the subsequent nitride when used for permanent magnets. Known methods for creating an alloy without free iron are either high temperature-long term annealing or addition of up to 5 at.% of Nb /2/ or Ta /3/.

There is much theoretical and experimental evidence of the nitrogenation of as-cast and homogenised alloys, but the diffusion parameters such as activation energy (E_a) and preexponential frequency factor (D_o) appear quite inconsistent. The activation energy for nitrogenation in pure nitrogen ranges from 66 to 133 kJ/mole and frequency factor (D_o) from 1 .02*10^{-6} to 1.95*10^{-10} m^2/s /4-7/. There are no data for Ta modified alloys. Therefore it was the aim of this work to study comparatively the nitrogenation of as cast and annealed standard and Ta modified alloy to obtain diffusion parameters which would help to predict optimal processing parameters.

* present address: Robert BOSCH GmbH, FV/FLW, POB 106050, D-70049 Stuttgart

The nitrogenation was carried out on induction melted Sm_2Fe_{17} and $Sm_2Fe_{16}Ta_1$ alloys in pure nitrogen. The stoichiometric composition of cast Sm_2Fe_{17} was additionally homogenised for one week at 1100°C in argon to obtain nearly single phase material. The approximate nitrogenation temperature was determined by means of a thermopiezic analyser (TPA). Alloys were nitrided in 1 bar of pure nitrogen at temperatures from 350 to 550°C for different times (from 1 to 16 h) and examined with optical (Zeiss) and scanning electron microscopy (SEM Jeol EPMA 840 A). From the depth of the nitrogenated layer, activation energy and frequency factor were calculated. The $Sm_2Fe_{16}Ta_1$ alloy was also milled in a ball mill to study the nitrogenation behaviour of powder. Powder was nitrogenated for different times at 1 bar of pure nitrogen at 450 °C. The nitrogenated powder was then characterised by means of scanning electron microscopy (SEM, Jeol EPMA 840 A), X-ray diffraction (XRD Philips, Cu Kα source, step scan mode, step 0.02°, time/step 10 s, Ag as a standard) and thermomagnetic analysis (TMA, Manics DSM 8, horizontal Faraday principle, H_{ext} = 100).

Results and discussion

The results of the diffusion experiments are shown on Fig.1. The square of the average depth of the nitrided layer (and therefore the nitrogen diffusion) in the stoichiometric alloy is slightly larger than that in the Ta

modified alloy. From the measurement the activation energy for Sm_2Fe_{17} alloy was determined to be 82.32±8.97 kJ/mole with frequency factor of $1.7*10^{-10}$ m^2/s and activation energy for Sm-Fe-Ta alloy 92.82±11.96 kJ/mole with frequency factor of $5.3*10^{-10}$ m^2/s. From the data obtained it was possible to calculate that sufficient nitrogenation time for spherical particles of 10 μm diameter would be around 10 hours, according to the equation published in /7/.

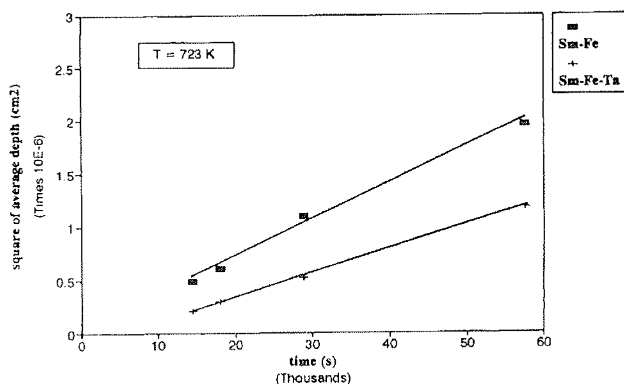

Fig. 1: Square of the average nitrogen layer depth vs. time at 723 K

For the nitrogenation and magnetic properties measurements the milled powder was used. The average particle size of the powder was about 10 μm (as determined with Cilas Alcatel Laser particle sizer) but its irregular morphology has to be noted as well as the broad particle size distribution. Due to these features slightly different nitrogenation behaviour was anticipated as predicted in theoretical modelling /7/. XRD diffraction of the Sm-Fe-Ta powder nitrided for 10 hours showed characteristic peak shifts due to lattice expansion of the Sm_2Fe_{17} phase (Fig. 2a) when compared with the XRD trace of the non nitrided Sm-Fe powder (Fig 2b). The $TaFe_2$ phase didn't change upon nitrogenation and there is no free Fe detectable in the Ta modified non nitrided alloy (see Fig 2c). There was also a small peak attributed to free Fe observed in the nitrided powder (Fig. 2a). Since the average nitrogenation temperature was too low to induce the overall decomposition of the nitride this was attributed to the combined effect of the decomposition of the $Sm_2Fe_{17}N_x$ into SmN and secondary Fe during nitrogenation due to surface effects as reported in /2/ and possible presence of the remanent primary Fe from the cast material.

Several features are apparent from the thermomagnetic scans of fully, partially and non nitrided Sm_2Fe_{17} alloy which are shown on Fig. 3. Only the magnetisation curves of non nitrided and the alloy nitrided for 6 hours exhibit one Curie point corresponding to Sm_2Fe_{17} and $Sm_2Fe_{17}N_{3-\delta}$ phase respectively.

The other traces exhibit contribution from both the nitrided shell and the core. The Curie point of the $Sm_2Fe_{17}N_{3-\delta}$ shell (470°C) remains virtually unchanged irrespective of the nitrogenation times. This shows, that, even after a short nitrogenation time, a layer of nitrogen saturated shell is formed. The Tc of the core increases with nitrogenation time over the range of 100°C. This shift may be caused by the expansion of the core, due to the strain caused by the volume expansion of the nitrogenated shell. Another possibility is that it is due to a combination of this factor together with the presence of regions of intermediate nitrogen concentration, as shown in the Sm-Fe-Nb system /8/.

The Sm-Fe-Ta powder appeared to be fully nitrided even after 6 hours of nitrogenation (for the given processing parameters) which is not in agreement with calculations in which temperature, time, N2 pressure and average particle size were used as the defined values. This difference was therefore attributed to the state of the milled powder i.e. irregular morphology, possible cracks or even anisotropic diffusion through the lattice, geometrical factor, particle size distribution and the surface condition which were omitted from the calculation.

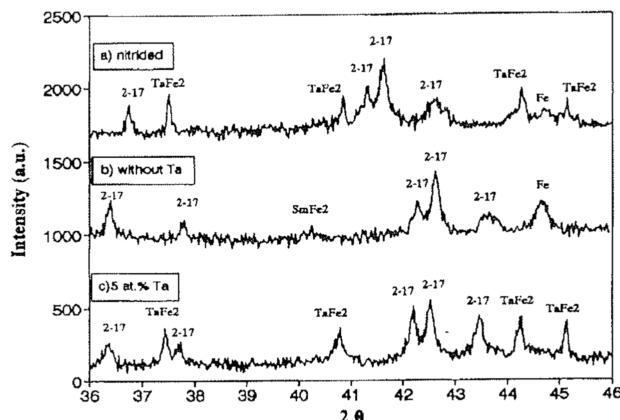

Fig. 2: XRD traces of
a) nitrided Sm-Fe-Ta alloy,
b) as-cast Sm_2Fe_{17} alloy, and
c) as-cast Sm-Fe-Ta alloy.

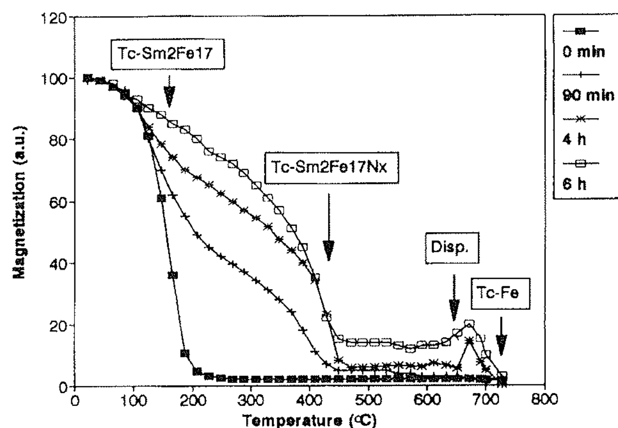

Fig. 3: TMA traces of Sm-Fe-Ta powders nitrided for various times.

Another feature apparent from the graphs on Fig. 3 is the increase of the magnetisation after the Curie temperature of the $Sm_2Fe_{17}N_3$ which was attributed to secondary free Fe formation due to decomposition of the nitride.

Activation energy for Sm_2Fe_{17} alloy was determined to be 82.32±8.97 kJ/mole with frequency factor of $1.7*10^{-10}$ m^2/s and activation energy for Sm-Fe-Ta alloy 92.82±11.96 kJ/mole with frequency factor of $5.3*10^{-10}$ m^2/s.The nitrogenation times to obtain fully nitrided alloy were around 6 hours for the powder with average grain size of 10 μm (for the given processing parameters) which is less than predicted by calculations assuming spherical powder particles with uniform grain size distribution. The discrepancy between the idealised powder used for theoretical calculations and real powder was attributed to the condition of the milled powder.

References

/1/ J. M. D. Coey, Sun Hong, J. Magn. Magn. Mat., 87, 1990, L251.

/2/ A. E. Platts, I. R. Harris, J. M. D. Coey, J. Alloys and Compounds, 185, 1992, 251.

/3/ B. Saje, A. E. Platts, S. Kobe Beseničar, I. R Harris, D. Kolar, IEEE Trans. Magn. , 30, 1994, 690.

/4/ J. M. D. Coey, J. F. Lawler, Sun Hong, J. E. M. Allan, J. Appl. Phys., 69, 1991, 3007.

/5/ H. Kaneko, T. Kurino, H. Uchida, Proc. 7th Int. Symp. Mag. Anisotropy and Coercivity in Re-TM Alloys, Canberra, 1992, 320.

/6/ R. Skomski, J. M. D. Coey, J. Mat. Eng. Perf., 2, 1993, 241.

/7/ J. M. D. Coey, R. Skomski, S. Wirth, IEEE Trans. Magn, 28, 1992, 2332.

/8/ D.S. Edgley, B. Saje, A.E. Platts, I.R. Harris, J. Magn. Magn. Mat., 138, 1994, 6.

Dr. Boris Saje,
Magneti Ljubljana d.d.,
Stegne 37, 1000 Ljubljana, Slovenia
Jo'ef Stefan Institute,
Jamova 39, 1001 Ljubljana, Slovenia
159 87 64/159 26 69/boris.saje @ijs.si

Dr. Spomenka Kobe-Beseničar,
Jo'ef Stefan Institute,
Jamova 39, 1001 Ljubljana, Slovenia
177 32 51/126 3 126/spomenka.kobe @ijs.si

Prof. dr. Drago Kolar,
Jo'ef Stefan Institute,
Jamova 39, 1001 Ljubljana, Slovenia
177 32 92/126 3 126/drago.kolar @ijs.si

Dr. Bernd Reinsch
Max Planck Institute for Metals Research, PML,
Heisenbergstr.5, D-70569 Stuttgart, Germany
fvflw_rb @sh_x4.bosch.de

Prof. Dr. I.R. Harris
School of Metallurgy and Materials,
University of Birmingham,
Birmingham B15 2TT, United Kingdom
I.R.Harris @bham.ac.uk

Prispelo (Arrived): 28.5.1996 ***Sprejeto (Accepted): 18.6.1996***

ON LOW FREQUENCY C-U RELATIONSHIP OF THE IONIZED CLUSTER BEAM, ICB, DEPOSITED Ag/n-Si(111) SCHOTKY DIODES

Bruno Cvikl
Faculty of Civil Engineering, University of Maribor,
and "J. Stefan" Institute, University of Ljubljana, Ljubljana, Slovenia

Key words: Schottky junction, Schottky diodes, C-U relationships, Low frequency C-U relationships, capacitance diodes, energy gaps, semiconductors, ICP, Ionized Cluster Beam, Ag/n-Si depositions, acceleration voltages, DIGS, Disorder Induced Gap States, UHV, Ultra-High Vacuum

Abstract: The low frequency capacitance- voltage, C-U, relationship has been investigated on the basis of the postulated model of the semiconductor energy bands for samples of ionized cluster beam, ICB, deposited Ag/n-Si(111) Schottky diodes for nonzero Ag ions acceleration voltage. In the derivation the fundamental assumption made is the existence, within the Si energy gap, in addition to usual P shallow levels also Ag deep donor and acceptor impurity energy levels which, however, are assumed to be spatially confined to the narrow region at Ag/Si junction, only. The electrical activation of Ag, within this region homogeneous distributed, impurities is biased voltage dependent. The Ag impurity levels are extending up to the maximal penetration length L, which is a function of silver ions acceleration voltage U_a. It is argued, that it is only for small values of L and/or small Ag impurity concentrations, that the C-U relation is expected to exhibit the linear relationship, in accordance with the measurements.

The observed bias dependence of the semiconductor series resistance, at constant temperature, as well as the strong temperature dependency of the I-U measurements as reported previously are, in terms of the proposed model, explained on the phenomenological grounds.

It is argued, that the relationship between the disordered, enriched semiconductor (interface) layer, formed at the metal/semiconductor junction, presumably responsible for the occurrence of the disorder induced gap states (DIGS), and the Fermi level pinning effect, might be most conveniently investigated by carefully controlled and suitably designed ICB experiments in UHV conditions.

O nizkofrekvenčni C-U odvisnosti Ag/n-Si(111) Schottky-jevih diod, nanešenih po metodi curka ioniziranih skupkov, CIS

Ključne besede: Schottky spoj, Schottky diode, C-U karakteristike, , C-U karakteristike nizkofrekvenčne, diode kapacitivne, reže energijske, polprevodniki, ICB nanašanje s curkom skupkov ioniziranih, Ag/n-Si nanosi, napetosti pospeševalne, DIGS stanja energijska nereda v reži energijski, UHV vakuum ultravisoki

Povzetek: Na osnovi modela energijskih pasov v reži polprevodnika za primer po metodi curka ioniziranih skupkov nanešenih Ag/n-Si(111) Schottky-jevih diod za različne vrednosti pospeševalne napetosti Ag ionov, je v limiti nizkih frekvenc raziskana odvisnost kapacitivnosti diod od velikosti zunanje napetosti. Osnovna podmena, ki je bila privzeta v toku izpeljave C-U odvisnosti, zadeva predvideni obstoj omejenega prostorskega področja polprevodnika znotraj katerega se, poleg fosforja, še dodatno nahajajo električno aktivni in nevtralni srebrovi ioni enakomerne koncentracije. Srebrovi atomi se v polprevodniku vedejo kot ali donorji ali akceptorji, njihova električna aktivnost na pripadajočih energijskih nivojih, ki so uvrščeni globoko znotraj energijske reže, pa v splošnem zavisi od zunanje napetosti. Srebrove nečistoče v notranjosti polprevodnika segajo od stika kovina polprevodnik pa vse do največje globine L, ki zavisi od zunanje pospeševalne napetosti, U_a. Na osnovi izvedenih izračunov je pokazano, da je samo v limiti zanemarljivo majhne dolžine L in/ali majhne koncentracije srebra, v splošnem C-U odvistnost lahko linearna, v skladu z opazovanji.

Na osnovi postavljenega modela je v delu podana fenomenološka razlaga odvisnosti serijskega upora od zunanje napetosti, kot tudi temperaturna odvistnost električnega toka in napetosti, I-U, na omenjeni način izvedenih Schottky-jevih diod.

V članku je podan predlog, da je mogoče medsebojno razmerje med neurejeno, z srebrovimi nečistočami obogateno polprevodniško vmesno plastjo ob stiku kovina polprevodnik ter s tem povezanim pojavom nastanka novih elektronskih energijskih stanj (DIGS) v reži polprevodnika in vpetjem Fermijevega nivoja, prikladno proučevati prav z skrbno nadzorovanimi in ustreznimi, v ultra visokem vakuumu, izvedenimi eksperimenti rasti tankih heteroplasti po metodi curka ioniziranih skupkov.

1. Introduction

Formation of thin films of various electric, magnetic, and even organic substances on the suitably chosen substrata is among the other well established methods, also conveniently accomplished by Takagi /1,2/ ionised cluster beam, ICB, vacuum deposition method.

The essential idea of ICB deposition method is illustrated on fig. 1. The material to be deposited is contained in a closed crucible with a small nozzle on top. The vapours, while escaping through the nozzle, undergo adiabatic, supersonic expansion and during this process some of the atoms may reportedly /2/ aggregate in clusters of up to a few dozen atoms. Subsequent

to their formation, through the nozzle ejecting atoms and atomic clusters are the subject of electron impact ionisation and are, on their path towards the substrate, accelerated in the static electric field, U_a. It has been generally observed that ejecting atoms or clusters are singly positively ionised.

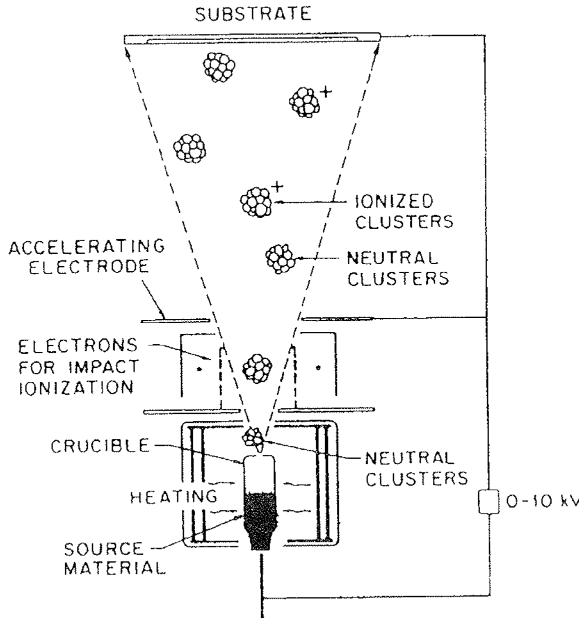

Fig. 1. Schematic drawing of an ion cluster beam, ICB, deposition experiment /1/.

It is rather a well documented fact /2/, that ICB low temperature thin film growth method produces a very good quality thin layers. The reason is attributed to the still unexplained effects which generally accompany this particular ion assisted method of film growth. In addition, there exist at least two additional important features contributing to the quality thin film growth, namely the fact that there are no extra atomic species involved which could contaminate or be incorporated in the growing process, as well as the observation, that the amount of damage on the substrate due to the impinging particles, depending on the experimental condition, might be very small indeed.

The potential barrier height, ϕ_b, of Ag/n-Si(111) Schottky diode when deposited by conventional UHV vacuum deposition methods as derived from I-V measurements /3/, is reported to be 0.78 eV. However, if deposited by ionised cluster beam, ICB, deposition method /1/, depending on the acceleration voltage, U_a, the apparent potential barrier height of the above structure, seemingly could be tailored to vanish. For our purpose it is to be noted, that by the proper choice of U_a, the silver ions possess enough kinetic energy to penetrate the Si substrate.

Since the accelerated Ag+ ions may, for large enough U_a, penetrate the Si wafer a few nm in depth, they might strongly contribute to an additional doping density /4/ within this region. In this respect an attempt /4/ has just recently been made to analyze the experiment in terms of the theory of thermally assisted tunneling of electrons (thermionic field emission current). This theory /5/ expresses the I-U characteristics in term of a parameter E_{oo} (which is a function of semiconductor doping density) and in certain cases, as evidenced in the literature, could account for the lowering of the **effective** potential junction barrier as a function of increasing semiconductor (homogeneous) doping. From the reverse part of I-U characteristics of our ICB deposited samples the extracted values of the "effective" Schottky barrier height, ϕ_b, the ideality factor, n, (defined as $n=(q/kT)\partial V/\partial(\ln J)$), and the donor doping density, determined separately for each case of the Ag+ ions acceleration voltages, U_a, failed to correctly predict the measured I-U temperature variation of the ICB deposited Ag/Si structures /4/.

The drastic changes as seen in the reverse part of the I-U diagram of ICB deposited Ag/n-Si(111) Schottky junctions, for U_a=0, 300 V and 1 kV, are presented on fig. 2. The details of the deposition and the analyses of the results are thoroughly discussed in ref. /4/. In general, the I-U electrical characteristics of such samples (for U_a nonzero) exhibit, within the small range of the *reverse applied voltage U*, almost linear I-U dependence before the saturation, fig. 2. The interval of almost linear I-U relationship is a monotonic function of U_a, the acceleration voltage of Ag^+ ions, however accompanied by the corresponding increase of the (reverse) saturation current, fig. 2. For large enough acceleration voltages (say for U_a = 6 kV) the diode rectifying characteristics disappear altogether as thought the effective Schottky barrier height has virtually diminished. The metal/semiconductor structure, in the reverse direction, than effec-

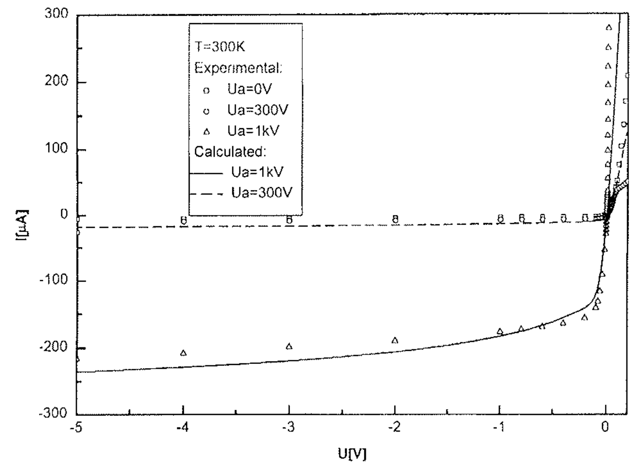

Fig. 2. An example of the room temperature measured reverse I-U characteristics of ionized cluster beam deposited Ag/n-Si(111) Schottky diodes for Ag^+ ions acceleration voltages U_a=0, 300 V (these measurements on the drawing coincide) and 1kV, is presented /6/. The circles, squares and the triangles are the calculated values, derived for the case of thermionic-diffusion theory of the majority charge carriers transport taking the Schottky barrier height as a parameter, as described in ref. /6/.

tively behaves as a linear element, however in the forward direction the conditions, due to the experimental difficulties, are presently still not yet determined in details.

In the latter work /6/ it was shown that the distinct features of the reverse I-U temperature dependent measurements (i.e. the appearance of the "knee bend" as well as the large differences of the reverse saturation current densities) of these ICB deposited Schottky junctions could be sufficiently well described in terms of the thermionic-diffusion theory of the charge carrier transport. In the computation the existence of the distinct Ag+ donor additionally enriched region in n-Si sample extending from the Ag/Si junction up to the Ag+ ions maximum penetration length, L, (which is a function of U_a) has been assumed. The doping effect of oxygen, carbon, sulfur and other surface impurities, which are for U_a nonzero also present within Si wafer, have been neglected. The results obtained seem to imply the fact,

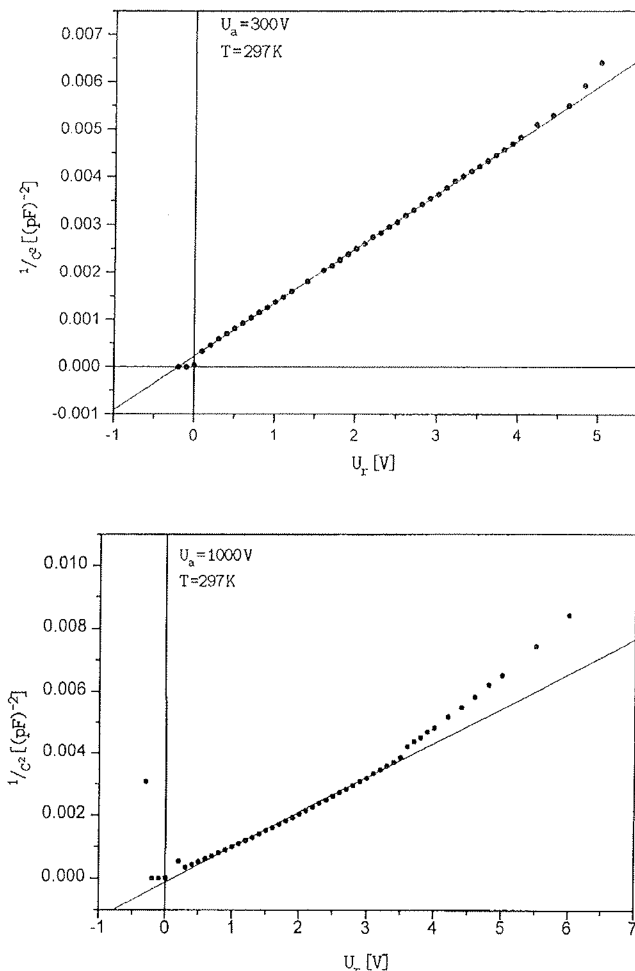

Fig. 3. *Two examples of low frequency, ν =2 kHz (the amplitude of the ac measuring signal was set to 10 mV), room temperature measurements of the C-U relationship of ionized cluster beam deposited Ag/n-Si(111) Schottky diodes for Ag^+ ions acceleration voltages of U_a=300 V and 1 kV, are exhibited /13/. The lines are guides to the eyes only.*

that by the ICB deposition method it might be possible directly to modulate the Schottky barrier height.

The measured low frequency capacitance-voltage, C - U, relationship exhibit similar peculiarities, fig. 3. in the sense that for low values of silver ions acceleration voltages the diagram C^{-2} versus applied voltage U (fig. 3) exhibit well defined linear relationship as predicted by the theory /3/, however, say, for acceleration voltages U_a > 2 kV, it may soon become nonlinear.

It is a well established fact /7/, that the Si wafer, following the surface preparation, is under normal laboratory atmospheric conditions almost immediately covered by extremely stable (for the period up to one year) dielectric thin film consisting of about 0.7 nm thick native oxide layer on top of which about 0.2 nm thick organic contamination layer is in general also present. Obviously, the extent of the Ag^+ enriched n-Si regions is most conveniently expressed in terms of the penetration lengths, L, which is accessible to Ag^+ ions (at a given value of U_a) within the n-Si wafer. This distances have been correspondingly calculated (including the 1.2 nm thick oxide layer on the Si surface) and have been found to be L=2.4 nm for U_a=300 V, and L=4.0 nm for U_a=1 kV /8/. As it is well known /3/ the impurity silver atoms incorporated within the Si substrate can act either as donors (E_d (Ag) in Si = 0.370 eV above E_V) or as

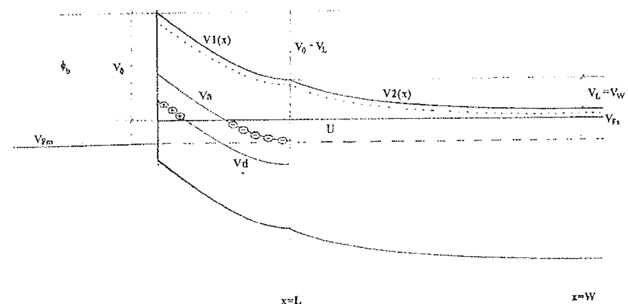

Fig. 4. *Schematic drawing (not to scale) of forward biased ionized cluster beam deposited Ag/n-Si(111) metal/semiconductor junction. The region within the semiconductor, up to the abrupt plane at depth L, contains additional (besides electrically activated shallow phosphorous dopant level denoted as dots) deep lying Ag donor and acceptor impurities, which are assumed to be homogeneously distributed. L denotes the maximum penetration range, of silver ions for the given value of the external acceleration voltage, Ua. Within the region 0<x<L the two deep Ag impurities levels explicitly exhibit the activated donor and acceptor ions. Note that the density of electrically activated Ag impurities is (within the certain voltage range) a function of the external DC bias U. The distance L, being a function of the Ag ions acceleration voltage U_a, is usually of the order of a few nm, while the edge of the depletion region, W, is at least an order of magnitude larger.*

acceptors (E_a (Ag) in Si = 0.717 eV above E_V). Consequently, these impurity deep-levels lie within the Si energy gap and the expected resulting energy band diagram is schematically depicted on fig. 4.

The present work is an extension of earlier results /10,11/ on the general capacitance voltage, C-U, relationship as applied to the case (of the spatially homogeneous concentration) of the deep-lying impurity atoms in Si wafer confined within the metal/semiconductor junction region. The region in question is of the characteristic length, L, which is expected to be of the order or even smaller than the usual Debye length, L_D, defined as $L_D = \sqrt{\varepsilon_s kT/q^2 N_D}$. Here, N_D is an effective dopant density, k denotes the Boltzman constant, q electronic charge, T the absolute temperature and $\varepsilon_s = \varepsilon\varepsilon_0$. For $N_D = 10^{16}$ cm^{-3} at T = 300 K, the Debye length in Si is about 40 nm and is approximately 3 nm for $N_D = 10^{18}$ cm^{-3} at the same temperature. In this connection one remembers that at thermal equilibrium (and zero applied voltage) depletion layer width, W, is for Si, of the order of $8L_D$. Consequently, depending upon the impurity concen-trations, one expects L to be at most comparable to L_D but it might be smaller. Nevertheless, the excess space charge variation, which is strongly dependent upon the value of an applied external bias U, might be responsible for the unusual features in electrical characteristics of IBC deposited Ag/n-Si Schottky junctions. In this work the effect of the space limited, deep-energy Ag impurity levels confined in the vicinity of metal/semiconductor junction, on low frequency C-U relationship is investigated on a qualitative basis.

It will be shown that these effects might be, under specific conditions, marked.

The notion of the so called disorder induced (semiconductor) gap state spectrum, DIGS, has recently appeared in the literature /9/. It is characterised by the energy E_0, interpreted as Fermi energy of DIGS spectrum at the energy point where the charge neutrality occurs. The DIGS density spectrum consists of bonding (donor-like) and antibonding (acceptor-like) states and E_0 represents the Fermi level location of the DIGS spectrum at the plane within the gap where the charge neutrality is achieved. According to this model, deposition of insulator or metal on semiconductor produces a thin disordered semiconductor layer. This layer is characterised by fluctuations of bond lengths and angles due to stress and due to the interface irregularity and consequently Anderson localisation leads to DIGS continuum in the energy gap whose density depends on degree of the disorder. The unified DIGS model is able to explain the behaviour of the metal/semiconductor interface when formed on the bare or oxide covered metals as well as the various features of the interface state density distribution. According to DIGS model, for cases when the interfacial degree of disorder is high, the Fermi level is firmly pinned at values very close to E_0, effectively resulting in the so called Bardeen limit, according to which the barrier height does not depend on the metal work function. An important feature of the DIGS model over MIGS model is the fact that the former is able to offer an explanation of the Fermi level pinning on the oxide covered Schottky barriers while the later can not. Since the crucial feature of the DIGS model is the assumption of the presence of a disorder at the interface, a fact which is difficult to characterise experimentally, it is quite evident that by an ICB deposition method one posses-ses the means of an experimentally controlled induce-ment of such type of disorder at the metal/semicon- ductor interface.

DIGS are usually studied by the measurements of the interface state density distributions as for instance provided by the careful interpretation of the frequency dependent C-V measurements in conjunction with the photocapacitance transient spectroscopy.

The ICB deposited samples, among other features, might be of a great potential value for investigation of certain aspects of DIGS model. It is the purpose of this paper to present the basic fundamentals of (low frequency) C-U relationship of such samples which are characterized, as explained earlier, by the coexistence of two adjacent distinct semiconductor doping regions of substantially different spatial extensions.

2. Theoretical outline

As described in the introduction the ICB deposited Ag/n-Si(111) Schottky diodes are characterized, for the ions acceleration voltage $U_a \neq 0$, by the fact that Ag^+ ionized clusters as well as ions, depending on the initial kinetic energy imparted to them by the voltage Ua, can penetrate the silicon substrate up to the maximum depth denoted by the distance L. In what follows we assume that the maximum penetration range, L, is attainable to the single ionized Ag^+ silver ions, while in general the penetration range of the individual clusters, depending on the number of atoms forming the cluster, is correspondingly shorter. In what follows, for the ease of the computation, we assume that the individual silver ions are uniformly distributed within the penetration range from the Si surface up to the largest range L. As well known /3/ the electrically activated impurity silver atoms incorporated within the Si substrate can act either as donors (E_d (Ag) in Si = 0.370 eV above E_V) or as acceptors (E_a (Ag) in Si= 0.717 eV above E_V). The impurity levels lie within the Si energy gap and the expected energy band diagram is schematically depicted on fig. 4.

Our purpose is to derive an expression for the differential capacitance per unit area, $C = dQ/(SdV_d)$, as a function of the external voltage, U, applied between the metal and the semiconductor, where dQ/dV_d represents the charge increment per infinitesimal change of the diffusion potential and S is the cross section of the Schottky diode (interface) /12/.

For this purpose one starts the derivations by the usual approach using the expressions, $div\mathbf{D} = \rho$, where $\mathbf{D} = \varepsilon_0\mathbf{E} + \mathbf{P} = \varepsilon_s\mathbf{E}$ and $\varepsilon_s = \varepsilon\varepsilon_0$, but since $\mathbf{E} = -grad\ V$,

(obviously a quasi-static field approximation is adhered to) where V is the electrical (scalar) potential, the Poisson equation in one dimension reads,

$$\frac{d^2V}{dx^2} = -\frac{\rho}{\varepsilon_s} \tag{1}$$

where $\rho = \rho(x)$ denotes the excess charge density within the semiconductor. The charge density distribution for the described model Schottky diode as a function of x is schematically depicted on Fig. 4. Since in general the electrical potential, V, is a single value function of the coordinate x, from which it follows that the inverse function, $x=x(V)$, also exists, the above expression may be written in a modified form. Namely, observing the following identity,

$$\frac{d}{dx}\left(\frac{dV}{dx}\right)^2 = 2\left(\frac{dV}{dx}\right)\frac{d^2V}{dx^2} \tag{2}$$

it consequently follows that,

$$\frac{d^2V}{dx^2} = \frac{1}{2}\frac{d}{dV}\left(\frac{dV}{dx}\right)^2 \tag{3}$$

and after the multiplication by the factor (-1) from which evidently follows that ρ is an even function of the scalar potential V, the following expression is to be solved,

$$d\left[\left(\frac{dV}{dx}\right)^2\right] = \frac{2}{\varepsilon_s}\rho(V)dV. \tag{4}$$

According to the described model of an ICB deposited Schottky diode, Fig. 4, the excess charge density discontinuously changes at the maximum Ag ions penetration length $x = L$ within the Si substrate. Consequently, the integration of the above expression is to be performed separately within each region such that $\rho = \rho_1(x) \rightarrow \rho_1(V)$ for $0 \le x \le L$ and $\rho = \rho_2(x) \rightarrow \rho_2(V)$ for $L \le x \le W$, where W is the width of the free carriers depletion range within the semiconductor. As usual we adhere to the approximation that $\rho = 0$ for $W \le x \le \infty$. Integration the expression, eq. (4), within the Ag enriched region of the Si semiconductor gives,

$$\left(\frac{dV}{dx}\right)^2_{x=L} - \left(\frac{dV}{dx}\right)^2_{x=0} = \frac{2}{\varepsilon_s}\int_{V_0}^{V_L}\rho_1(V)dV \tag{5}$$

from which it follows,

$$\left(\frac{dV}{dx}\right)_{x=0} = -\sqrt{\left(\frac{dV}{dx}\right)^2_{x=L} - \frac{2}{\varepsilon_s}\int_{V_0}^{V_L}\rho_1(V)dV} \tag{6}$$

and the minus sign is taken on account of potential V decrease with an increasing depth x. At this point it has to be mentioned that at $x=L$, due to the discontinuity of the excess charge density the electric potential V, while itself continuous, possesses the discontinuous derivatives.

Similarly, the integration of the eq. (4) within the range $L \le x \le W$, results in

$$\left(\frac{dV}{dx}\right)_{x=L} = -\sqrt{\frac{2}{\varepsilon_s}\int_{V_L}^{V_W}\rho_1(V)dV} \tag{7}$$

since due to potential being flat at the end of the depletion region $(dV/dx)_{x=W} = 0$ and once again the minus sign is taken on account of potential V decrease with an increasing distance x.

From the fig. 4. it is evident that the redistribution of space-charge due to the deep impurities present is expected to occur within the region $0 \le x \le L$ for small applied forward and reverse voltages. Specifically, for large forward U, all deep lying Ag^+ donors will be electrically neutral and the Ag^- acceptor states will be completely populated resulting in an effective decrease of the net positive space charge within this region. And conversely, for larger reverse applied voltages U the acceptor states are empty and the excess positive space charge $\rho_1(x)$ within the same region exceeds that of the normal conditions as provided by the phosphorous doping in n-Si substrate. Obviously, for each value of the silver ions concentrations N_{Ag} within this enriched region there exists an interval of the applied external voltage to which monotonically corresponds the space charge density variations $\rho_1(x)$ for $0 \le x \le L$. For this reason the electron potential energy $qV(x)$, for concentrations of electrically activated silver atoms N_{ag} large enough, may considerably vary for different values of the applied voltage and it is just this variation which presumably might be responsible for the observed C-V behavior of ICB deposited Schottky diodes. In order to compare the experimental I-V characteristics to the predicted ones based upon the model depicted in fig. 4., the detailed numerical evaluation of the electron potential $V(x)$, for $0 \le x \le W$, at each value of the applied external voltage U is required. This, however, is a subject of a future publication /13/. The general characteristics of the differential capaci-tance per unit area, C, of the model diode defined as,

$$C = \frac{\partial Q_d}{\partial V_d} \tag{8}$$

can be for the above case discussed in the sufficient particulars without adhering to such the detailed numerical procedures. In the eq. (8), the term ∂Q_d represents the infinitesimal change in the total charge per unit area due to all uncompensated electrically active impurities in the depletion region, which is occurring due to the ∂V_d, the infinitesimal change in the so called diffusion potential V_d. The diffusion potential, as well known,

is for an ordinary Schottky diode defined as the difference between the potential at the junction metal/semiconductor interface (i.e. x=0) and the potential evaluated at the edge of the depletion region, x=W, thus $V_d = V(x=0) - V(x=W)$.

In what follows we adhere to the approximation (termed the low frequency approximation) according to which occupations of donor or acceptor energy levels instantaneously respond to the capacitance measuring test small signal (alternating) voltage which is superimposed on an externally applied direct voltage bias.

Viewing fig. 4., the low frequency depletion-layer capacitance C per unit area can be evaluated as a resultant capacitance of two capacitors, C_1, and C_2, connected in series. In order to see this one introduces at x=L two connected, infinitely closely spaced, conducting plates. On account of induced charges appearing on each plate, the charges are equal in magnitude but of opposite signs. Consequently, one may immediately generalize,

$$C_i = \frac{\partial Q_i}{\partial V_{di}} \qquad i = 1,2 \tag{9}$$

where,

$$V_{d1} = V(x=0) - V(x=L) \tag{10}$$

and similarly

$$V_{d2} = V(x=L) - V(x=W), \tag{11}$$

respectively. From here onwards the following abbreviations; $V(x=0) = V_0$ and $V(x=L) = V_L$ will be adhered to.

The internal electric field in the semiconductor is oriented in the negative direction of x-axis from the edge of the depletion region (where V(x=W)=constant and consequently E=0) towards the metal/semiconductor interface junction. Applying the Gauss's law, $\oint DdS = \rho$, first on the surface of the cylinder placed between x=0 and x=L, and secondly on the surface of the one placed at x=L and x=W one obtains,

$$E_o - E_L = \frac{Q_1}{\varepsilon_s} \tag{12}$$

where Q1 denotes the excess charge density per unit (junction) area within the first, i.e. Ag enriched, region. Similarly, one obtains

$$E_L = \frac{Q_2}{\varepsilon_s} \tag{13}$$

yielding the two expressions to be evaluated as,

$$\left(\frac{dV}{dx}\right)_{x=L} - \left(\frac{dV}{dx}\right)_{x=0} = \frac{Q_1}{\varepsilon_s} \tag{14}$$

$$\left(\frac{dV}{dx}\right)_{x=L} = \frac{Q_2}{\varepsilon_s}. \tag{15}$$

The excess charge densities for the two regions remains to be defined. In the lowest approximation one writes, noting that the excess charge density per unit area of eq. (12), Q_1, is directly related to ρ_1 of the eq. (7) simply as $Q_1 = \rho_1/S$, and similarly for Q_2, where the net excess charge density in the region (1) is brought about by the electrically activated phosphorous shallow donors (of density N_P^+) in conjunction with the deep lying Ag (donor as well acceptor) impurity atoms of densities N_{Ag}^+ and N_{Ag}^-,

$$\rho_1 = q(N_p^+ + N_{Ag}^+ - N_{Ag}^-) \tag{16}$$

$$\rho_2 = q(N_p^+ - N_e^-(x=L)). \tag{17}$$

Here, $N_e^-(x=L)$ denotes the density of the displaced free carriers (i.e. electrons) at the edge of the enriched region, x=L /4/, but the rough estimate shows that this contribution can be, if one is not being interested in the C-V frequency dependence, in the first approximation, neglected. Generally speaking, this contribution also varies (on account of the electrical activation or deactivation of deep lying silver donors and acceptors) with the change of the applied external bias DC voltage. For the exact calculations, the shape of the conduction band in the vicinity around x=L has to be calculated in details. The probability, w(E), for donor or acceptor to be electrically activated is given by /3/,

$$w(E_d) = \frac{N_d^+}{N_d} = \frac{1}{1 + g_d e^{-(E_d - E_F)}} \tag{18}$$

where, E_d is the donor energy level (as defined with respect to the conduction, E_C, or alternatively valence energy band, E_V, respectively), E_F the Fermi energy in the semiconductor and g_d is the ground state degeneracy of the donor impurity level, equal to $g_d=2$. Obviously the factor $(1-w(E_d))$ is the probability, that the donor is not electrically activated. Similarly, the probability that the acceptor level is electrically active is provided by the expression,

$$w(E_a) = \frac{N_a^-}{N_a} = \frac{1}{1 + g_a e^{-(E_a - E_F)}} \tag{19}$$

where g_a, the ground state degeneracy factor is equal to $g_a=4$, for acceptor levels of energy E_a.

As schematically indicated on fig. 4, due to the metal/semiconductor junction potential barrier the elec-

tronic potential V(x), or equivalently the conduction band E_C, exhibits relatively strong curvature in the interval $0 \leq x \leq L$, consequently the energy difference of both activated impurities levels is a function of the potential V(x), i.e. the position along the x-axis of the activated impurity within (the silver enriched part of) the semiconductor. Written in terms of the potential V(x), this difference reads,

$$E_d - E_F = q(V_1(x) - V_m) - q\,U - z_d \qquad (20)$$

and similarly,

$$E_a - E_F = q(V_1(x) - V_m) - q\,U - z_a\ , \qquad (21)$$

where, z_d = 0.75 eV, and z_a = 0.40 eV, for Ag impurity levels within the Si bandgap, and the potential V(x) is now referred with respect to the metal Fermi level characterized by the potential, V_m, and U denotes the externally applied DC bias voltage, see fig. 4. The corresponding transformation for the shallow phosphorous donor level, valid throughout the region $0 \leq x \leq W$ (since, the P donor level never crosses the semiconductor quasi-fermi level) reads,

$$(E_d - E_F)_P = q(V_i(x) - V_m) - q\,U - z_0, \quad i=1,2 \qquad (22)$$

where z_0 = 0.05 eV.

Using the eqs. (6) and (7), the net charge density Q_1 in the region x being between 0 and L as obtained from eq. (14) reads,

$$Q_1 = \sqrt{2\varepsilon_s}\left[\sqrt{\int_{V_W}^{V_L}\rho_2(V)dV + \int_{V_L}^{V_0}\rho_1(V)dV} - \sqrt{\int_{V_W}^{V_L}\rho_2(V)dV}\right] \qquad (23)$$

and similarly for Q_2, one obtains,

$$Q_2 = \sqrt{2\varepsilon_s\int_{V_L}^{V_W}\rho_2(V)dV}. \qquad (24)$$

These expressions are to be evaluated using the eqs. (16) to (22). After the appropriate transformation of the integral limits, noting the relevant integrals can be easily evaluated, the results are given by,

$$I_1(V_{d1}) = \int_{V_L}^{V_0}\rho_1(v)dV = \int_{V_0}^{V_{d1}}\rho_1(s+V_L)ds =$$

$$= q\left\{N_{d,Ag}\left[V_{d1} - \frac{1}{\beta q}\ln\frac{1+b_1e^{\beta qV_{d1}}}{1+b_1}\right] + N_{d,P}\left[V_{d1} - \frac{1}{\beta q}\ln\frac{1+b_2e^{\beta qV_{d1}}}{1+b_2}\right] - N_{a,Ag}\left[V_{d1} - \frac{1}{\beta q}\ln\frac{1+b_3e^{\beta qV_{d1}}}{1+b_3}\right]\right\} \qquad (25)$$

where the symbols b_i, (i=1,3) stand for the following functions,

$$b_1 = g_{d,Ag}\, e^{\beta q(U-\phi_b)}\, e^{\beta z_d} \qquad (26)$$

$$b_2 = g_{d,P}\, e^{\beta q(U-\phi_b)}\, e^{\beta z_0} \qquad (27)$$

$$b_3 = g_{a,Ag}\, e^{-\beta q(U-\phi_b)}\, e^{-\beta z_a}. \qquad (28)$$

In the transformations above, the following relation has been used, $V_{d1} = V_0 - V_L = \phi_b - U - V_L$, fig. 4, where ϕ_b, is the Schottky barrier height.
Likewise, the evaluation of the second integral yields,

$$I_2(V_{d2}) = \int_{V_W}^{V_L}\rho_2(V)dV = \int_0^{V_{d2}}\rho_2(s+V_W)ds =$$

$$= qN_{d,P}\left[V_{d2} + \frac{1}{\beta q}\ln\frac{1+b_4e^{-\beta qV_{d2}}}{1+b_4}\right] \qquad (29)$$

and b_4 is given by,

$$b_4 = g_{d,P}\, e^{-\beta q\xi}\, e^{-\beta z_0} \qquad (30)$$

In the derivation the relation, $V_{d2} = V_L - V_W = V_L - (U + \xi)$, where $\xi = (kT/q)\ln(N_C/N_d)$, and N_C is the effective density of states in the conduction band has been employed.

Finally, performing the indicated operations as suggested by the eq. (9), noting that $Q_1 = Q_1(V_{d1}, V_{d2}, V_d)$, where the diffusion potentials are defined by the eqs. (10), (11), consequently

$$\frac{\partial Q_1}{\partial V_{d1}} = -\frac{\partial Q_1}{\partial V_L} + \frac{\partial Q_1}{\partial V_{d2}} = \frac{\partial Q_1}{\partial V_0} - \frac{\partial Q_1}{\partial V_d} = \text{etc.},$$

the following capacitance's per unit area are derived:

$$C_1 = q\sqrt{\frac{\varepsilon_s}{2}}\;\frac{\dfrac{N_{d,Ag}}{1+b_1e^{\beta qV_{d1}}} + \dfrac{N_{d,P}}{1+b_2e^{\beta qV_{d1}}} - \dfrac{N_{a,Ag}}{1+b_3e^{-\beta qV_{d1}}}}{\sqrt{I_1(V_{d1}) + I_2(V_{d2})}} \qquad (31)$$

and similarly,

$$C_2 = q\sqrt{\frac{\varepsilon_s}{2}}\;\frac{\dfrac{N_{d,P}}{1+b_4e^{-\beta qV_{d2}}}}{\sqrt{I_2(V_{d2})}}. \qquad (32)$$

The resultant low frequency capacitance, C, of the ICB deposited Ag/n-Si(111) Schottky diode is than obtained as,

$$\frac{1}{C}=\frac{1}{C_1}+\frac{1}{C_2}. \qquad (33)$$

The expressions as given by eqs. (31) and (32) are the central result of the present calculations. One notes that they have been derived without an explicit solution of the Poisson equation, eq. (1). For the interpretation of the I-V measurements, this equation has to be, however, solved explicitly.

3. Results and discussion

On account of complicated expressions as provided by eqs. (31) and (32), it is not self evident in general, that the C^{-2} versus externally applied DC voltage U should yield the straight line. Since the electron potential at x=L, i.e. V_L, is itself an implicit function of the applied bias voltage U, the linear relation obviously is expected to be an exception rather than a rule. However, the above derived results can be simply checked in the limit of very low concentrations of silver impurities in Si substrate as compared to phosphorous concentration doping, i.e. $N_P >> N_{a,Ag}$ and $N_{d,Ag}$, In the lowest approximation (neglecting the Ag impurities in Si substrate), $\rho_1(V) = \rho_2(V) = \rho(V)$, and one therefore obtains from the eq. (23),

$$Q_1=\sqrt{2\varepsilon_s}\left[\sqrt{\int_{V_W}^{V_0}\rho(V)dV}-\sqrt{\int_{V_W}^{V_L}\rho(V)dV}\right] \qquad (34)$$

and likewise,

$$Q_2=\sqrt{2\varepsilon_s\int_{V_L}^{V_W}\rho(V)dV}. \qquad (35)$$

In this limit the depletion capacitance of a Schottky diode if evaluated at L = 0, i.e. when $V_L = V_0$, yields $Q_1 \equiv 0$, consequently $C_1 = 0$, and the resulting capacitance is given by,

$$C\equiv C_2=\sqrt{\frac{q\varepsilon_s N_{d,P}}{2V_d}} \qquad (36)$$

where $V_d = V_0 - V_W$. This is, however, the exact result /3/ for the depletion capacitance of on ordinary Schottky diode, as expected. Setting now the opposite limit, i.e. L=W, hence $V_L=V_W$, only the first term in eq. (34) survives, Q_2, and consequently $C_2 = 0$, and the resulting capacitance C is once again written in terms of the right side of the expression (36), as it should in the presence of only one homogeneously distributed shallow donor in a semiconductor.

On account of the discussion just presented above it is now possible to offer rather an obvious explanation of the experimental observation concerning the low frequency C-U measurements of Schottky diodes deposited for small values of the ionized silver atoms acceleration voltage $U_a < 0.6$ keV, (say), by the ionized cluster beam, IBC, deposition method. Apparently, as follows from the stopping power calculations, for these small acceleration voltages the penetration range of Ag ions in Si is small, $L \approx 0$, $V_L \approx V_0$, and consequently $C_1 \approx 0$. The resulting capacitance, C, is then given by the eq. (36) and since,

$$V_d = V_0 - V_W = \Phi_b - U - \xi \qquad (37)$$

where $q\Phi_b = 0.78$ eV, is the Schottky potential barrier height /3/ and $q\xi$ is the energy difference between the semiconductor quasi fermi level and the conduction band, E_C, at the position $x \geq W$, the edge of the depletion region ($q\xi = kT \ln(N_C/N_d)$ and N_C is the effective density of states in the conduction band). Consequently, combining eqs. (36) and (37) the usual linear C^{-2} versus U relationship is obtained, in accordance with the C-U measurements for $U_a = 0$ and 300 V samples, as indicated on fig. 3., respectively. Some relevant examples of the low frequency C-U relationships, calculated for the various values of the deep level impurity concentrations, taking the potential, V_L, as an independent parameter, are explicitly exhibited on figs. 5-7.

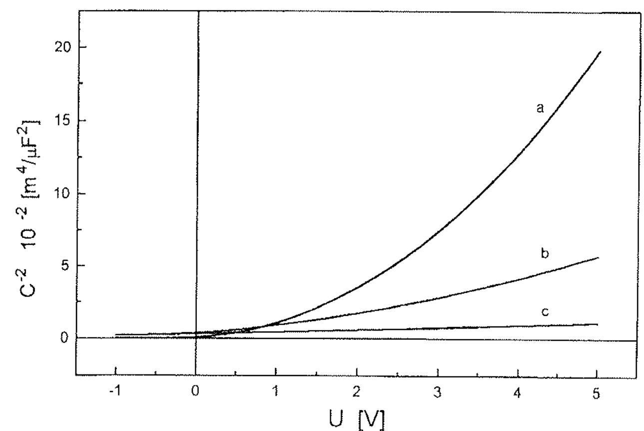

Fig. 5. The calculated values of the resulting capacitance, $1/C^2$, based on the eq. (33) of the text, versus the external applied DC bias, U, is presented for various values of the parameters. The lines shown are calculated for the following values of parameters expressed in terms of the constant $N_o=10^{16}$ cm^{-3}:
line a) $V_L=0.45$ V, $N_{d,Ag}=10\ N_o$, $N_{d,P}=1\ N_o$, $N_{a,Ag}=40\ N_o$;
line b) $V_L=0.65$ V, $N_{d,Ag}=10\ N_o$, $N_{d,P}=1\ N_o$, $N_{a,Ag}=40\ N_o$;
line c) $V_L=0.65$ V, $N_{d,Ag}=0$, $N_{d,P}=1\ N_o$, $N_{a,Ag}=0$.
The latter curve represents the usual case of the homogeneously doped metal/Si semiconductor junction.

For the discussion of C-U relationship at large values of Ag ions acceleration voltages, one has to adhere to the full numerical analysis, originating from the exact solution of the Poisson equation /13/.

Nevertheless, the simplified model, as depicted on fig. 4., of ICB deposited Ag/Si diodes might possibly provide a direction towards understanding of the findings presented in ref. /6/, where an unusual feature was reported. Namely, applying the usual I-V evaluation procedure /14/ on the raw experimental data, it was found, quite contrary to the expectations, that the ideal-

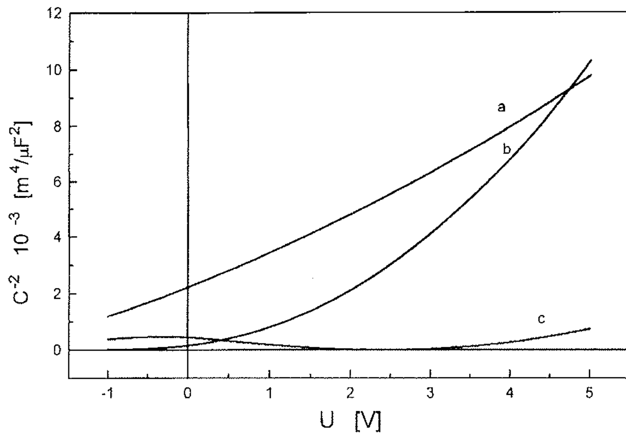

Fig. 6. The calculated values of the resulting capacitance, $1/C^2$, based on the eq. (33) of the text, versus the external applied DC bias, U, is presented for various values of the parameters. The lines shown are calculated for the following values of parameters, expressed in terms of the constant $N_o=10^{16}$ cm^{-3}: line a) $V_L=0.45$ V, $N_{d,Ag}=0$, $N_{d,P}=1$ N_o, $N_{a,Ag}=0$; (the curve represents the usual case of the homogeneously doped metal/Si semiconductor junction); line b) $V_L=0.45$ V, $N_{d,Ag}=1$ N_o, $N_{d,P}=1$ N_o, $N_{a,Ag}=40$ N_o; line c) $V_L=0.45$ V, $N_{d,Ag}=10$ N_o, $N_{d,P}=1$ N_o, $N_{a,Ag}=100$ N_o.

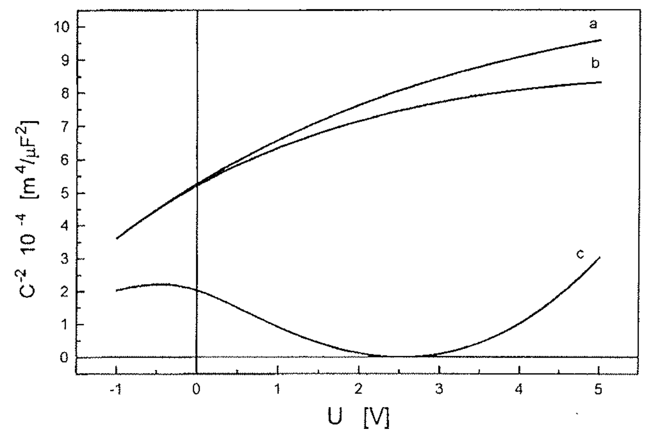

Fig. 7. The calculated values of the resulting capacitance, $1/C^2$, based on the eq. (33) of the text, versus the external applied DC bias, U, is presented for various values of the parameters. The lines shown are calculated for the following values of parameters, expressed in terms of the constant $N_o=10^{16}$ cm^{-3}: line a) $V_L=0.45$ V, $N_{d,Ag}=0.3$ N_o, $N_{d,P}=1$ N_o, $N_{a,Ag}=90$ N_o; line b) $V_L=0.45$ V, $N_{d,Ag}=0$, $N_{d,P}=1$ N_o, $N_{a,Ag}=90$ N_o; line c) $V_L=0.45$ V, $N_{d,Ag}=2$ N_o, $N_{d,P}=1$ N_o, $N_{a,Ag}=60$ N_o. Note that the shape of the calculated curves exhibits different curvatures, depending upon the values of parameters.

ity factor, n, as well as the series resistance, R_s, are bias dependent. The results of an alternative, rather involved and more general, analysis /15/ seem to support the above findings. One notes, that the results of ref. /6/, are based upon the assumption, that the n-Si enriched region is characterized by the constant density of electrically activated silver donors throughout the whole interval of bias investigated. Now, according to the model of fig. 4, this assumption is certainly no longer valid; for forward biases, due to the increasing density of activated acceptor silver impurities accompanied by the corresponding density decrease of the Ag^+ donors, the net excess space charge within $0 < x < L$ interval ought to be bias dependent and at all times smaller than if only shallow donor P impurities would have been present. Consequently, the series resistance ought to be bias dependent all the way up to its given upper limit above which the net space charge ought to remain constant. Similar characteristic feature, but in the reversed order, is expected to exists for the case of an applied reverse bias. This behavior would be expected to appear always, providing the enriched range exceeds certain minimal L_{min} and/or certain minimal Ag impurities densities, which are yet to be determined and thoroughly investigated. Strictly speaking, the presented ICB Ag/n-Si structures consequently may not be truly considered to be a typical representative of an ordinary Schottky metal/semiconductor diodes.

The measured strong temperature I-U dependency /4/ of the ICB deposited Ag/n-Si(111) Schottky diodes might now be possible, on the basis of the proposed model exhibited on fig. 4., to assign primarily to the effect of the strong temperature dependent activation of the additional Ag donors and acceptors rather than (in conjunction with the variation of P donors activation) to the direct 1/kT variation itself.

There exists another very important feature which deserves a comment. Namely, as reported in ref. /4/ and /6/ the *effective* Schottky barrier height presumably decreases with an increased silver ions acceleration voltage Ua in clear disagreement with the DIGS model prediction of the strong Fermi level pining at the metal/semiconductor interface for all cases of strong disorders of a semiconductor interface region. Consequently, as DIGS model is generally considered to work well in clear cases of interface disorders, and as an ICB deposition method is certainly expected to produce just such an effect, the question how the effective Schottky barrier is related to the true Schottky barrier height is an important question which still requires to be answered.

4. Conclusions

The low frequency capacitance- voltage, C-U, relationship of ionized cluster beam, ICB, deposited Ag/n-Si(111) Schottky diodes for nonzero acceleration voltage of the silver ions, has been investigated on the basis of the postulated model of the semiconductor energy bands. In the derivation the fundamental assumptions made is the homogenous, spatially limited distribution, laying within the semiconductor energy gap, of the bias voltage dependent activated deep Ag

donor and acceptor impurities energy levels. These are (in addition to the shallow phosphorous donor level throughout the Si sample) spatially confined within the Si region extending up to the maximal silver ions penetration length L, which is a function of the silver acceleration voltage Ua. It is argued, that it is only for small values of L and/or small Ag impurity concentrations, within the described impurity additionally enriched semiconductor region, that the C-U relation is expected to exhibit the linear relationship, in accordance with the measurements.

The previously observed bias dependence of the semiconductor series resistance, at constant temperature, as well as the strong temperature dependency of the previously reported I-U measurements, are being phenomenologically explained in terms of the proposed model.

The effects of the additional, within the Si energy gap placed impurity levels arising on account of surface atoms, like O, C, N and traces of S, to be in the process of the Ag impact also transferred into the semiconductor, have been neglected. These impurities may contribute to the additional space charge within the Ag enriched n-Si region, but very likely their importance, as traps, ought to be taken into account if one is concerned with C-V frequency dependency. However, their possible effect, as microcluster formations, on the Schottky barrier height formation, in a sense as first proposed by Freeouf and Woodall /16/, is not to be neglected.

It is argued, that the relationship of the disordered (due to Ag and surface atoms) enriched semiconductor layer (at small penetration lengths L), on the Fermi level pinning and consequently on the DIGS implications concerning the metal/semiconductor junction, might be most conveniently investigated by carefully controlled and suitably designed ICB experiments in UHV conditions.

Acknowledgment

The endeavors of Mess. M. Ko'elj, T. Mrđen, F. Moškon, E. Krištof and D. Korošak, at the Division of Reactor Physics, in the course of very involved ionized cluster beam experiments and data treatment, as well as to Professor A. Levstek and M. Sc. C. Filipič at the Condensed Matter Physics Division of the "J. Stefan" Institute, for having made the equipment available and for helping us in C-V measurements, are all greatly appreciated. The acknowledgment is also due to M. Sc. R. Jecl, Faculty of Engineering, for numerical evaluations serving as a basis for some of the arguments presented in this presentation.

5. References

/1/ T. Takagi, Vacuum 36, (1986) 27.

/2/ W. L. Brown, M.F. Jarrold, R.L.McEachern, M. Sosnowski, G. Takaoka, H. Usui and I. Yamada, Nucl. Instr. and Meth. in Phys. Research, B59, (1991) 182.

/3/ S.M. Sze in Physics of Semiconductor Devices, 2nd Edition, John Wiley & Sons, New York (1981).

/4/ B. Cvikl and T. Mrdjen, Fizika, A4, (1995) 2, 403.

/5/ F. A. Padovani and R. Stratton, Solid-State Electron. 9, (1966) 695, see also C. R. Crowell and V. L. Rideout, Solid-State Electron., 12, (1969) 89. The discussion of their results is also presented in the reference /12/.

/6/ B. Cvikl, Zs. J. Horvath, T. Mrđen, 23rd International Conference on Microelectronics, MIEL'95 and 31st Simposium in Devices and Materials, SD'95, Proceedings, p. 391 -396. September 27.-29, 1995, Terme Čatež, Slovenia.

/7/ T. Takahagi, I. Nagai, A. Ishitani, H. Kuroda, Y. Nagasawa, J. Appl. Phys. 64 (1988) 3516.

/8/ J. F. Ziegler, J. P. Biersack and U. Littmark in The Stopping and Range of Ions in Solids, Pergamon Press, New York, (1985).

/9/ H. Hasegawa and Hideo Ohno, J. Vac. Sci. Technol., B 4, (1986) 1130, see also K. Koyanagi, S. Kasai and H. Hasegawa, Jpn. J. Appl. Phys., 32, (1993) 502.

/10/ R. R. Senechal and J. Basinski, J, Appl. Phys., 19, (1968) 3723.

/11/ G. I. Roberts and C. R. Crowell, J. Appl. Phys., 41, (1970) 1767.

/12/ E.H. Rhoderic and R.H. Williams in Metal-Semiconductor Contacts, 2nd Edition, Clarendon Press, Oxford, (1988).

/13/ T. Mrdjen, B. Cvikl and D. Korošak, to be published.

/14/ S.K. Cheung and N.W. Cheung, Appl. Phys. Lett., 49, (1986) 85.

/15/ D. Donoval, M. Barus and M. Zdimal, Solid-State Electronics, 34, (1991) 1365.

/16/ J. L. Freeouf, J. Woodall, J. Appl. Phys. Letts, 39, (1981) 727.

Dr. Bruno Cvikl
Fakulteta za gradbeništvo, Univerza v Mariboru,
Smetanova 17, 2000 Maribor, ali
Institut "J. Stefan", Univerza v Ljubljani,
Jamova 39,1000 Ljubljana
Tel.: +386 (0)61 188 54 50
Fax: (0)61 374-919;
Email: bruno.cvikl@ijs.si

Prispelo (Arrived): 31.5.1996 ***Sprejeto (Accepted): 18.6.1996***

UDK 621.3:(53+54+621+66), ISSN0352-9045 Informacije MIDEM 26(1996)2, Ljubljana

IZVEDBA NEREKURZIVNEGA DIGITALNEGA SITA S STANDARDNIMI INTEGRIRANIMI KOMPONENTAMI V MODIFICIRANI OBLIKI PORAZDELJENE ARITMETIKE

K. Korošec, A. Vesenjak, B. Jarc, M. Solar, R. Babič
Fakulteta za elektrotehniko, računalništvo in informatiko, Univerza v Mariboru
Maribor, Slovenija

Ključne besede: DSP procesiranje signalov digitalno, filtri digitalni, filtri nerekurzivni, FIR filtri s trajanjem omejenim impulza odzivnega, filtri digitalni s trajanjem omejenim impulza odzivnega, izvedbe praktične, aritmetika porazdeljena, koeficienti v aritmetiki porazdeljeni, deli sestavni integrirani standardni, CMOS vezja EPROM pomnilniki, H CMOS vezja hitra, frekvence vzorčenja

Povzetek: V članku je opisana izvedba univerzalne strukture nerekurzivnega digitalnega sita s 15 koeficienti v porazdeljeni aritmetiki s standardnimi integriranimi komponentami. Pri tem smo uporabili novi modificirani postopek izračunavanja delnih vsot koeficientov, ki omogoča povečanje dinamičnega območja izhodnega signala vsaj za 6 dB, obenem pa dosežemo tudi zmanjšanje aparaturne kompleksnosti strukture. Pri uporabi standardnih hitrih CMOS vezij in nezahtevnega EPROM pomnilnika za shranjevanje vnaprej izračunanih delnih vsot koeficientov smo pri 12-bitni kvantizaciji vhodnega signala dosegli frekvenco vzorčenja fv=143 kHz. S simulacijskimi rezultati smo ilustrirali povečanje dinamičnega območja izhodnega signala po predlaganem modificiranem postopku izvedbe porazdeljene aritmetike, prikazana pa je tudi primerjava med teoretičnimi, simulacijskimi in merilnimi rezultati frekvenčnih karakteristik nizkoprepustnih in visokoprepustnih digitalnih sit, ki smo jih načrtali s programskim paketom DF-PAK.

The FIR Digital Filter Realization with Standard Integrated Circuits in the Modified Distributed Arithmetic Structure

Keywords: DSP, digital signal processing, digital filters, nonrecursive filters, finite impulse response digital filters, practical implementations, distributed arithmetic, coefficients in distributed arithmetic, standard integrated components, CMOS circuits, EPROM, H CMOS circuits, sample frequencies

Abstract: In this article the hardware realization of 15 tap general FIR digital filter structure with standard integrated circuits for the implementation of digital filters with arbitrary frequency responses is presented. A new modified distributed arithmetic structure is used for the computation of output signal sequence with the purpose to increase the dynamic range of output signal. Apart from concentrated arithmetic mechanization where the output sample calculation is determined with the sum of products of two vectors, the distributed arithmetic technique permits this calculation only with summing and shifting operations of the precalculated partial sums of the coefficients. When the bipolar input signal is converted into unipolar form the offset binary format of input samples is obtained. In this way a new approach to the modified partial products calculations is necessary. Then the output sample calculation is also distinguished from the classical distributed arithmetic technique in one significant step that in the last calculation step no subtraction is needed.

Our digital filter is realized in the structure with 12 bits analog to digital and digital to analog conversion for input and output signals, 14 bit memory register length for partial sums of coefficients presentation in look up table and with 16 bits register length of arithmetic unit. With standard H CMOS circuits and EPROM memory with access time of 200 ns the sample frequency of 143 kHz is obtained. As this structure is also suitable for FPGA implementation, higher sampling frequencies are expected. In comparison with classical distributed arithmetic structure the increasing of 6 to 8 dB of the dynamic range of output signal is obtained. This increasing depends slightly on the number of digital filter coefficients and on parameters of predetermined frequency characteristics. Filter coefficients are designed with digital filter design software DF-PAK. The frequency responses with theoretical, simulated and measured results for low pass and high pass digital filter implementations are also presented.

1. Uvod

Pri aparaturni izvedbi digitalnih sit, je pomembna izbira realizacijske oblike. Osnovni kriteriji, ki vplivajo na izbiro, so: - dobro ujemanje med teoretičnimi in želenimi oziroma zahtevanimi lastnostimi, - čim manjši vpliv kvantizacije na spremembo frekvenčnih karakteristik in velikost šumnega signala na izhodu, - mala aparaturna kompleksnost ter - velika hitrost delovanja. Porazdeljena aritmetika ali ROM akumulator struktura /1, 2/ predstavlja določen prispevek pri izbiri izvedbene oblike. Posebej je zanimiva zaradi manjše in nezahtevne aparaturne kompleksnosti, tako da postaja aktualna za izvedbo tudi s programabilnimi polji logičnih vrat.

S porazdeljeno artimetiko je označen postopek izračunavanja skalarnega produkta dveh vektorjev na elementarnem bitnem nivoju brez uporabe običajnih množilnikov, tako da ga lahko s pridom izkoristimo pri izvedbi nerekurzivnih digitalnih sit. Nerekurzivna digitalna sita so zaradi dodelanih postopkov načrtovanja,

svoje enostavnosti in predvsem linearnega faznega pomika zelo zanimiva za področje digitalne obdelave signalov.

Za nerekurzivno digitalno sito zapišemo odziv *y(k)* v obliki konvolucijske enačbe

$$y(k)=\sum_{n=0}^{N-1} h(n)\,x(k-n)\,, \qquad (1.1)$$

ki ima tudi obliko skalarnega produkta dveh vektorjev $\mathbf{y} = \mathbf{h}^T \cdot \mathbf{x}$. S h(n), n = 0, 1, ... , N-1 je označena končna sekvenca N koeficientov impulznega odziva, ki obenem določa vektor koeficientov nerekurzivnega digitalnega sita h, z x(k-n) pa je označena sekvenca časovnih odtipkov vhodnega signala, ki določajo komponente vektorja x.

2. Porazdeljena aritmetika in modificirani izračun delnih vsot koeficientov

Če so vrednosti vhodnega signala x(k) omejene na intervalu [-1, +1], jih lahko zapišemo tudi v dvojiški binarni obliki s končno dolžino besede B_X bitov

$$x(k-n)=-b_0(k-n)+\sum_{i=1}^{B_X-1} b_i(k-n)\cdot 2^{-i}, n=0,1,\ldots N-1. \qquad (2.1)$$

Z $b_i(k-n)$ so označene binarne spremenljivke, ki zavzemajo vrednosti 0 ali 1, pri tem je $b_0(k-n)$ najbolj utežni bit, ki predstavlja predznak, $b_{Bx-1}(k-n)$ pa je najmanj utežni bit.

S povezavo obeh izrazov po enačbah 1.1 in 2.1 dobimo osnovo za izračun trenutne vrednosti izhodnega signala za nerekurzivno digitalno sito po principu porazdeljene aritmetike /2/.

$$y(k)=-\sum_{n=0}^{N-1} h(n)\cdot b_0(k-n)+\sum_{i=1}^{B_X-1}\sum_{n=0}^{N-1} h(n) b_i(k-n)2^{-i} \qquad (2.2)$$

Če z

$$v_i(k)=\sum_{n=0}^{N-1} h(n) b_i(k-n) \qquad (2.3)$$

označimo delne vsote koeficientov, ki predstavljajo vmesni korak pri računanju y(k), dobimo poenostavljeno obliko zapisa izračunavanja izhodnih vrednosti v obliki

$$y(k)=-v_0(k)+\sum_{i=1}^{B_X-1} v_i(k)2^{-i}\,. \qquad (2.4)$$

Pri uporabi konstantnih koeficientov digitalnega sita so delne vsote odvisne le od nabora N binarnih spremenljivk $b_i(k-n)$. Za določitev trenutne izhodne vrednosti potrebujemo le postopek seštevanja (odštevanja) in množenja z 2^{-i}. Za seštevanje uporabimo seštevalnike, ki so dovolj enostavna in hitra vezja, za odštevanje je potrebno posebej tvoriti dvojiški komplement, množenje z 2^{-i} pa se preprosto izvaja s pomikom vsebine v aritmetični enoti za i-bitov in z zakasnilnimi elementi T. Zaradi pridobitve na hitrosti odziva vse možne delne vsote koeficientov običajno izračunamo vnaprej in jih zapišemo v pomnilnik vrste ROM, njihove vrednosti pa pri izračunu izhodnih vrednosti sproti določa naslovni vektor vhodnih spremenljivk, ki ga definiramo z vhodnim poljem. Na sliki 2.1 je prikazana bločna shema osnovne strukture nerekurzivnega digitalnega sita v porazdeljeni aritmetiki.

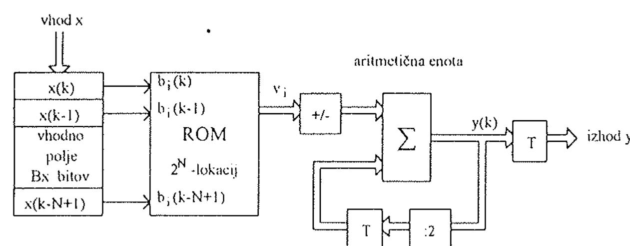

Slika 2.1: Osnovna struktura nerekurzivnega digitalnega sita v porazdeljeni aritmetiki

V tabeli 2.1 so prikazane delne vsote koeficientov $v_i(k)$ v odvisnosti od naslovnega vektorja brez upoštevanja potrebnega normiranja.

Tabela 2.1: Delne vsote koeficientov pri osnovni strukturi porazdeljene aritmetike

	naslovni vektor	$v_i(k)$
0	0...000	0
1	0...001	h_0
2	0...010	h_1
3	0...011	h_0+h_1
4	0...100	h_2
.	.	.
.	.	.
2^{N-1}	1...111	$h_{N-1}+h_{N-2}+\ldots+h_0$

Ker raste število delnih vsot koeficientov eksponentov s številom koeficientov sita N, potrebujemo pomnilnik z 2^N pomnilniškimi lokacijami. Pri današnjem stanju tehnologije je neekonomično izvajati sita z N≥21 koeficienti impulznega odziva. V našem primeru smo izbrali kompromisno rešitev z N = 15, pri čemer potrebujemo ROM s kapaciteto 32 K x 16 bitov.

Pri dvojiškem zapisu vhodnega signala je v vhodnem polju z 1000 ... 0 zapisana najmanjša (negativna) vred-

nost, z 0111 ... 1 pa največja (pozitivna) binarna vrednost.

Modificirano obliko porazdeljene aritmetike dobimo, če pred vpisom v vhodno polje vhodni bipolarni signal pretvorimo v unipolarno obliko

$$x_p(k-n)=\sum_{i=0}^{B_x-1} b_i(k-n)2^{-i} \quad n=0,1,\ldots N-1. \quad (2.5)$$

Tedaj preide izraz za izračunavanje izhodnega signala po enačbi 2.4. v

$$y(k)=y_m(k)=\sum_{i=0}^{B_x-1} v_{im}(k)\cdot 2^{-i}, \quad (2.6)$$

pri čemer so z $v_{im}(k)$ označene modificirane vrednosti delnih vsot koeficientov /3/.

S primerjavo izrazov pod enačbama 2.4 in 2.6 vidimo, da v slednjem primeru ne potrebujemo več posebnega postopka odštevanja v aritmetični enoti. S tem se zmanjša kompleksnost prikazane strukture na sliki 2.1, obenem pa se še izognemo možnosti prelivanja vmesnih rezultatov preko normirane vrednosti ena v aritmetični enoti pred končnim odštevanjem vrednosti $v_0(k)$.

Zaradi spremenjenih vrednosti vhodnega signala v vhodnem polju je potrebno delne vsote koeficientov simetrirati in normirati. Postopek simetriranja je odvisen od vrste uporabljene frekvenčne karakteristike sita in ga izvedemo za vsako sito posebej. Modificirane delne vsote koeficientov $v_{mi}(k)$ so prikazane v tabeli 2.2.

Tabela 2.2: Delne vsote koeficientov pri modificirani obliki porazdeljene aritmetike.

	naslovni vektor	$v_{mi}(k)$
0	0...000	$1/2(-h_0-h_1-h_2-\ldots-h_{N-1})$
1	0...001	$1/2(+h_0-h_1-h_2-\ldots-h_{N-1})$
2	0...010	$1/2(-h_0+h_1-h_2-\ldots-h_{N-1})$
3	0...011	$1/2(+h_0+h_1-h_2-\ldots-h_{N-1})$
4	0...100	$1/2(-h_0-h_1+h_2-\ldots-h_{N-1})$
	.	
	.	
2^{N-1}	1...111	$1/2(+h_0+h_1+h_2+\ldots+h_{N-1})$

Novo modificirano strukturo porazdeljene aritmetike pri izvedi nerekurzivnih digitalnih sit kaže bločna shema na sliki 2.2. Na vhodni strani je sicer potreben dodatni pretvornik bipolarnega signala v unipolarno obliko, zato pa se izognemo postopku odštevanja delnih vsot koeficientov, ki jih določa naslovni vektor najbolj utežnih bitov v vhodnem polju pri izračunu vsakokratne trenutne izhodne vrednosti.

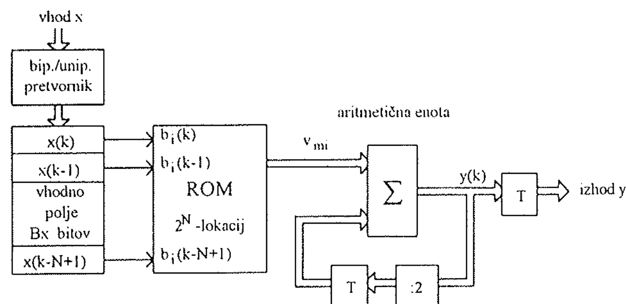

Sl. 2.2: Digitalno sito v modificirani obliki porazdeljene aritmetike

Pri skrbnem simetriranju in normiranju modificiranih delnih vsot koeficientov dosežemo povečanje dinamičnega območja izhodnega signala za najmanj 6 dB. Primerjavo simulacijskih rezultatov frekvenčnih karakteristik nizkoprepustnega sita s petnajstimi koeficienti po klasičnem in modificiranem postopku porazdeljene aritmetike kaže slika 2.1.

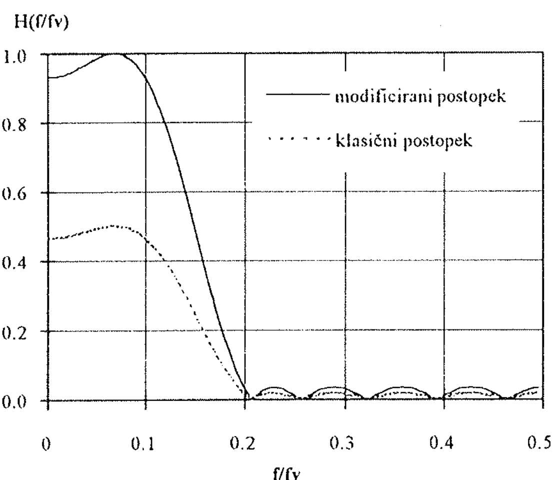

Slika 2.3: Primerjava frekvenčnih odzivov nizkoprepustnega sita s petnajstimi koeficienti po klasičnem in modificiranem postopku

Izhodni signal iz nove strukture je tudi unipolarne oblike, vendar imamo tudi na izhodu na voljo več enostavnih postopkov za njegovo spremembo v običajno bipolarno obliko.

3. Izvedba

Digitalno sito v modificirani porazdeljeni aritmetiki smo izvedli v laboratorijski obliki s standardnimi integriranimi komponentami. Zasnova vezja je univerzalna, tako da omogoča realizacijo nerekurzivnih digitalnih sit s 15 koeficienti s poljubno frekvenčno karakteristiko.

Za pretvorbo analognega signala v digitalno obliko smo izbrali 12-bitni A/D pretvornik MAX 122, ki omogoča vzorčenje signala z maksimalno vrednostjo f_{vmax} = 333 kHz = 1/T. Pretvorbo binarnega vhodnega signala x(k)

v unipolarno obliko smo izvedli z invertiranjem najbolj uteżnega bita. Tako pretvorjen signal vodimo preko 12-bitnega vzporedno-zaporednega pomičnega registra v zaporedni pomični register vhodnega polja z velikostjo 180 bitov. Sestavili smo ga iz CMOS gradnikov HCT 164. Vsebina vhodnega polja v trenutku $t = kT$ določa toliko različnih naslovnih vektorjev kot je število bitov vhodne binarne besede $B_x = 12$.

Za usklajeno delovanje skrbi krmilno vezje s kvarčnim oscilatorjem $f_0 = 2$ MHz, ki generira vse potrebne časovne signale: - osnovne urine impulze u_1, - invertirane urine impulze u_2, - impulze za startanje analogno-digitalne pretvorbe u_3, - za čitanje vrednosti A/D pretvornika v vzporedno zaporedni pretvorik u_4, - za krmiljenje vhodnega polja u_5, - za brisanje stare vrednosti iz zadrževalnih celic aritmetike u_6 ter - za krmiljenje izhodnih zadrževalnikov u_7. Časovne poteke signalov iz krmilnega vezja prikazuje slika 3.1.

Osrednji del strukture je pomnilnik za shranjevanje delnih vsot koeficientov. Uporabili smo dve EPROM vezji 27256 saj potrebujemo pomnilnik s kapaciteto $2^{15} \times 14$ bitov. Za zapis delnih vsot koeficientov smo uporabili 14 bitov. Vsebina EPROM pomnilnika določa obliko frekvenčne odvisnosti izhodnega signala. Programski paket BRUMEC /3/ omogoča natačni izračun delnih vsot koeficientov, 14-bitno kvantizacijo pa smo opravili pred vpisom v pomnilnik.

Aritmetično logična enota je sestavljena iz seštevalnega in zadrževalnega vezja. Zaradi zmanjšanja vplivov pogreška kvantizacije aritmetične enote na izhodni signal smo uporabili 16-bitno strukturo. Osnovni gradniki so 4-bitni seštevalniki 4008. Vezje izvaja postopek seštevanja in deljenja z dve. To je izvedeno med posameznimi seštevanji s pomikom vsebine v desno, postopek krmili negirana osnovna ura u_2. Po dvanajstih seštevanjih je zaključen izračun trenutne izhodne vrednosti y(k). Na izhodu seštevalnika se pojavi 16-bitni

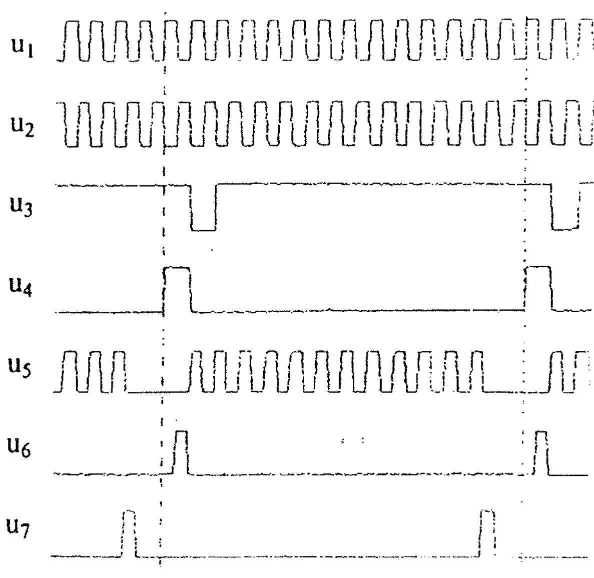

Slika 3.1: Časovni poteki signalov iz krmilnega vezja

Tabela 3.1: Koeficienti nizkoprepustnega in visokoprepustnega digitalnega sita

h(n)	nizkoprepustno sito $f_p=0,1\ f_v$; $f_z=0,2\ f_v$	visoko prepustno sito $f_z=0,2\ f_v$; $f_p=0,3\ f_v$
h(0)=h(14)	0.132637E-01	0.264990E-01
h(1)=h(13)	-0.227501E-01	-0.133865E-05
h(2)=h(12)	-0.447545E-01	-0.440890E-01
h(3)=h(11)	-0.380495E-01	-0.202039E-06
h(4)=h(10)	0.271117E-01	0.934248E-01
h(5)=h(9)	0.141917E+00	-0.518952E-06
h(6)=h(8)	0.254379E+00	-0.313903E+00
h(7)	0.301295E+00	0.500000E+00

podatek. Ker smo na izhodu uporabili 12-bitni pretvornik digitalnega v analogni signal MAX 507 smo uporabili le dvanajst najbolj uteženih bitov $b_{15}, b_{14}, ... b_4$. Vezalno shemo celotne strukture prikazuje slika 3.2.

Pri izbrani frekvenci urinih impulzov smo ob dvanajst bitni kvantizaciji vhodnega signala dosegli pri izvedeni strukturi frekvenco vzorčenja $f_v = 143$ kHz. Z uporabo vezij večje stopnje integracije ali s programabilnimi polji logičnih vrat bi zaradi zmanjšanja vplivov ožičevanja elementov, zlahka to vrednost frekvence še povečali.

Izvedeno univerzalno strukturo digitalnega sita za 15 koeficientov v modificirani obliki porazdeljene aritmetike smo uporabili za prikaz vezja z nizkoprepustno in visokoprepustno frekvenčno karakteristiko. Za spremembo frekvenčne odvisnosti je potrebno le zamenjati EPROM pomnilnike z vpisanimi delnimi vsotami koeficientov. Digitalni siti smo načrtali s programskim paketom DF-PAK /4/. Uporabljene koeficiente obeh sit, ki so osnova za izračun delnih vsot koeficientov, podaja tabela 3.1.

Na slikah 3.3 in 3.4 so prikazane teoretične, simulacijske in izmerjene frekvenčne karakteristike obeh sit. Pri simulacijskih rezultatih smo zajeli vse vplive kvantizacije /5/. Na vhodu in izhodu sita smo dodali A/D in D/A pretvornik, meritve frekvenčnih karakteristik pa smo opravili z generatorjem spremenljive frekvence na vhodu in meritvijo temenske vrednosti izhodnega signala z merilnikom vršne vrednosti. Pri izbranem nizkoprepustnem situ načrtanem po optimalnem postopku s prepustno frekvenco $f_p = 0,1\ f_v$ in zaporno frekvenco $f_z = 0,2\ f_v$ smo dosegli slabljenje A= - 28 dB. Pri realizaciji visokoprepustnega sita z zaporno frekvenco $f_z = 0,2\ f_v$ in prepustno frekvenco $f_p = 0,3\ f_v$ pa smo dosegli slabljenje A= - 30 dB. S primerjavo teoretičnih, simulacijskih in izmerjenih frekvenčnih odzivov vidimo, da smo dosegli dokaj dobro ujemanje frekvenčnih potekov, odstopanje vrednosti slabljenja v zapornem frekvenčnem področju pa je bilo v obeh primerih manjše od približno $\Delta A = 2$ dB.

Slika 3.2: Vezalna shema celotnega vezja digitalnega sita

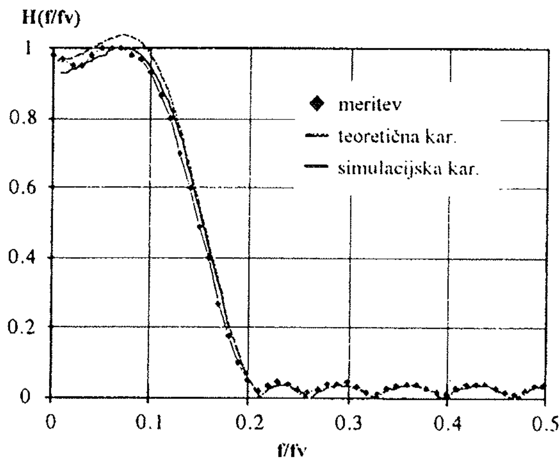

Slika 3.3: Frekvenčna karakteristika nizkoprepustnega sita

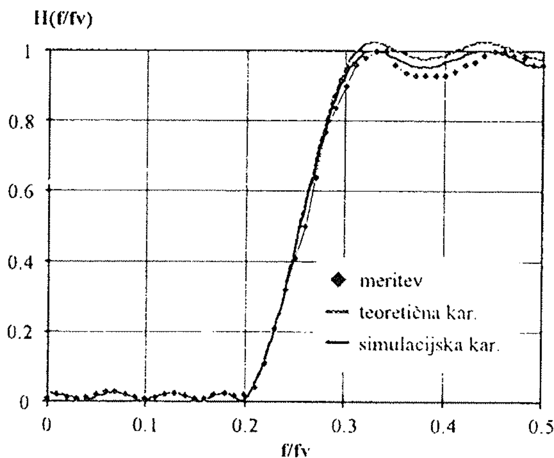

Slika 3.4: Frekvenčna karakteristika visokoprepustnega sita

4. Zaključek

Prikazali smo izvedbo univerzalne strukture nerekurzivnega digitalnega sita s standardnimi integriranimi komponentami za realizacijo sit s poljubno frekvenčno odvisnostjo. Pri tem smo uporabili modificirano obliko porazdeljene aritmetike, s katero smo pri zmanjšani aparaturni kompleksnosti strukture dosegli povečanje dinamike izhodnega signala od 6 do 8 dB. Povečanje dinamike je odvisno od števila koeficientov digitalnega sita in od vrste frekvenčne odvisnosti. Pri isti kompleksnosti aritmetične enote dosežemo tako praktično dva krat manjši vpliv kvantizacije aritmetične enote na izhodni signal. S simulacijskimi frekvenčnimi poteki nizko prepustnega sita s 15 koeficienti smo ilustrirali povečanje dinamike izhodnega signala in s tem tudi ojačenja digitalnega sita v prepustnem frekvenčnem področju.

Z uporabo nezahtevnih standardih integriranih komponent smo pri 12-bitni kvantizaciji vhodnega signala dosegli frekvenco vzorčenja f_V = 143 kHz. Frekvenca vzorčenja je sorazmerna številu bitov za zapis vhodnega signala. Njeno povečanje bi pri izbranih komponentah dosegli že s skrbnejšo izdelavo ožičenja vezja, s katerim bi zmanjšali vplive parazitnih kapacitivnosti. Praktično pa bomo dosegli boljše rezultate z uporabo programabilnih polj logičnih vrat saj predstavlja opisana struktura digitalnega sita le osnovo za izvedbo digitalnega sita z integiranimi komponentami večje stopnje integracije (FPGA elementi).

V rezultatih smo prikazali še dve frekvenčni odvisnosti. Pri realizaciji nizko prepustnega sita s prepustno frekvenco f_p = 0,2 f_v in zaporno frekvenenco f_z = 0,3 f_v smo dosegli slabljenje A = - 28 dB. S preprogramiranjem EPROM pomnilnika z vpisanimi delnimi vsotami koeficientov pa smo realizirali še visoko prepustno sito z zaporno frekvenco f_z = 0,2 f_v in prepustno frekvenco f_p = 0,3 f_v ter dosegli slabljenje A = - 30 dB. V obeh primerih smo dosegli v splošnem dobro ujemanje frekvenčnih potekov med teoretičnimi, simulacijskimi in izmerjenimi odzivi, zaradi več vplivov pa je le prišlo do odstopanja vrednosti slabljenja v zapornem frekvenčnem področju ΔA = 2 dB.

5. Literatura

/1/ B. Liu, A. Peled. A New Hardware Realization of Digital Filters. IEEE Trans. on A. S. S. P., Vol. ASSP 22, pp. 456-462, Dec 1974

/2/ Stenley A. White. Applications of distributed arithmetic to digital signal processing: A tutorial review. IEEE ASSP Magazine, pages 4-19, Jul. 1989

/3/ M. Brumec, Izvedba digitalnega sita 14 stopnje v porazdeljeni aritmetiki, diplomsko delo, TF Maribor, ERI, Maribor 1993

/4/ F.J. Taylor, T. Stouraitis, Digital Filter Design Sotfware for IBM PC, Marcel Dekker Inc., New York, 1987

/5/ R. Babič, M. Solar, B. Stiglic, Analiza vplivov kvantizacije pri izvedbi digitalnih sit v porazdeljeni aritmetiki. Zbornik prve elektrotehniške in računalniške konference ERK'92, strani 13-16, Portorož, Slovenija, 1992.

Karl Korošec, dipl. inž.,
doc. dr. Rudolf Babič, dipl. inž.,
doc. dr. Mitja Solar, dipl. inž.,
Bojan Jarc, dipl. inž.,
Anton Vesenjak, inž.,
Univerza v Mariboru,
Fakulteta za elektrotehniko, računalništvo in informatiko
2000 Maribor, Smetanova 17
tel.: +386 62 25 461
fax: +386 62 211 178

Prispelo (Arrived): 28.5.1996　　*Sprejeto (Accepted): 18.6.1996*

UPORABA PLAZME V ELEKTRONIKI
APPLICATION OF PLASMA IN ELECTRONICS

PLASMA PROCESSES

PART II : APPLICATIONS IN ELECTRONICS

I. Šorli*, W. Petasch, B. Kegel, H. Schmid, G. Liebel, W. Ries
*MIKROIKS d.o.o., Ljubljana, Slovenia
Technics Plasma GmbH, Kirchheim, Germany

1.0 INTRODUCTION

Plasma is obtained by producing a discharge in gases or gas mixtures under vacuum through the application of high frequency alternating voltage. The gas in the chamber is brought to an excited (ionized) state. As well, active radicals and UV radiation are released. Electrons and UV light, resulting from the recombination processes are essential for maintaining the plasma. These components are the actual energy carriers, which are ultimately responsible for the production of chemically active radicals. This highly active process gas is capable of reacting with the surface of the material to be treated even at low temperatures. During the process fresh gas is continuously fed into the chamber. The reaction products are evacuated by the vacuum pump.

Plasma excitation via microwaves (2.45 GHz) has proved especially effective, since the efficiency of the gas discharge increases considerably with increasing frequency but still requiring very low electrical power. This results in strong, intensive ionization and production of radicals and thus a more cost effective process. Today's microwave excitation technology makes it possible to use the low pressure plasma processes economically in industrial mass production in either continuous or batch systems using large process chambers. Small bulk parts, as well as large components can be effectively cleaned and activated.

Very important issue of low pressure plasma is its penetrability. The gas enters the smallest crevices, making it possible to process three - dimensional parts with complex geometries. Another very important fact is that plasma processes are environmentally friendly and as such are alternatives to CFC cleaning processes.

Thus, main advantages of low-pressure plasma technology are:

- dry process
- energy saving through low power consumption
- inexpensive supplies, cost - effective gases
- switch - off chemistry: the process stops immediately when the power is turned off, no disposal of waste
- cleaner, safer workplace, simple operation
- high penetration power into narrow spaces - an advantage in degreasing or activating parts with complex shapes
- constant process conditions, good reproducibility
- meets or exceeds air emission standards
- parts are absolutely dry after treatment

2.0 SUPER FINE CLEANING WITH LIQUID PHASE PRECLEANING AND SUBSEQUENT PLASMA TREATMENT

2.1 GENERAL

Cleaning and degreasing is a widely used industrial procedure. Stricter environmental requirements and recently discovered facts regarding the effect of previously used cleaning and drying agents on atmosphere chemistry make a radical review of the conventional cleaning technologies necessary.

The plasma process is especially well suited for removing organic contaminants and residual films (such as greases, oils, waxes or solvents) when the films are very thin and super clean surfaces are required. A very important characteristic of low pressure plasma is its penetrating power. The gas penetrates into small pores that are difficultt or impossible for liquids to access. Thus, even parts with complex shapes can be easily processed with plasma (cutouts, small radii, bore holes, slots). The penetration capability allows the plasma to reach even cracks with micrometric dimensions.

Since most cleaning problems are concerned with the removal of organic substances from the surface, oxygen is used in most cases as the reactive gas. Oxygen is so one of the most important process gases in the treatment of almost all types of materials, In the case of polymer activation which is discussed in Part III, best results are achieved with oxygen for the most common polymers.

Mechanical abrasion through particle bombardment (sputtering effect) has a subordinate role in the type of equipment used for this purpose.

The effect of oxygen is enhanced by the admixture of small amounts (five to ten percent) of argon or helium. Slightly preheating the parts to between 80 and 100°C, whenever the material to be treated allows, is also helpful.

Since the process gas immediately returns to its original state after the gas discharge has been shut off, possible residues capable of causing long term corrosion represent no problem.

Plasma cleaning means that organic impurities are removed by chemically transforming them in volatile products CO, CO_2 and H_2O, figure 1. In short, the process is a dry one, no submerging of the parts into a liquid takes place and energy cost for a separate drying phase can be saved.

Thus, when oxygen is used the cleaning effect consists of oxidative conversion of the organic contaminants.

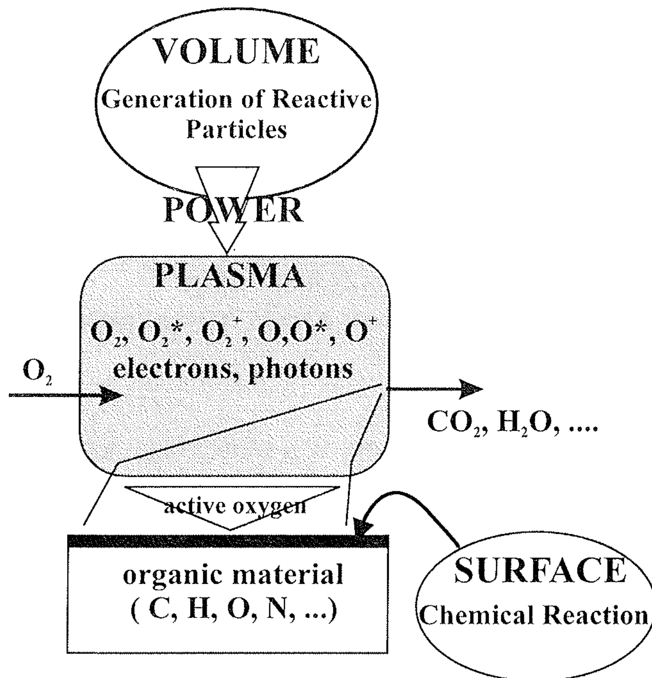

Figure 1: Oxygen plasma cleaning principle

2.2 ENVIRONMENTAL PLUSES TO PLASMA

The plasma process does not use acids, lyes, solvents or liquid halogenated hydrocarbons. The reaction with the process gas takes place in hermetically sealed chambers. For operation, this means no disposal problems and clean workplace conditions, since no poisonous gases or vapors are produced and no hazardous liquids are handled. A plasma system can be easily operated by semi - skilled personnel. The process is simple and does not require special education. Waste gas emissions satisfy and exceed TA clean air standards. There is no fire or explosion hazard.

2.3 DOWNSIDE TO PLASMA

Critical examination discloses the following limitations of this process:

1. Intensive contamination is always irregularly distributed. Thus, the treatment period is long.
2. Photochemical reactions within the surface layer may lead to a crosslinking reaction of the layer material which results in a reduction in the etching rate.
3. Inorganic components (machininng chips, debris and other particles) cannot be removed. They tend to form non-volatile oxides or salts remaining on the surfaces.

A solution is provided by a precleaning step, in which the inorganic components are removed and the processing agent amounts are reduced. This leaves a relatively uniform residual layer, which can be removed by means of plasma in a few minutes.

2.4 PRECLEANING WITH DIFFERENT MEDIA

As discussed above, precleaning may be required depending on the initial conditions. The medium used for preclean, the material to be cleaned and the chemical composition of the contamination have an influence on the results of the subsequent plasma cleaning. In the following example, solvent in the form of glycol ether and water, are used as cleaning agents. The part must be dry prior to plasma fine cleaning.

Plant design with the respective peripherals (distilling unit, water treatment and purification) are shown in figure 2.

Examples and Results of Cleaning Procedures

Application:
Degreasing of metallic parts

Case Description:
Cleaning of brass, aluminum and steel parts prior to assembly

Cleaning requirements:
Minimum grease level (low residue carbon)

Former cleaning process:
Aqueous and CFC

Alternative solution:
Aqueous precleaning and final plasma cleaning.

Results showing residual carbon (mg/cm^2) left after cleaning are presented in table 1.

TABLE 1

Material	Aqueous Cleaning	Aqueous + Tri	Aqueous + Plasma
X12CrNiS188	29.3	6.8	2.7
CuZn39Pb3	20.7	5.3	3.5
AlCuMgPb	19	7.5	3.7

Additionally, the good cleaning results are confirmed by quantitative measurements of the adhesion of the cleaned parts, table 2. Test setup: copper tube with 3 mm diameter, glued into an aluminum block, both suitably cleaned; glue used: Gupalon 30, setting for four hours at 120°C

TABLE 2

Cleaning method	Tear Strength (N)
Aqueous	531
Aqueous + Tri	642
Aqueous + Plasma	785

Parts: Injection molded and stamped parts
Material: Non-ferrous metals, silver, plastic
Contamination: stripping agents, stamping and bending oils, flux
Cleaning agent: Glycol ether (Zestron LP)
Water: demineralized, continuously recirculating
Cleaning requirements: visually spotless, greaseless, low electrical resistance, imprintability
Capacity/cycle time: process - dependent
Batches: 40 x 50 x 20 cm perforated baskets

Floorspace required: approx. 40 m^2
Installed power: 65 kW

Figure 3: Combination wet/plasma cleaning of metal and plastic parts for the automotive industry

Combination solvent/water and plasma treatment

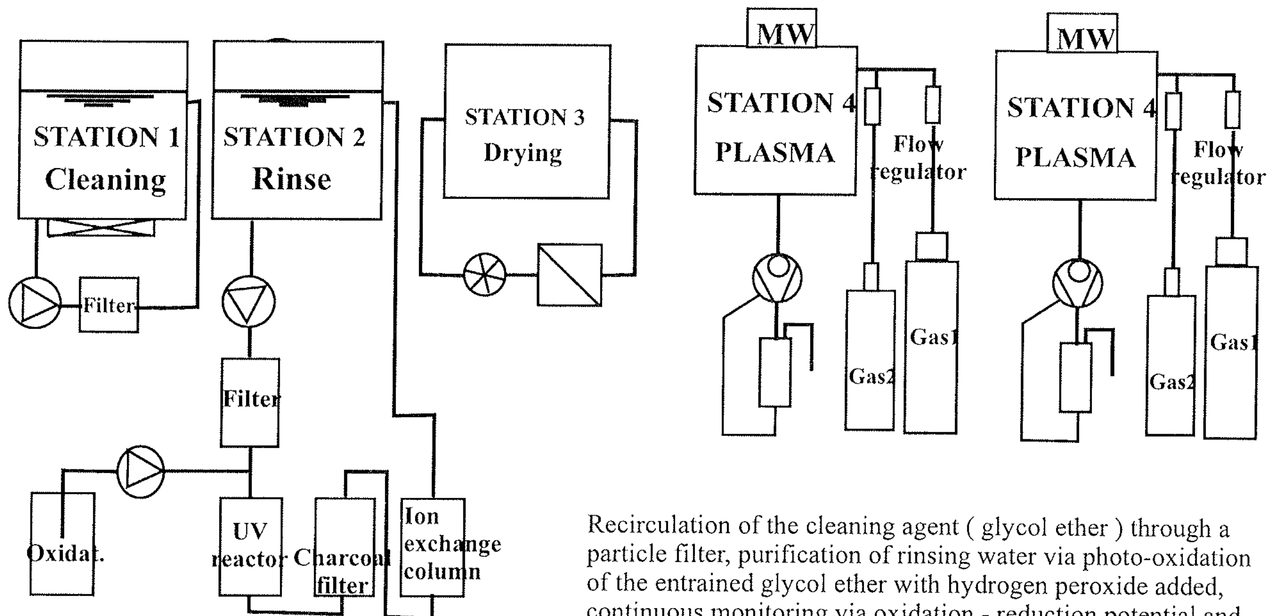

1st stage : Cleaning - dipping with ultrasound(glycolether)
2nd stage : Cleaning - rinsing (DI water)
3rd stage : Drying in a forced-air oven, at 70 deg.C
4th stage : Oxygen plasma cleaning

Recirculation of the cleaning agent (glycol ether) through a particle filter, purification of rinsing water via photo-oxidation of the entrained glycol ether with hydrogen peroxide added, continuous monitoring via oxidation - reduction potential and conductivity measurement after ion exchange, temperature control in furnace, totally enclosed with central exhaust system, automatic handling, automatic process control. Other process versions are possible (e.g. plasma only, aqueous precleaning and plasma, precleaning only, etc.)

Figure 2: Combination of solvent/water and plasma treatment

3.0 APPLICATION OF PLASMA TECHNOLOGY IN ELECTRONIC PACKAGING

Prohibition of CFC's and, in addition increasing surface quality requirements make new solutions for electronic board cleaning necessary. As well, plasma applications of great interest are metal finishing prior to fluxless soldering, device cleaning for reliable wire bonding and surface treatment for adhesive bonding.

3.1 WIRE BONDING ON CRITICAL SURFACES

The yield of plasma treatment is demonstrated by comparative experiments with and without plasma pre-treatment. Parameters of practical significance such as the strength of wire bonds are used as evaluation criteria.

In particular, for bonding wires to printed circuit board substrates, bonding to the connection metal platings is a frequent source of problems. In addition to the inhomogenity of the circuit board's matrix structure, the quality of the bond pad surface is a frequent cause of failures. Preceding process steps such as soldering and adhesive bonding cause organic contamination, which may precipitate on the bond pads, e.g. in the chip - on - board (COB) technology. With the introduction of a plasma process, prior to bonding wet chemical cleaning can be completely omitted.

Wire bonds are characterized using strength tests such as the pull test according to MIL-STD 883D. Then a metallographic ground cross section of a wire bond is prepared in order to make the joint area visible.

Mechanical Strength Test: Pull Test

The destructive pull test (MIL - STD 883D, Method 2011) is a standard test for determining the strength and reliability of wire bonds. The wire bridge is pulled with a hook under the effect of a continuously increasing pulling force until rupture. The maximum force is measured, making sure that the individual measurements are reproducible.

When evaluating the pull test, one should basically distinguish between different rupture characteristics or failure modes. We distinguish between the failure modes of bond detachment from metallization and wire rupture in the deformation zone.

The different qualities of substrate surfaces can affect bond detachment, but also influence the introduction of ultrasonic energy in the bond, which leads to different kinds of wire deformation at the bond with the resulting effects on wire strength in the heel area.

In figure 4 possible failure modes in the pull test are shown.

A, B: Failure in bond at interface between wire and metallization (bond detachment), 1st or 2nd bond

E, F: Wire rupture at the bond heel, 1st and 2nd bond

H: Bond failure: no bond was made

Well defined contamination of the bond surfaces

Laboratory tests were performed with well defined contamination on bond surfaces.

Surface: Chemically deposited Ni/Au on FR4 substrate.

Bonding process: Ultrasonic wedge bonding with 25 μm AlSi1 wire.

In order to investigate the effectiveness of a plasma cleaning process, a contamination was applied which represents a real - life contamination actually occuring during electronic manufacturing. The surface contamination and its effect on bondability was tested using a reflow soldering process. The soldering paste on the substrate was melted. The flux component constituted the bond pad contamination. Prior to bonding, the substrates were subjected to plasma cleaning. Then over 100 bonded wire edges were placed on each substrate and tested with the destructive pull test.

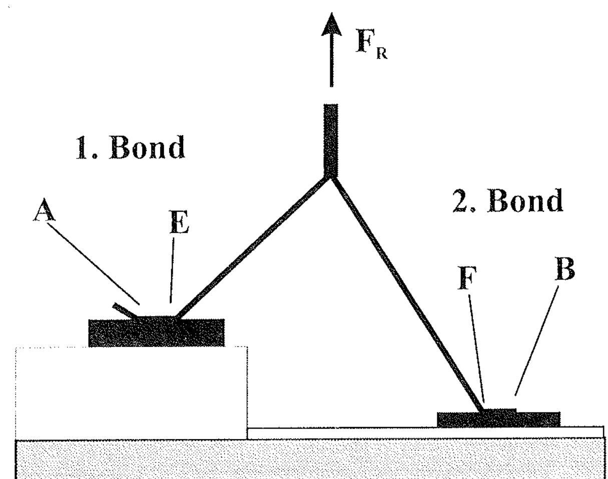

Figure 4: Failure modes in the pull test

Plasma cleaning

Two different plasma processes were used with the samples contaminated with the flux residue of the reflow soldering. The O_2 plasma has an oxidizing effect on the organic deposits; the Purigon (trade name of Linde AG) plasma also has a reducing effect on the metal oxides due to the H_2 component.

Results and discussion

Table 3 shows the results of the individual test series. The average force for all failure modes (bond strength) is given with the standard deviation σ, as well as the distribution by individual failure modes, including the corresponding average force.

Test series a) shows the succesful optimization in relation to the initial conditions. Bond detachment is minimized and the average force of 7.2 cN is significantly larger than the suggested value of 4.0 cN. With contaminated surfaces (series b)) the average rupture force

TABLE 3

Test series	F cN	σ cN	Distribution (%) Average force (cN) for different failure modes					Remarks
			A	B	E	F	H	
a) initial state	7.2	0.8	8.0 6.1	1.0 6.1	66.0 7.2	25.0 7.6	0 -	Bond optimization: A, B min.
b) contaminated	5.5	2.9	24.8 4.8	6.0 6.8	35.0 7.5	15.4 7.5	17.1 -	Bonding results significantly inferior
d[1]) O_2 plasma	6.9	1.8	0.7 7.0	2.2 6.3	81.0 7.3	10.9 7.4	5.1 -	Bonding results almost as good as a). Failure modes A, B drastically reduced
d[2]) Purigon plasma	6.2	2.2	19.6 5.7	6.5 5.2	44.2 7.3	21.0 7.1	8.7 -	Improvement but clearly inferior to O_2 plasma
c) contaminated - with parameter optimization	6.0	2.0	38.5 4.5	0.7 9.2	28.1 7.3	29.6 7.2	3.0 -	No substantial improvement. Effect of contamination cannot be eliminated by parameter optimization
e) O_2 plasma - with parameter optimization	7.6	0.8	0 -	5.5 6.8	3.7 8.1	90.8 7.7	0 -	Slight improvement compared to d[1]

drops down to 5.5 cN, while the standard deviation increases dramatically to 2.9 cN. Bond detachment increases drastically, and bonding errors are also observed.

This negative effect of the contamination can be eliminated by plasma cleaning in an O_2 plasma. In particular, bond detachment types A and B disappear nearly completely. Purigon plasma is not as effective as O_2 plasma, because the organic deposits only respond to oxidizing action. The main component of Purigon, hydrogen, cannot be active, but it reduces the partial pressure of oxygen,

For test series c) we attempted to compensate for surface contamination by optimizing the bonding parameters. Since bond detachment A cannot be reduced below the 38.5% limits, the procedure was not successful. Thus the effect of contamination cannot be eleiminated by optimization only.

In the case of O_2 plasma cleaning, however, the subsequent optimization results in a slight improvement of the bond strength (series e)).

3.2 ENHANCE HYBRID RELIABILITY THROUGH PLASMA CLEANING

Poor wire bonding is the primary cause of failure in hybrid integrated circuits. To create a successful wire bond, strong intermetallic contact between pads on a hybrid and the bond wires must be achieved. This is possible only when the two surfaces are brought into close contact. Once forced together, interatomic forces create a bond. Wire or pad contamination, however, hinders this process. To remove organic and inorganic contaminants and form strong, low failure bonds, hybrid components should be plasma cleaned prior to wire bonding.

To plasma clean hybrids, plasma of inert gases or a mixture of inert/reactive gases - such as Ar, Ar/O_2, Ar/N_2 - chemically removes molecular layers of contamination. Argon mechanically dislodges contaminants, while Ar/O_2 is a mechanical dislodge and chemical oxidation process.

Contaminants can form on hybrids and ICs during assembly. For example, organic contaminants due to poor rinsing after wet chemical photoresist, strip or etch appear on semiconductor die. Hybrids assembled with an epoxy die attach may suffer from resin bleed. When organic resin runs over the adjacent surface of the ceramic and conductors through capillary action, wire bond strength can be reduced. Another contaminant is outgasses produced during epoxy cure. Although modern epoxies are classified as solventless, they contain low molecular weight diluents, which control epoxy viscosity and rheology. By formulation, diluents bind chemically with the epoxy as it polymerizes. Nonetheless, even with an exhaust system in operation, some diluents can be outgassed during epoxy cure and can build up on the hybrid and impede bonding.

The dicing process for wafer segmentation is another source of contaminants. Water used to cool the dicing diamond saw blade may have impurities, catalyze contaminants from previous process steps, or result in bond pad corrosion. In addition, the aluminum metallization from which most semiconductor bond pads are made

readily oxidizes. If this oxidation layer is too thick, bond pad reliability can suffer.

The hybrid assembly environment also inroduces contamination from hand oils used by machine operators, oil fumes and particulates in the air, and more. Containers for hybrid substrates, waffle packs for ICs, and other storage materials can be contamination sources.

Careful handling and processing during hybrid and IC assembly can only minimize contamination; therefore, assembly techniques must incorporate a cleaning step in the process flow.

Removing epoxy resin bleed is a good method to test plasma cleaning effectiveness - if resin bleed can be eliminated, any nonvisible contaminants present also can be removed.

Innitially only Ar gas was used to clean the contamination, but long processing times required were unsuitable for a production environment. A 98% Ar / 2% O_2 mixture provided a sufficiently fast process time, although there is always fear that oxygen might discolor the silver filled die attach epoxy. In figure 5a) and 5b) a comparison between AES spectra of an uncleaned and plasma cleaned bond pad (plasma condition: 98%Ar/2%O_2, 500 W, 15 min, 0.75 torr) demonstrates a sharp reduction in the metallization's carbon peak after plasma clean which also means a reduction in organic contaminant level.

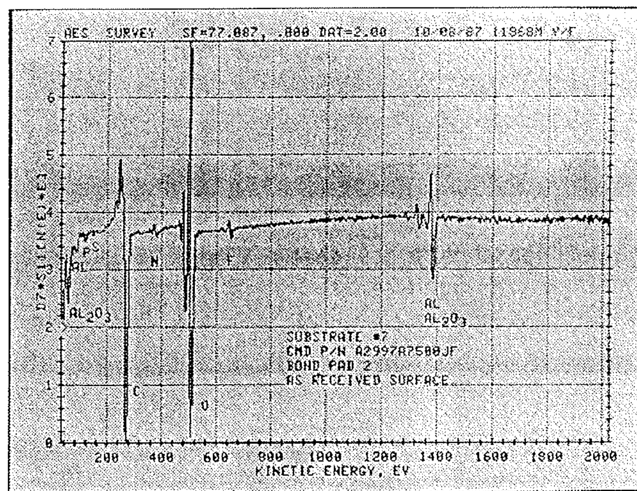

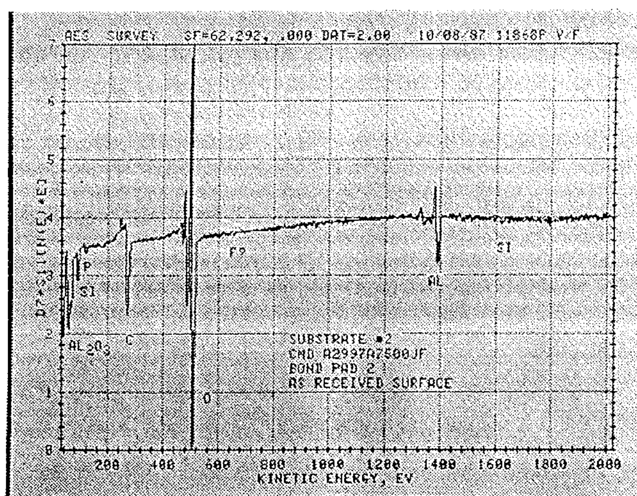

Figure 5: AES - Scanning Auger microanalysis of a bond pad on a component
a) before plasma cleaning
b) after plasma cleaning

Wire bond test results

Test results shown in table 4 clearly show the efficacy of plasma cleaning. Samples thermosonically bonded on a semiautomatic gold bonder with 6 to 8 g tensile strength and a 3 to 5 percent elongation wire boasted stronger bonds than did hybrids that had not been plasma cleaned. Bond pull strength increased 13 to 25 % with a 13 to 17 % reduction in the standard deviation.

TABLE 4

DESTRUCT PULL TEST SAMPLES	
SAMPLE I	
Before Cleaning	After Plasma Cleaning
X = 5.3 g	X = 6.65 g
S = 1.89 g	S = 1.57 g
Failure Mechanism	Failure Mechanism
8 - Bond lifts 7 - Neck downs	10 - Neck downs 5 - Wire breaks
SAMPLE II	
Before Cleaning	After Plasma Cleaning
X = 6.78 g	X = 6.65 g
S = 1.31 g	S = 1.57 g
Failure Mechanism	Failure Mechanism
11 - Bond lifts 23 - Neck downs 1 - Wire break	31 - Neck downs 5 - Wire breaks
NON-DESTRUCTIVE WIRE BOND PULL TEST	
Product 1	Product 2
Uncleaned	Plasma Cleaned
Total bonds tested - 28.050	Total bonds tested - 18.305
Total bonds falied - 317	Total bonds falied - 12
% Failure 1.13%	% Failure 0.066%
Plasma Cleaned	
Total bonds tested -11.826	
Total bonds falied - 15	
% Failure 0.13%	

A more significant result was a shift in the failure mechanism of the bond when pulled to destruction - failures shifted to neck down and wire breaks versus bond lifts. The cleaner components permitted a reduction in ultrasonic power levels on the bonder and less rework of parts coming off the bonder due to missed bonds.

Conclusion

Plasma cleaning of hybrids and ICs can increase bond pull forces and reduce standard deviations of destructive pull tests, decrease ultrasonic power levels, and wide the effective bond window. In addition, life tests and non-destructive bond pull tests demonstrate an improvement in long - term reliability.

4.0 APPLICATION OF PLASMA TECHNOLOGY IN PCB PRODUCTION

4.1 PLASMA DESMEARING AND ETCHBACK OF MULTILAYER PRINTED CIRCUIT BOARDS

Technics Plasma offers manufacturers of multilayer printed circuit boards a reliable, clean, easy - to - use production tool for removing drill smear from either flex or rigid boards.

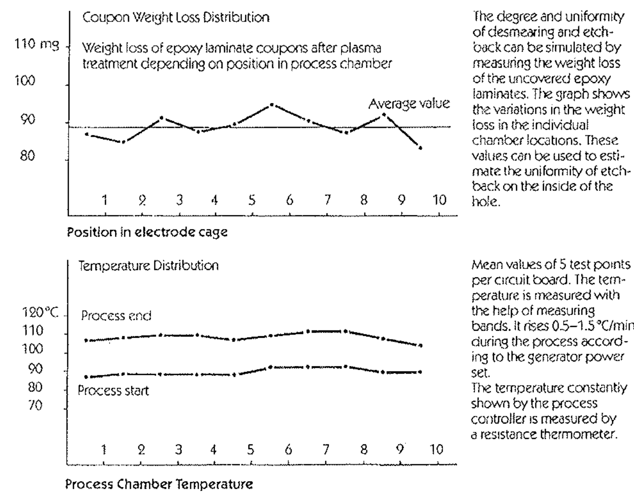

Figure 6: a) etch uniformity versus laminate position in the chamber
b) process temperature versus laminate position in the chamber

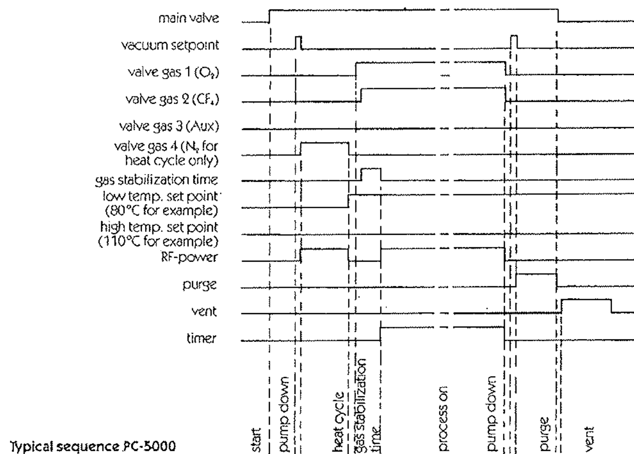

Figure 7: Typical process sequence for drill smear removal

The drill smear found inside drilled holes can be safely removed in an Oxygen - Freon plasma. When desired the system can also be used to perform controlled etch back in multilayer polyimide and epoxy glass boards.

The uniformity across one board, from board to board and batch to batch is usurpassed due to patented Planartube electrodes which are driven by low frequency RF generators.

Typical performance results are shown in figure 6 where etch rate and laminate temperature uniformity are displayed. As well, in figure 7 typical process sequence is displayed.

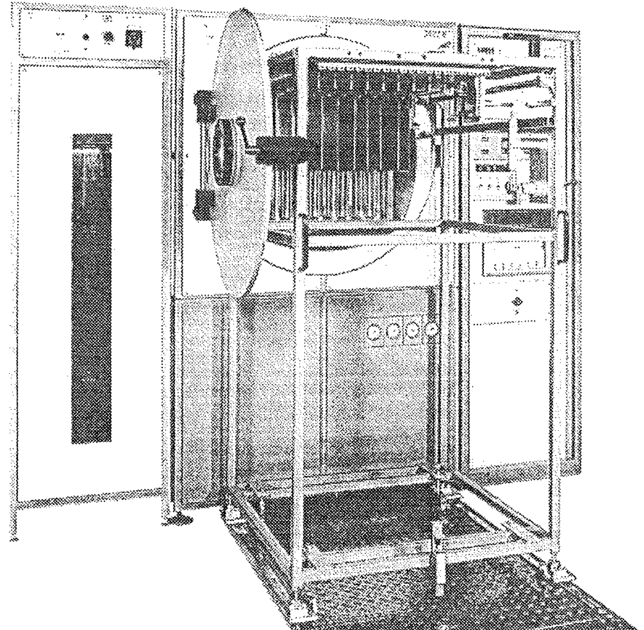

Figure 8: Technics Plasma desmear system

4.2 FLUXFREE SOLDERING WITH PLASMA PRETREATMENT

Introduction

During the wave soldering process the active and passive components are connected with the circuit carrier of the PCB by a collective soldering procedure and thus made an operative flat pack group. The jointning partners are in general supplied in an unsolderable status, covering layers impede the wetting procedures in the solder melting, figure 9.

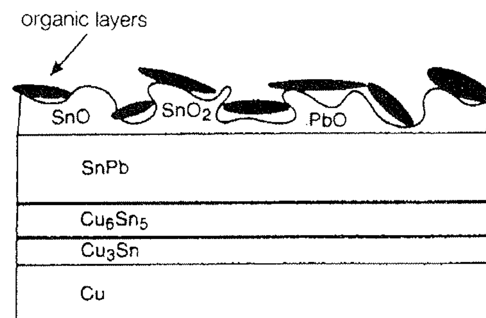

Figure 9: Covering layers impair the soldering

These layers are organic, they cover as part of industry atmospheres all surfaces and have the even more impeding effect the longer the molecule chains of the hydrocarbons are.

Further layers are metal oxides originated by reactions with oxygen. Before the solder process can be started a preparation is necessary to ensure the jointing ability. Usually flux is used. Therefore everybody associates wave soldering with flux. A procedure without flux, however, shows differently. The active ingredient in modern, low solid content flux is an organic acid. Heat supply effects the transformation from metal oxide to metal complexes respectively to metal. Due to the unknown supply status of components and PCBs (quality and thickness of the covering layers are usually not known) one has to work with a surplus of flux so that the chemical process may be incomplete and not wanted residues remain on the flat pack groups. These residues may effect the long term reliability by decreasing the surface resistance respectively by migration. In principle these processes apply to all flux variations no matter whether they are conventional colophony formations, low solid content types or formic acid in protective atmosphere solder systems.

Principle of fluxfree soldering

SnO, SnO_2, PbO form a porous monolith with a very high melting point (1000°C). The surface failure spots are bare after the plasma treatment, since oxygen plasma ashes away all organic contaminants as well as activates the surface increasing its wettability. Now, an appropriate vaporized process material (purified water) is applied to the surface. Condensate precipitates in the fine openings of the oxide layer. When the SnPb layer prepared this way contacts the solder wave the temperature rises fast (500 K/s) and leads to the quick volume expansion of the precipitated condensate amounts. The volume increase (1000 : 1) lifts the oxide layers, fragments are washed away by the moving solder wave and the solder connection is formed by the copper - tin diffusion at the oxide free areas, figure 10.

Solder connections generated by such a new method have of course to undergo a line of tests in order to prove their quality and long term reliability. All visual, structural, electrical, physical and burn in tests turned out to be successful.

There are no restriction in the range of components that can be processed. All available component shapes are suitable for the plasma method.

System Concept

A piling device collects pallets (5 off per batch) from the feeder and passes them on to the receptacle drawer of the plasma chamber, figure 11. The chamber closes and evacuates. After completion of the plasma treatment the pallets are extended, separated again, and by means of band conveyor they run into the preheating, used only for tempering. Then the condensation process is effected and the conveyance to the dual wave.

The solder process is executed under the protective atmosphere wherease the concentration of the remaining oxygen may be higher than in the conventional protective atmosphere systems. The gas consumption runs at 14 - 15 m^3/h. The flat pack groups leave the system completely clean and free of any residues.

Perspective: Fluxfree reflow soldering under plasma

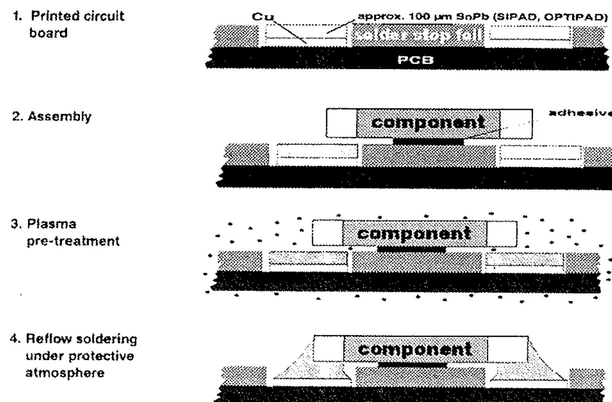

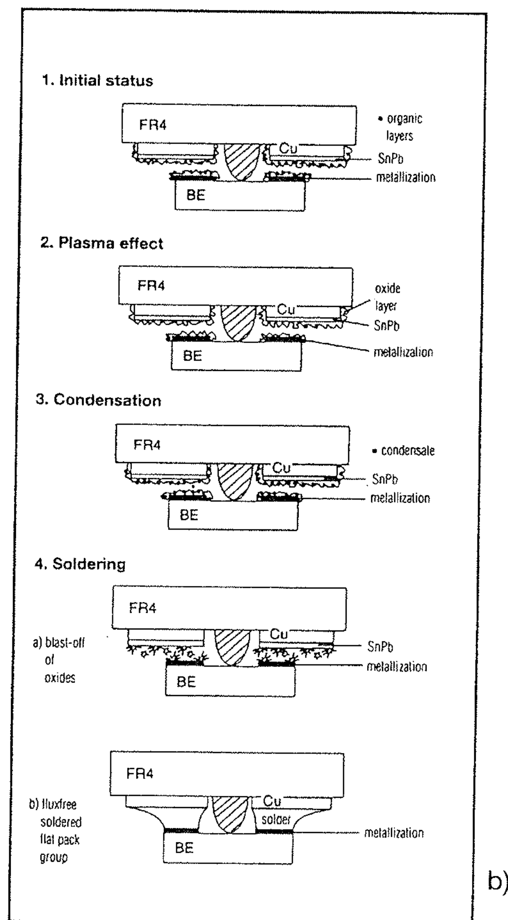

Figure 10: a) Principle of fluxfree soldering
b) Detailed mechanism behind fluxfree soldering

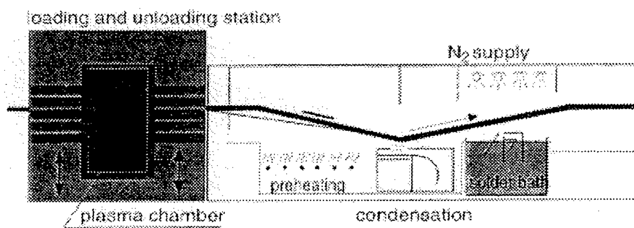

Figure 11: Fluxfree soldering system concept

5.0 LITERATURE

/1/ S.Wolf, R.N.Tauber, SILICON PROCESSING FOR THE VLSI ERA, Volume1: Process Technology, Lattice Press 1986, ISBN 0-961672-3-7

/2/ R.Buck, ENHANCE HYBRID RELIABILITY THROUGH PLASMA CLEANING, Hybrid Circuit Technology, December 1988

/3/ H.Schmid, Super Fine Cleaning with Liquid Phase Precleaning and Subsequent Plasma Treatment, PC, October 1995

/4/ Technics Plasma GmbH, Application Reports

For more information about Technics Plasma systems and their applications, please call:

MIKROIKS d.o.o., Mr. Iztok Šorli
Dunajska 5, 1000 Ljubljana, Slovenia
tel. +386 (0)61 312 898
fax.+386 (0)61 319 170

PREDSTAVLJAMO PODJETJE Z NASLOVNICE
REPRESENT OF COMPANY FROM FRONT PAGE

ISKRA Kondenzatorji
Industrija kondenzatorjev in opreme d.d.

Iskra Kondenzatorji d.d. praznuje v letošnjem letu 45 let delovanja. Skromni začetki proizvodnje navitih kondenzatorjev na sedanji lokaciji v letu 1951 so bili nadaljevanje razvojnega dela na institutu IEV v Ljubljani, ki je bil ustanovljen z namenom, da razvija elektronske komponente za nastajajočo slovensko elektronsko industrijo.

V začetku je bila proizvodnja prilagojena možnostim in zahtevam domače industrije. Kmalu se je pojavila zahteva za širjenje programa proizvodov za nove aplikacije. Že po 10-tih letih delovanja je proizvodnja obvladovala širok program kondenzatorjev za različne namene uporabe, tako v elektroniki, kakor tudi na področju elektroenergetike. Proizvodnja je bila delno velikoserijska in pa maloserijska in prilagojena posameznim kupcem.

V 70-tih letih se je tovarna začela intenzivno usmerjati v prodajo preko meja domovine. Izvoz je postal izziv, še bolj pa potreba za nadaljnji razvoj. Prodaja, predvsem v industrijsko visoko razvite države, je zahtevala absolutno izpolnjevanje zahtev kakovosti in solidnega poslovanja. Raziskave in aplikativni razvoj je bilo potrebno usmeriti v produkte, ki so obetali ekonomično proizvodnjo in konkurenčnost na trgu. Razvoj je sledil trendom v svetu s široko paleto proizvodov za uporabo na področju elektronskih naprav, naprav elektroenergetike in odprave radiofrekvenčnih motenj. Večina proizvodov mora ustrezati mednarodnim in celi vrsti nacionalnim predpisom in standardom tako v Evropi kakor v ZDA in Kanadi. Ustreznost tem predpisom in standardom mora biti potrjena z atesti, ki so obvezni za plasma proizvodov na tehnično in komercialno izredno zahtevnem tržišču. Zahteve na področju razvoja, proizvodnje, trženja in na področju ostalih segmentov poslovanja so privedle do spoznanj, da je možno zagotavljati zahtevano kakovost le s certificiranim sistemom ISO 9001, kar je bilo tudi realizirano v letu 1995.

Danes firma Iskra Kondenzatorji samostojno obvladuje vse poslovne aktivnosti. Preko 90% proizvodov proda na tujih trgih. Kupci in uporabniki proizvodov Iskre Kondenzatorji so svetovno znani proizvajalci elektronskih naprav, računalnikov, bele tehnike, električnih orodij, elektroenergetskih sistemov, električnih strojev itd. Tovarna predstavlja pomembnega proizvajalca kondenzatorjev v svetovnen merilu, tako po količini, kakor po kvaliteti.

Za uveljavitev v svetovnem merilu je bilo potrebno veliko strokovnega dela, ki je vseskozi potekalo v sklopu tovarne ob sodelovanju z domačimi strokovnjaki in znanstveno-raziskovalnimi institucijami. V razvoj proizvodov, ki obsega ob bazičnem predvsem aplikativni razvoj, je bilo vloženo ogromno interdisciplinarnega znanja iz vseh področij naravoslovnih ved, še posebej, ker firma ob osnovnem programu obvladuje tehnologijo proizvodnje praktično vseh sestavnih delov.

Ob osnovnem programu proizvodnje vseh vrst kondenzatorjev, katerih glavni sestavni del predstavlja dielektrik iz termoplastičnih materialov (poliester, polipropilen) in specialnega kondenzatorskega papirja, pa je firma preko celotnega obdobja delovanja razvijala proizvodno opremo za proizvodnjo kondenzatorjev in sestavnih delov. V zadnjem obdobju je na tem področju dosežen poseben viden uspeh, ko je večina zahtevnih strojev in naprav v proizvodnji izdelek lastnih strokovnjakov. Tak koncept lastnega razvoja izdelkov in proizvodnje opreme daje tovarni popolno tehnološko neodvisnost brez tujih licenc in omejitev na trgu.

Tovarna Iskra Kondenzatorji d.d. Semič ob svoji 45. letnici prodaja proizvode v 40. državah, ustvari letno 60 mio DEM prihodka in ob proizvodnji tudi večino sestavnih delov, nudi zaposlitev preko 1300 delavcem. Načrti za bodočnost so optimistični in predvidevajo nadaljnji razvoj proizvodnje in izdelkov, prilagojenih aplikacijam v najzahtevnejših napravah na vseh področjih elektronske in elektro industrije.

Proizvodni program obsega naslednje proizvode:

- kondenzatorji za elektroniko - enosmerni-metalizirani, folijski poliester, polipropilen,
- kondenzatorji za visoko impulzne obremenitve,
- kondenzatorji za elektroniko - miniaturni,
- kondenzatorji in filtri za odpravo radiofrekvenčnih motenj razreda X1, X1Y,
- kondenzatorji za odpravo radiofrekvenčnih motenj - samoozdravljivi - X1 in X2,
- kondenzatorji za pogon elektromotorjev,
- kondenzatorji za kompenzacijo fluorescenčnih svetilk,
- kondenzatorji za kompenzacijo jalove energije na nizki in srednji napetosti,
- avtomatske naprave za kompenzacijo jalove energije,
- specialni kondenzatorji za elektroenergetiko in druga področja uporabe,
- stroji in merilna oprema za proizvodnjo kondenzatorjev,
- manipulatorji in naprave za avtomatizacijo industrijskih procesov,
- orodja za predelavo plastike in preoblikovanje kovin,
- specialna oprema, orodja in stroji po zahtevah naročnika.

ISKRA KONDENZATORJI d. d.
Vrtača 1, 8333 Semič
Slovenija
tel. 068/67-709
fax. 068/67-110

MIDEM IN NJEGOVI ČLANI
MIDEM SOCIETY AND ITS MEMBERS

OBČNI ZBOR DRUŠTVA MIDEM

Spoštovani člani društva MIDEM!

Kot prilogo zapisniku občnega zbora društva MIDEM podajamo poročilo dosedanjega predsednika dr. R. Ročaka o delu v preteklem mandatnem obdobju, oz. okvirni plan dela društva za naslednje triletno obdobje, ki ga je pripravila novoizvoljena predsednica dr. M. Kosec in je podan kot uvodnik v tej številki Informacij MIDEM.

ZAPISNIK

občnega zbora društva MIDEM, ki je bil dne 15.05.1996 ob 18. uri v diplomski sobi Fakultete za elektrotehniko, Tržaška 25, Ljubljana.

Dnevni red:

1. Otvoritev občnega zbora
2. Izvolitev organov občnega zbora
3. Poročilo predsednika
4. Poročilo člana Izvršilnega odbora, zadolženega za finance
5. Poročila ostalih organov društva
6. Diskusija po poročilih
7. Razrešitev organov društva
8. Predlog kandidacijske komisije za izbiro novih organov društva
9. Izvolitev novih organov društva
10. Smernice delovanja društva za naslednje triletno obdobje
11. Razno

Prisotni: S. Amon, M. Kosec, M. Komac, F. Čuk, F. Jan, D. Belavič, I. Pompe, T. Mrdjen, M. Slokan, R. Ročak, I. Šorli in M. Limpel.

ad 1.

Ob 18. uri je predsednik društva MIDEM, R. Ročak predlagal, da prestavimo začetek občnega zbora za pol ure, da bi dosegli kvorum. Čeprav ob 18:30 kvorum ni bil dosežen, smo začeli z občnim zborom. Predsednik društva R. Ročak je otvoril občni zbor in predlagal izvolitev delovnega predsedstva.

ad 2.

Za delovnega predsednika je bil soglasno izvoljen I. Šorli, za zapisnikarja M. Limpel, za overovatelja M. Slokan in S. Amon.

V komisijo za sklepe so bili izvoljeni: M. Kosec, I. Pompe in D. Belavič, v volilno komisijo pa: M. Limpel, F. Čuk, F. Jan in T. Mrdjen.

ad 3.

Poročilo predsednika R. Ročaka je priloženo.

Nekaj odlomkov iz diskusije:

- potrebno je izboljšati stike med organi društva in članstvom,
- ponovno navezati stike z nekdanjimi člani iz BiH, Srbije in Črne gore,
- pridobiti študente v vrste članov,
- osnovati posebno študentsko sekcijo; za pridobivanje študentov je potrebno angažirati profesorje,
- problematičen je majhen vpis na tehniške fakultete v Ljubljani in v Mariboru,
- društvo naj vpliva na študijske programe,
- organizacija inženirskega programa - pri tem naj sodeluje Splošno združenje za elektrotehniko,
- v študij tehniških smeri je potrebno vključiti osnove ekonomije,
- potrebno je vzgajati kadre, ki bodo sposobni prenašati raziskovalne dosežke v industrijo,
- društvo lahko posreduje med iskalci zaposlitve in podjetji,
- društvo naj sodeluje pri izdelavi študijskih in raziskovalnih programov, pri tem naj se vključijo tudi ambasadorji znanosti, ki so člani našega društva: Z. Fazarinc, D. Kolar in S. Pejovnik.
- rast zaposlovanja je možna na dva načina: ali bodo tujci pokupili naša podjetja in z njimi začeli nov razvojni ciklus, ali z rastjo domačih novonastalih privatnih podjetij, kar bo počasnejše, trajalo bo 5 do 10 let,
- društva morajo biti organizirana civilna družba, delovanje društev mora dobiti v družbi večji odmev.

Sklep št.: 1 - Sprejme se poročilo predsednika.

Sklep št.: 2 - Akcijo za včlanitev študentov-dodiplomcev sprožimo. Organiziramo sestanek s profesorji in jim predstavimo dejavnost društva. To nalogo bi lahko opravil novi predsednik.

ad 4.

Poročilo člana IO, zadolženega za finance (poročilo je priloženo zapisniku).

Sklep št.: 3 - Finančno poročilo se sprejme.

ad 5.

Poročilo Nadzornega odbora je prebral njegov predsednik (poročilo je priloženo zapisniku)

Poročilo Častnega razsodišča je prebral delovni predsednik (poročilo je priloženo zapisniku).

ad 6.

Ker društvu kronično primanjkuje finančnih sredstev, je potrebno intenzivno iskati sponzorje, tudi med novimi malimi podjetji.

Sklep št.: 4 - Poročila organov društva se sprejmejo.

ad 7.

Občni zbor je soglasno razrešil vse organe društva.

ad 8.

Kandidacijska komisija je predlagala kandidate za nove organe društva, kandidatna lista je priložena zapisniku.

ad 9.

Volilna komisija je pregledala glasovalne listke in preštela oddane glasove prisotnih in tistih, ki so glasovali po pošti.

Vseh veljavnih glasovnic je bilo 24.

Posamezni kandidati so dobili naslednje število glasov:

dr. Marija Kosec, kand. za predsednico:	23.

Za člane IO je kandidiralo 21 članov.

Izvoljeni kandidati so dobili naslednje število glasov:

prof. dr. S. Amon:	24
dr. R. Ročak:	24
mag. I. Šorli:	21
mag. M.Limpel:	22
dr. R. Babič:	21
F. Jan:	22
dr. M. Komac:	22
mag. M. Kramberger:	17
I. Pompe:	20
prof. L. Trontelj:	21
dr. W. Pribyl:	19

ker je doseglo 16 glasov kar 5 kandidatov, smo z javnim glasovanjem izbrali štiri preostale člane IO.

Izvoljeni so bili:

J.Štefanič:	11 glasov
prof. dr. G. Soncini:	11 glasov

dr. I. Krivka:	11 glasov in
mag. G. Lipnjak	11 glasov

Za Nadzorni odbor so kandidirali 4 člani, izvoljeni so bili:

mag. F. Čuk:	20 glasov
E. Pirtovšek:	20 glasov in
mag. S. Solar:	19 glasov.

Za Častno razsodišče so kandidirali 4 kandidati; izvoljeni so bili:

dr. B. Lavrenčič:	23 glasov
mag. M. Slokan:	20 glasov in
dr. M. Gliha:	15 glasov.

ad 10.

Smernice za nadaljno delo društva je podala novoizvoljena predsednica, njen govor je priložen zapisniku.

POROČILO PREDSEDNIKA DRUŠTVA MIDEM ZA OBDOBJE OD 1.10.1992 DO 15.5.1996

Od zadnjega volilnega občnega zbora v Portorožu, dne 1.10.1992 do danes, je preteklo sedem in pol mesecev več, kot pa to predvidevajo pravila našega društva. Razlog temu ni pretirana želja za oblastjo, ki bi ga mogoče lahko kdo pripisal sedanjim organom društva, temveč je nastala zaradi spremembe termina skupščine in načina volitev, ki smo si ga prvič v zgodovini društva zastavili. Upam, da oba proceduralna "prekrška" nista tako velika, da bi kdo iz tega naredil problem.

Takrat, ko smo imeli skupščino v Portorožu, so po Zagrebu padale granate in bilo je precej jasno, da bodo nastopili težki časi za naše egzemplarno, rekel bi skoraj neverjetno, sodelovanje članov iz nekdanje Jugoslavije. Takrat smo poslali poziv našim članom, da povzdignejo glas proti noriji in možni moriji. Pred tem smo že zastavili nov program dela društva, nova pravila, ki so na tej skupščini bila tudi sprejeta. Ta pravila so omogočila tudi formalno včlanitev strokovnjakov, ki priznavajo naša pravila in so iz kateregakoli konca sveta. S tem smo tudi formalno zastavili popolno internacionalizacijo društva. Pravila so bila objavljena v Informacijah MIDEM 4/92, registracija društva z novimi pravili pa je bila potrjena 7.10.1993. Ob sprejemu slovenskega zakona o društvih lahko ugotavljamo, da so naša pravila v popolnem skladu z zakonom, čeprav predlagam, da se med sklepe današnje skupčine uvrsti možnost formalnih popravkov členov, ki bi jih bilo potrebno iz zakonskih razlogov preformulirati.

Delovanje društva je karakterizirano predvsem z aktivnostjo članov na konferencah društva in objavljanju strokovnih prispevkov v reviji. Preden dam nekaj statističnih podatkov o tem, naj navedem še nekaj podatkov o delovanju organov društva.

Izvršilni odbor in časopisni svet sta se sestajala enkrat letno, ožji sekratariat na formalnih sejah devetkrat, veliko več pa na neformalnih delovnih sestankih, posebej ob sestankih uredniškega odbora, ki se je sestal petintridesetkrat.

INFORMACIJE MIDEM

Vsa leta smo uspeli redno izdati vse štiri predvidene številke. Le pri ta četrti se je vedno malo časovno zatikalo. INSPEC je nadaljeval redno zajemanje podatkov iz časopisa, uspel pa nam je tudi "veliki met", da nas je ISI - Institute for Scientific Information izbral za zajemanje podatkov v tri svoje podatkovne baze: SciSearch, Research Alert in Materials Science Citation Index.

Nekaj statističnih podatkov je v priloženi tabeli, ki jo je pripravil odgovorni in glavni urednik Iztok Šorli. Iz tabele se lahko vidi, da je slovenskih prispevkov v zadnjih dveh letih 67%, v slovenščini pa 33%. To izkazuje uspešno realizacijo treh naših ciljev: da si pridobimo neslovenske avtorje, da slovenski avtorji pišejo v svetu razumljivem jeziku, da pa kljub temu še nadalje omogočamo gojenje in napredovanje slovenske strokovne terminologije.

Časopisni svet petnajstih priznanih strokovnjakov in članov ima 8 neslovencev, Uredniški odbor pa so sestavljali Slovenci in en Hrvat.

Informacije MIDEM
Pregled člankov, 1992 - 1995

	1992	1993	1994	1995
DOMAČI	24	21	15	15
TUJI	1	7	10	9
SLOVENŠČINA	14	7	8	8
ANGLEŠČINA	11	21	17	16
SKUPAJ	**25**	**28**	**25**	**24**
DOMAČI, %	96	75	60	62
TUJI, %	4	25	40	38
SLOVENŠČINA, %	56	25	32	33
ANGLEŠČINA, %	44	75	68	67

Verjetno se ne moremo ne strinjati s sklepom, da sta ta dva odbora v preteklem obdobju delovala izredno dobro, zato bi se vsem njunim članom javno zahvalili, predvsem pa Iztoku Šorliju, ki je bil motor in nosilec vseh dejavnosti.

KONFERENCE MIEL - SD

Uspešno sta bili vsako leto organizirani združeni posvetovanji o mikroelektroniki MIEL in sestavnih delih SD. Statistični podatki o referatih in udeležencih so v priloženi tabeli. Lahko se vidi trend zadrževanja skupnega števila referatov nad 50, vendar s tendenco zmanjševanja števila referatov iz Slovenije in povečevanja referatov iz drugih držav. Vse konference so bile izredno dobro organizirane, za kar smo kot društvo zmeraj dobili pohvale samih udeležencev, v prijetnih krajih. Naj samo spomnim:

1992 v Portorožu
1993 na Bledu

Konferenca MIEL-SD
Pregled udeležbe in referatov, 1992 - 1996

	MIEL-SD'92 Portorož	MIEL-SD'93 Bled	MIEL-SD'94 Rogla	MIEL-SD'95 Terme Čatež	MIEL-SD'96 Nova Gorica
Skupaj referatov	64	55	53	53	64
• domači	46	42	41	36	40
• tuji	18	13	12	16	24
Skupaj udeležencev	-	61	68	73	*
• domači	-	49	57	58	*
• tuji	-	12	11	15	*
Število držav - referati	9	7	6	9	11
Število držav - udeleženci	-	8	6	7	*

1994 na Rogli
1995 v Čatežu
1996 pa bo v Novi Gorici.

DRUGE DEJAVNOSTI

Društvo v preteklem obdobju ni oraganiziralo nobenih seminarjev, šol, ali kaj podobnega, če izvzamemo javno prezentacijo na stojnici Ministrstva za znanost Republike Slovenije ob razstavi Sodobna elektronika.

ČLANSTVO

Koliko nas je po tem zgodovinskem premetavanju v preteklem obdobju?

Uradno 402, iz petnajstih držav. Statistika je v prilogi. Pri tem niso šteti eventuelni člani iz bivših jugoslovanskih republik Srbije in Črne Gore, katerih članstvo smo ob embargu svetovne organizacije tudi mi zamrznili, ni članov iz Bosne in Hercegovine ter Makedonije, ki so se v vojni vihri razpršili, izgubili iz poštnih evidenc ali pa so bili ubiti. Predlagam sklep, da se strpno poskusi ponovno navezati stike z njimi in jih ponovno voditi v evidenci, saj kriterij o neplačanju članarine kot razlog izstopa ni v tem primeru sprejemljiv. Edini član, ki je bil na svojo eksplicitno željo izbrisan iz članstva že leta 1992, je bil Ljutica Pešić iz Beograda.

Zahvaljujem se vsem za podporo med mojim "vladanjem". Upam, da je bilo aktivno, uspešno in ne preveč svojeglavo. Zahvaljujem se vsem aktivnim članom, zahvaljujem se vsem podjetjem in njihovim direktorjem, ki so sponzorirali bodisi časopis, bodisi konference. Posebna zahvala gre tudi ministru za znanost Republike Slovenije za to obdobje, gospodu Radu Bohincu za njegovo izredno osebno podporo in podporo ministrstva, ki ga je vodil. Lahko pa se že zahvalimo tudi sedanjemu ministru gospodu Andreju Umeku, ki nadaljuje z isto politiko podpore. Sicer pa naj končam s postulatom: ni težko podpirati nekaj, kar je trdno. To pa naše društvo zagotovo je.

Pregled članov društva MIDEM, maj 1996

država	fizična oseba	pravna oseba
SLOVENIJA	274	36
ZDR. DRŽAVE	2	
AVSTRIJA	4	
NEMČIJA	4	
HRVAŠKA	92	2
ANGLIJA	2	
MAKEDONIJA	9	
ITALIJA	5	
FRANCIJA	2	
ČEŠKA	1	
ŠVICA	1	
UKRAJINA	1	
BELGIJA	1	
ŠVEDSKA	1	
DANSKA	1	
BOLGARIJA	1	
SKUPAJ	**402**	**38**
SLOVENIJA	274	36
TUJINA (15 držav)	128	2
SKUPAJ	**402**	**38**

V Ljubljani, 15.5.1996 *dr. Rudolf Ročak*

USTANOVITEV NOVEGA INŠTITUTA

Inštitut za tehnologijo površin in optoelektroniko (ITPO), ki ima status zavoda, deluje od prvega decembra leta 1995. Ustanovljen je bil v času lastninskega preoblikovanja Inštituta za elektroniko in vakuumsko tehniko, p.o. (IEVT), v sodelovanju z Ministrstvom za znanost in tehnologijo (MZT), ustanovitelj pa je Tehnološko-razvojni sklad Republike Slovenije. ITPO zaposluje štirinajst ljudi, od tega devet raziskovalcev, ki imajo na Teslovi 30 v Ljubljani na razpolago laboratorijske in druge prostore v izmeri nekaj več kot 500 m^2.

Verjetno ne bo odveč kratka razlaga, zakaj je do ustanovitve ITPO sploh prišlo. Ministrstvo za znanost in tehnologijo je že leta 1991 imenovalo štiričlansko komisijo, ki je analizirala kronično slabo stanje IEVT in predlagalo organizacijske spremembe, ki naj bi omogočile avtonomnost manjšinskega raziskovalnega dela IEVT in transparentnost porabe sredstev namenjenih raziskovalnemu in razvojnemu delu, ki so se tako ali drugače prelivala v večji, proizvodni del IEVT. Žal pa je bilo samo priporočilo MZT prešibko, da bi prišlo do korenite reorganizacije IEVT že v navedenem obdobju, in sledilo je nadaljnje triletno slabšanje razmer in močno osipanje raziskovalnega kadra IEVT, od približno petinštirideset raziskovalcev v letu 1992 na manj kot dvajset ob koncu leta 1995.

Ustanovitev ITPO je bila torej nujni izhod v sili za skupino raziskovalcev, ki so na svojem področju bili že do tedaj dokaj uspešni, pa tudi trdno vpeti v slovensko in mednarodno raziskovalno sfero ter industrijo. V okviru nove raziskovalne organizacije bomo še povečali aktivnost in kvaliteto dela na specializiranih raziskovalnih področjih. Inštitut za tehnologijo površin in optoelektroniko kot raziskovalni zavod opravlja temeljne, razvojne in aplikativne raziskave na področju naravoslovja in tehnologij. Njegova osnovna dejavnost je na področju preiskav in tehnologij površin trdnih snovi in tankih plasti, vakuumske optoelektronike, tehnike visokega in ultravisokega vakuuma, vakuumskih tehnologij, tehnike plazme, razvoja specialnih elektronk in optoelektronskih komponent. Teme petih mladih raziskovalcev nakazujejo smeri bodočega razvoja ITPO. Teme treh doktorandov so vakuumska ploskovna izolacija, interakcija vodikove plazme s površinami trdnih snovi ter preiskave površin z rentgensko fotoelektronsko spektroskopijo (XPS=ESCA), dva pa pripravljata magisterij s področja luminiscentnih materialov ter postopkov analize reflektometrskih merilnih rezultatov. Z Laboratorijem za analizo površin in tankih plasti smo vključeni v Nacionalni center za mikrostrukturno in površinsko analizo, v katerem sta še Laboratorij za mikrostrukturno analizo Odseka za keramiko ter Laboratorij za elektronsko mikroskopijo Odseka za fiziko trdne snovi z Inštituta Jožef Stefan. Laboratorij na ITPO je specializiran za preiskavo površin trdnih snovi (AES, SAM, SEM) in tankih plasti ter kompozitnih materialov in njihovih faznih mej (TFA). Opravljamo tudi mikroanalizo kovinskih, steklenih in keramičnih materialov (EMPA, EDX, WDX). ITPO dobro sodeluje z najpomembnejšimi slovenskimi tehničnimi inštituti, z univerzama v Ljubljani in Mariboru ter s slovensko industrijo, na primer s Fotono, Cryorefom, Iskro in drugimi.

Sodelavci ITPO imamo vzpostavljeno dobro bilateralno sodelovanje s priznanimi tujimi institucijami in v okviru mednarodnih projektov v Evropi in ZDA, kar nam omogoča dostop do raziskovalne opreme, ki je v Sloveniji še nimamo, in do najnovejših informacij, pomembnih za naša raziskovalna področja. Bolj pomembna kot naštevanje tujih institucij so področja dela, na katerih sodelujemo z njimi. Ta so preiskava reakcij na faznih mejah tankih plasti (MPI Stuttgart, DLR, Köln), preiskava večplastnih struktur iz superprevodnih tankih plasti in kovinskih oksidov (FZ, ITP, Karlsruhe), preiskava reakcij v trdni fazi (Müfi, Budimpešta), optimizacija profilne analize tankih plasti (PHI, München, PHI, Minnesota), sodelovanje pri izgradnji žarkovnih linij na sinhrotronih (Elettra, Trst, FZ, Karlsruhe, COPERNICUS), tehnike plazme in obdelava površin materialov (Univerza Bratislava, CEEPUS) ter v zadnjem času ionska implantacija (IAEA, Dunaj). Področje, na katerem ITPO deluje, je v zadnjih letih zapustilo več raziskovalcev, zato je ena glavnih nalog ITPO vzgoja novih kadrov za lastne potrebe in kasneje tudi za druge institucije. Področje preiskave površin zastopamo tudi pri rednem in podiplomskem študiju na obeh slovenskih univerzah. Poskrbeti bomo morali tudi za obnovo infrastrukturne opreme za področja, na katerih delamo, pri čemer pričakujemo sodelovanje z MTZ in z vsemi zainteresiranimi, ki tovrstne preiskave neobhodno potrebujejo pri svojem raziskovalnem delu ali v industriji.

Nekateri sodelavci ITPO aktivno sodelujemo v Društvu za vakuumsko tehniko Slovenije in v Mednarodni zvezi za vakuumsko znanost, tehniko in aplikacije, kot tudi v uredniških odborih domačih strokovnih časopisov in v tujih recenzijskih odborih.

A. Zalar

Sodelavci inštituta za tehnologijo površin in optoelektroniko

KONFERENCE, POSVETOVANJA, SEMINARJI, POROčILA
CONFERENCES, COLLOQUYUMS, SEMINARS, REPORTS

ISHM/NATO Workshop 1996 (poročilo s konference)

NATO Advanced Workshop and Exhibition on Microelectronic Interconnections and Microassembly

Udeležil sem se konference oz. delavnice za povezovanje v hibridni mikroelektroniki, ki sta jo sponzorirala NATO in ISHM (International Society for Hybrid Microelectronics). Konferenca je bila v dneh od 18. do 21. maja v Pragi. Na konferenci s približno 45 udeleženci iz 21 držav je bilo predstavljenih 32 referatov v petih sekcijah:

1. Trendi v pakiranju in povezovanju
2. Spajkanje in Flip Chip tehnologija
3. Žično bondiranje in TAB
4. Multi Chip Moduli
5. Povezovanje z debeloplastno tehnologijo

V poročilu bom na kratko opisal vsebino nekaterih zanimivejših predavanj, na razpolago pa je zbornik povzetkov. Zbornik referatov bo izšel predvidoma v prvi polovici naslednjega leta.

Registrirani udeleženci

1.	Združene države Amerike	9
2.	Češka	7
3.	Slovaška	3
4.	Belgija	2
5.	Finska	2
6.	Italija	2
7.	Japonska	2
8.	Madžarska	2
9.	Nizozemska	2
10.	Poljska	2
11.	Švedska	2
12.	Ukrajina	2
13.	Velika Britanija	2
14.	Bolgarija	1
15.	Danska	1
16.	Francija	1
17.	Irska	1
18.	Kanada	1
19.	Norveška	1
20.	Slovenija	1
21.	Španija	1
	Skupaj:	**47**

Mikroelektronika v Skandinavskih državah

Soren Noerlyng (Micronsult, Danska) je predstavil aktivnosti na področju hibridne mikroelektronike v štirih Skandinavskih državah: Danska, Norveška, Švedska in Finska. Posebej je osvetlil, dogajanja na sledečih povezovalnih tehnologijah: MCM (Multi Chip Modules), Flip-chip, TAB (Tape Automated Bonding), COB (Chip On Board), in PTF (Polimer Thick Film). Na področju raziskav so raziskovalne institucije in proizvodne firme povezane v skupne projekte omenjenih štirih držav in/ali v skupne projekte Evropske Unije.

Miniaturizacija v elektroniki za široko potrošnjo

Co Van Veen (Philips, Nizozemska) je predstavil zahtevo po miniaturizaciji tudi v elektroniki namenjeni za široko potrošnjo. Primerjal je tri tehnologije COB (Chip On Board), TAB (Tape Automated Bonding) in Flip-chip. Slednji tehnologij je dal prednost pred prvima dvema. Tehnologiji COB očita zahtevno čiščenje zaradi kombinacije tehnologij spajkanja in žičnega bondiranja. Tehnologiji TAB pa očita drago proizvodno opremo. Medtem ko tehnologija Flip-chip v zadnjem času dosega ponoven razvoj na področju zmanjševanja dimenzij in tehnoloških procesov za izdelavo in uporabo Flip-chip komponent.

Primerjava plastične in hermetične inkapsulacije

Nihal Sinnadurai (TWI, England) je predstavil obsežno študijo zanesljivosti elektronskih komponent (10.000.000 enot) v telefonskih centralah na 260 lokacijah v Veliki Britaniji in Indiji. Zasledovali so klimatske in ostale pogoje okolice ter analizirali katere komponente in zakaj odpovedujejo. Na osnovi rezultatov so določili pospeševalne faktorje degradacije komponent. Poleg tega so ugotovili, da plastično inkapsulirane elektronske komponente celo manj odpovedujejo kakor hermetično inkapsulirane komponente (?!).

Pogoji okolice, ki so vplivali na odpovedi:

1.	Temperatura	55%
2.	Vibracije	20%
3.	Vlaga	19%
4.	Prah	6%

Komponente, ki so odpovedovale:

1.	Transistorji	36%
2.	Integrirana vezja	32%
3.	Diode	15%
4.	Upori	9%
5.	Hibridna vezja	8%

Vzroki odpovedi:

1. Električna preobremenitev 44%
2. Nezanesljiva komponenta 40%
3. Vzrok odpovedi ni najden 10%
4. Napačna komponenta 2%
5. Ostalo 4%

Flip-chip tehnologija

Nekaj predavateljev (Bill Brox, IVF, Švedska; Peter Bodo, IMC, Švedska; Carlo Cognetti, SGS Thomson, Italija; I. Suni, VTT Electronics, Finska) je izrazito povdarilo perspektivnost Flip-chip tehnologije za povezovanje in pritrjevanje integriranih vezij. Po njihovih raziskavah s Flip-chip tehnologijo dosežejo večjo gostoto funkcij na hibridnem vezju in višjo delovno frekvenco. To dosežejo zaradi zmanjševanja dimenzij. Dimenzije zmanjšujejo, tako da razporedijo priključke oziroma kroglice po površini (Ball Grid Array), razmak priključkov zmanjšujejo proti dimenziji 80 µm, debelino Flip-chipa pa proti 700 µm. Poleg tega pa povečajo zanesljivost, saj se z uporabo Flip-chipa izognejo enemu niviju povezav (spajkanje oziroma žično bondiranje). Cenovna primerjava je tudi na strani Flip-chip tehnologije, saj bi se pri masovni produkciji Flip-chip komponente pocenile do 7 krat (?!).

Po trditvah enega izmed avtorjev so v firmi Erikson mnenja, da če bi prej poznali vse probleme, ki jih imajo z SMD tehnologijo, bi šli direktno na Flip-chip tehnologijo. Drugi avtor pa zatrjuje, da je SGS pripravljen za masovno produkcijo Flip-chip komponent. Poleg tega ocenjuje, da bodo te komponente cenejše od SMD verzije. Kasneje je to stališče omilil z izjavo, da bo vse odvisno od povpraševanja.

Multi Chip Module

V sekciji za multi chip module je Illyefalvi-Vitez (Tehnična univerza v Budimpešti, Madžarska) predstavil mednarodni projekt za cenene multichip module z udeležbo Velike Britanije, Belgije, Madžarske, Romunije in Slovenije.

G. Harsanyi (University Park Campus, Miami, Florida) je obravnaval zanesljivost večplastnih MCM z vidika elektromigracije kovinskih ionov. Trdi, da temperatura žganja močno vpliva na intenzivnost nastajanja dendritov v večplastnih MCM.

Računalniške simulacije

Kar nekaj predavateljev je predstavilo računalniške simulacije in/ali matematično modeliranje temperaturnih razmer na mikroelektronskem debeloplastnem vezju, mehanskih lastnosti različnih spojev, ter mehanske napetosti v komponentah, substratu in spojih.

V sekciji "Povezovanje z debeloplastno tehnologijo" je bil predstavljen tudi naš referat, ki obravnava posebnosti, ki jih mora upoštevati projektant pri izdelavi senzorjev in pretvornikov, katerih pretvorniški del je izdelan s hibridno mikroelektronsko tehnologijo.

Naslednja konferenca oz. delavnica (ISHM/NATO Workshop 1997) naj bi bila organizirana maja 1997 v Sloveniji.

Darko Belavič
HIPOT-HYB, Šentjernej
RO HV Ljubljana

Delavnica COST 514: Feroelektrične tanke plasti

Za uvod: feroelektrične tanke plasti na siliciju so potencialni kandidati za vrsto novih mikroelektronskih, optoelektronskih in mikromehanskih komponent. Najpogosteje se omenjajo spominski elementi, kjer imajo omenjene plasti bodisi aktivno bodisi pasivno funkcijo, valovodi, preklopniki, modulatorji, mikrosenzorji in makroaktuatorji. Zato je to, kakšnih 10 let staro raziskovalno področje, ki združuje raziskovalce in inženirje s področja materialov in mikroelektronike, v zadnjih letih deležno izjemne pozornosti.

Pred tremi leti se je v Evropi začel izvajati koordiniran projekt COST 514, Feroelektrične tanke plasti. Njegov namen je intenzivirati in povezati raziskave materialov, tehnologij in potencialnih aplikacij in na ta način hitreje rešiti tehnološke probleme, ki so upočasnili vpeljavo feroelektričnih tankih plasti v komercialne produkte. Danes v tem projektu, v katerega je vključena tudi skupina iz Odseka za keramiko IJS, sodelujejo vse pomembne evropske raziskovalne institucije (19), ki delajo na tem področju. Projekt povezuje pet podprojektov: Zanesljivost feroelektričnih tankih plasti, Procesiranje tankih plasti z laserji, Feroelektrični materiali za kondezatorje v neposrednem kontaktu s silicijem, Razvoj plasti za SAW aplikacije in Materiali in tehnologije za optoelektroniko.

V okviru projekta je bila že tretjič zapovrstjo organizirana delavnica, katere namen je bil predstaviti delo in rezultate raziskovalnih skupin ter skupnega projekta. Letos je drugega in tretjega marca to delavnico organziral Inštitut za materiale iz Madrida. Poleg sodelavcev projekta COST 514 so na njej sodelovali še gostje iz Amerike, gost iz Siemensa iz Münchna in gost iz Instituta za fiziko iz Rige.

Posebej velja omeniti predavanje prof. Kingona iz North Carolina University, ki je predstavil vsebino raziskav pa tudi finančni angažma Japonske in Amerike na področju raziskav feroelektričnih spominskih elementov. Tu predvidevajo največjo proizvodnjo in finančni uspeh feroelektričnih tankih plasti. Po njegovem mnenju se je na tem področju zgodilo tisto, kar so raziskovalci že nekaj let pričakovali (in upali): resničen prodor feroelek-

tričnih tankih plasti v industrijske raziskave. Predavatelj je naštel vrsto industrijskih gigantov, ki so se za to odločili. To je potrdil tudi dr. Wersing iz Siemensa.

Sicer pa zelo na kratko nekaj strokovnih zaključkov z delavnice. Raziskave kažejo, da se med materiali največkrat pojavlja trdna raztopina na osnovi $Pb(Zr,Ti)O_3$. Za mikromehanske aplikacije zaenkrat sploh nima pravega tekmeca, medtem ko za pasivne elemente v spominskih celicah (DRAM) iščejo druge materiale. Med procesnimi tehnologijami se vsaj Evropa največ ukvarja s sol-gelom, manj pa z naprševanjem in nanašanjem iz parne faze (MOCVD).

Uveljavlja se tudi nanašanje plasti z laserji (PLD), kjer se, poleg ostalega, intenzivno dela na modifikaciji opreme in postopka, tako da bi metoda omogočala nanašanje plasti na velike površine. Napredovali so tudi postopki pri nadaljnjem procesiranju elementov, ki so v veliki meri preneseni iz polprevodnih tehnologij.

Kot sem omenila, v COST 514 sodeluje tudi skupina iz Odseka za keramiko Instituta "Jožef Stefan". Ukvarjamo se s sol-gel postopkom nanašanja plasti in strukturno karakterizacijo plasti. V projekt smo se vključili tudi zato, ker verjamemo, da je uporabnost in zahtevnost proizvodnje teh elementov tako raznolika, da je tu lahko mesto tudi za slovenska podjetja. Če kogarkoli strokovno in podjetniško to področje podrobneje zanima, smo tu z dodatnimi informacijami.

dr. Marija Kosec
Odsek za keramiko
Institut "Jožef Stefan"
Jamova 39, 1001 Ljubljana
Tel.: 1773-368
Faks: 1263-126
Elektronska pošta: Marija.Kosec @ijs.si

"TRIBOLOGY - SOLVING FRICTION AND WEAR" poročilo s simpozija

Od 9. do 11. januarja 1996 je v Esslingenu (Nemčija) potekal 10. mednarodni simpozij z naslovom "Tribology - Solving Friction and Wear" Problems. Simpozija sem se udeležila s prispevkom "Comparison of the Fretting Wear in 100Cr6/100Cr6, Si_3N_4/Si_3N_4 and Si_3N_4/100Cr6 Contacts in Lubricated and Dry Conditions". Delo je nastalo v sodelavi s Centrom za tribologijo in tehnično diagnostiko, zato je del stroškov potovanja krila Fakulteta za strojništvo.

Srečanje je potekalo na Tehnični akademiji Esslingen, ki je bila tudi glavni organizator. Udeležilo se ga je preko 800 ljudi, predstavljenih je bilo okoli 300 polurnih govornih prispevkov. Predavanja, ki jih je spremljala razstava raziskovalne opreme, so potekala v sedmih vzporednih sekcijah. Precejšen poudarek je bil na obrabi raznih strojnih delov, orodij za obdelavo in na metodah zmanjševanja trenja in obrabe. Najbolj obiskane so bile vsekakor sekcije, ki so obravnavale mazanje. Govora je bilo o različnih vrstah maziv in dodatkov, pri čemer je bilo največ zanimanja za nova - biorazgradljiva olja. Odpadna olja namreč predstavljajo veliko obremenitev za okolje, zato v zadnjem času intenzivno poskušajo mineralna in druga olja zamenjati z razgradljivimi, ki pa zaenkrat še ne kažejo povsem zadovoljivih rezultatov. Simpozija se je udeležila tudi relativno velika skupina predstavnikov različnih podjetij za proizvodnjo ali prodajo maziv iz Slovenije.

Nekaj sekcij je bilo posvečenih materialom, pri čemer so glavni predstavniki obrabno odpornih materialov različni keramični materiali. Tako se v firmah, ki se sicer ukvarjajo z mazivi (npr. Lubrizol, ki je eden najmočnejših proizvajalcev olj in aditivov), vedno bolj intenzivno posvečajo raziskavam materialov in ustreznih maziv za keramične elemente, saj vedno več kovinskih delov (tudi v boljših avtomobilih) zamenjujejo s keramičnimi.

Glavna predstavnika sta Si_3N_4 in SiC, katerih prednosti so predvsem nizek koeficient trenja in majhna obraba na dolge roke ter odpornost na povišane temperature, predvsem pa manjša občutljivost na eventuelno pomanjkanje maziva v primerjavi s kovinami. Predstavljena je bila vrsta zanimivih prispevkov o obnašanju različnih keramičnih materialov pri različnih triboloških pogojih. Glavno sporočilo, ki ga je poslušalec lahko razbral iz predavanj, je bilo, da so tribološke lastnosti keramike zelo odvisne od pogojev uporabe. Glavni parameter, ki določa vrsto in intenzivnost obrabe, je temperatura na stiku, pri čemer se lahko visoka temperatura (preko 1000^oC) pojavlja zelo lokalno. Pri teh pogojih pa kljub pregovorno visoki kemijski stabilnosti keramičnih materialov prihaja do tribokemijske reakcije. V primeru Al_2O_3 prihaja do hidratacije, pri ZrO_2 pride lahko do fazne transformacije, značilnost neoksidne keramike pa je velika odvisnost od mazalnega sredstva. V prisotnosti vodnih molekul nastajajo oksidi, katerih lastnosti zavisijo od vrste gibanja elementov.

V sekciji o tribologiji kostnih nadomestkov v človeškem telesu je bil med drugimi predstavljen prispevek, ki je opisoval nenavaden pristop skupine raziskovalcev iz ZDA in Nemčije. Izhajali so iz dejstva, da je idealen tribološki sistem katerikoli sklep v človeškem telesu, zlasti pa kolčni, ki mora dolga leta prenašati relativno velike obremenitve. Do obrabe v sklepu pride le v redkih primerih, ki jih večinoma povzroči kakšna bolezen. To pomeni, da je - dokler ne pride do spremembe v sestavi mazalne tekočine v sklepu, mazanje idealno in vredno posnemanja vsaj v primeru vgradnje umetnih kolkov. Predstavljena je bila tudi študija možne povezave med obrabo sklepov in osteoartritisom. V mnogih primerih so namreč v obolelih sklepih našli obrabne delce, ki bi lahko povzročili razvoj bolezni. Rezultati opazarjajo na pomembnost pravilne izbire materiala za kostne nado-

mestke in njihove geometrije v tribološkem kontaktu. Predstavljeni so bili rezultati primerjave obrabne odpornosti različnih biokompatibilnih materialov pri pogojih, ki simulirajo realne.

Splošni vtis, ki sem ga dobila na srečanju, je bil, da je kljub zadržkom pri uporabi keramičnih materialov v konstrukcijskih delih, ki so sledili začetnim pretirano optimističnim napovedim, keramika material, ki v strojnih delih sicer počasi, vendar uspešno zamenjuje klasične materile. Ovira za hitrejše uvajanje je še vedno skeptika uporabnikov (konstrukterjev) in zaenkrat slabo obvladovanje primernih mazalnih sredstev. Vendar pa kaže, da se keramični materiali vendarle vztrajno uveljavljajo v strojnih elementih.

Saša Novak
Odsek za keramiko
Institut "Jožef Stefan"
Jamova 39, 1001 Ljubljana
Tel.: 1773-368
Faks: 1263-126

POROČILO S KONFERENCE ISPSD'96 (The 8th international symposium on power semiconductor devices and IC's)

Od 20. do 23. maja je bila na Maui, Hawaii, ZDA, konferenca oz. simpozij o močnostnih elementih in integriranih vezjih. Konferenca zajema zelo ozko a obenem pomembno vejo polprevodniških elementov, ki jih potrebujemo praktično v vsaki električni napravi za regulacijo, krmiljenje in zaščito elektronskih delov. Na konferenci se zberejo vsi pomembnejši raziskovalci iz tega področja, predvsem pa je to konferenca, kjer se zberejo vsi pomembnejši proizvajalci elektronskih komponent. Zato je konferenca še posebno zanimiva in zelo koristna, saj je industrija tista, ki narekuje razvoj novih elementov in določa prihodnje trende razvoja. Največ udeležencev konference je prišlo iz ZDA, na drugem mestu je bila Japonska, nato pa Evropa. Izkazalo se je, da Japonci vodijo predvsem na področju diskretnih elementov, američani in evropejci pa na področju integracije le teh v močnostna integrirana vezja oziroma tako imenovane pametne močnostne elemente (smart power devices).

Sam sem predstavil delo z naslovom "Diffused spiral junction termination structure: modeling and realization", soavtorja Prof. dr. Slavko Amon (Laboratorij za elektronske elemente, Fakulteta za elektrotehniko, Ljubljana) in dr. Georges Charitat (LAAS/CNRS, Toulouse, Francija). Predstavili smo rezultate nove zaključitve planarnih spojev, ki omogoča zelo visoke prebojne napetosti in je obenem zelo robustna in enostavna za izdelavo. Delo je bilo zelo dobro sprejeto, posebno glede na dejstvo, da smo pokazali tudi eksperimentalne rezultate struktur, ki so bile procesirane v našem laboratoriju. To je posebno velik uspeh glede na relativno skromno opremo našega laboratorija, ki se ne more primerjati z raziskovalnimi možnostmi velikih polprevodniških firm kot so Motorola, SGS-Thomson, International Rectifier, Texas Instruments, Daimler-Benz, Mitsubishi Electric, Philips, Toshiba, Fuji Electric, Hitachi, itd. Glede na močno udeležbo velikih industrijskih podjetij, ki so prikazali najnovejše raziskovalne dosežke, je bilo iz akademskih raziskovalnih organizacij le 17% vseh predstavljenih del.

Konferenca je pokazala, da se akademske organizacije lahko enakomerno kosajo z industrijskimi le z zelo domiselnimi novimi koncepti in raziskavami novih struktur, ki bodo morda vgrajeni v prihodnje generacije polprevodniških elementov.

Več o smereh razvoja visoko-napetostnih in močnostnih elementov bom poskusil pripraviti v posebnem prispevku za MIDEM, kogar pa zanimajo članki predstavljeni na konferenci, tako na papirju kot na CD disku (zgoščenki), se lahko oglasi pri avtorju članka.

Aloha,

dr. Dejan Križaj
Laboratorij za elektronske elemente
Fakulteta za elektrotehniko, Ljubljana

VSE ČLANE DRUŠTVA MIDEM VLJUDNO PROSIMO, DA PORAVNAJO ČLANARINO ZA LETI 1995 IN 1996.
ALL MIDEM MEMBERS AREKINDLY ASKED TO PAY MEMBERSHIP FEE FOR 1995 AND 1996.

HVALA LEPA!
THANK YOU VERY MUCH!

VESTI - NEWS

News from AMS

The year 1995 - the most successful to date in the history of the company!

For a number of reasons the year 1995 was an exceptional one for Austria Mikro Systeme International AG:

1) The **business development of the AMS Group** with extraordinary high growth rates of sales, profit and cash earnings:

The sales increased by **71**% from 1,107 MATS in 1994 **to 1,887 MATS in 1995**. This represents a significant outperformance compared with most competitors.

The **profit on ordinary activities** increased by **82**% from 147 MATS in 1994 to **267 MATS**, including the 26 MATS losses of the two new consolidated subsidiaries. This represents **a return on sales of 14%**.

The **cash earnings** with a more than 60% growth of **431 MATS** reached a new record.

Key Figures 1995

	AMS AG	AMS Group[1]
Sales (MATS)	1,698	1,887
Sales growth absolute (MATS)	+ 592	+ 780
Sales growth in %	+54%	+71%
Profit on ordinary activities (MATS)	292	267
Profit growth	+99%	+82%
Return on sales	17%	14%
Cash earnings (MATS)	406	431
Cash earnings in % of sales	24%	23%
Total assets (MATS)	2,653	3,782
Equity (MATS)	1,527	2,166
Equity ratio	58%	57%

[1] Consolidation of SAMES for 9 months, of Thesys for 2 months.

The ÖVFA result and the cash earnings according to ÖVFA will be published on April 24, 1996.

2) **The majority participations:**

In July 1995 Austria Mikro Systeme acquired 51 % of SAMES in South Africa - ASIC specialist for solid state electronic current metering, security and identification applications - and in October 1995 51.25% of THESYS in Germany - ASIC specialist for multimedia, communications, industrial and automotive electronics - inline with the longterm company strategy to expand the customer base and to improve the market position as a result of the increased product and process offerings of the partnerships.

Both subsidiaries, though having achieved a high increase in sales and having improved their earnings in the past business year are as planned in a loss situation.

3) **The capital increase**:

The nearly complete exercise of the acquisition rights on the new shares by the existing shareholders documents the confidence of the employees and shareholders in the longterm strategy of the company.

The proceeds from the rights issue of around 733 MATS were used partially for financing the participations; the remainder will be used for the further expansion at company headquarters in Unterpremstatten to finance the further growth of Austria Mikro Systeme.

4) **The future potential created:**

With the establishment of the AMS Group **approximately 1,500 highly qualified and motivated employees** at three manufacturing locations as well as in the worldwide design centres and in the sales offices are available to assist customers more efficiently and to better utilize the possibilities of the international ASIC market.

Outlook for 1996:

The situation on the international semiconductor market at the beginning of 1996 has been characterized by a general decrease in demand. The AMS Group will not be able to disengage completely from this worldwide trend. Thus, the pace of sales and earnings development will not be sustained. However, we expect that there will be no fundamental change in the midterm growth outlook for the relevant markets which the AMS Group serve.

The First Quarter 1996 of the AMS Group

The AMS Group reports the results for the first quarter 1996 (in MATS):

	AMS Group,1 - 3 '96
• Order Entry	405
• Net Sales	572
• Backlog	870
• Employees	1,526
• Capital Expenditure	153
• Profit before Taxes (after minority interests)	38

The AMS Group with its members Thesys, Austria Mikro Systeme and Sames is a company group that specializes in the design and production of ASICs (application specific integrated circuits) for the market segments communications, multimedia, automotive and industrial electronics and meets the customer challenges with state-of-the-art technology and know how. The AMS Group, formed in 1995, reported net sales of 1,887 million ATS for the year 1995 (after consolidation of Sames for 9 months and Thesys for 2 months).

Since the beginning of the year main emphasis was placed on capacity competences and the AMS Group was optimized by the simultaneous use of the synergies in design, mask lithography, production, test and quality. Hence, the prerequisites were established to strengthen the better basis for the future in the changed environment of the general sluggishness of the economy, especially in the field of semiconductors.

The AMS Group will not be able to disengage completely from this worldwide trend. Thus, the pace of sales and earnings development will not be sustained. However, we expect that there will be no fundamental change in the midterm growth outlook for the relevant markets which the AMS Group serve.

AMS
Schloß Premstätten
A-8141 Unterpremstätten Austria
Fax: +43 (03136) 52 501, 53 650
Tel.: +43 (03136) 500
Email: info @ams.co.at
http: //www.ams.co.at

News from "Solid State Technology"

AMD: $3 billion for MPU fab and design center in Dresden

As anticipated, Advanced Micro Devices has announced a ten-year plan to invest $3 billion in a microprocessor center in Dresden, Germany. The plan has been approved by the company's board of directors and is now subject to final approval by the German state of Saxony, the Federal Republic of Germany, and the European Economic Community. Both Saxony and the German federal government will provide substantial financial assistance through grant allowances and loans.

The new facility will be AMD's first wafer fab in Europe. Chairman and CEO Jerry Sanders noted that Germany is the biggest market in Europe and cited the highly skilled workforce as one reason for choosing the location. About 1400 people will be employed at the new center.

Over the next five years, the company will spend $1.5 billion to construct an 87,000-square-meter plant, to be named Fab 30. It will include about 9000 square meters of cleanroom space, and have a capacity of up to 6000, 200-mm wafers/week. Initial production, commencing by the end of 1998, will be at 0.25 micron, with later migration to 0.18 micron planned. Groundbreaking will take place before the end of 1996, said Sanders.

The initial investment phase also includes a design center which will begin operations about two years after groundbreaking.

Siemens recently opened its own DRAM fab in Dresden, where 16-Mbit and 64-Mbit devices will be produced. The former East German city is also home to Zentrum Mikroelektronik Dresden, a state-controlled producer of ASICs, fast SRAMs, and other devices with annual sales of about DM 40 million ($29 million).

AT&T to expand Spanish wafer fab

AT&T Microelectronics recently celebrated the 10th anniversary of its fab in Madrid, Spain, with the word that it will invest an additional $145 million to add capacity and extend the facility's capability to 0.35 micron during 1996. ASICs, FPGAs, and DSPs utilizing the new technology will start coming off the line in 1997; wafer output is expected to grow to 5000/week by the middle of 1996.

IMEC to handle ADEQUAT+ work

The Belgian IMEC research institute has been selected to coordinate advanced development work on 0.25- and 0.18-micron CMOS processes under the 15-month ADEQUAT+ project, which is funded by the Esprit Framework IV program. The $3 million effort will develop interconnect processing steps and modules for 0.25-micron CMOS by the end of this year; these back-end modules will then be combined with front-end capabilities developed in the just-completed ADEQUAT-2 project. Concept testing and patterning feasibility for 0.18-micron front-end modules is expected to be complete by the end of this year, and a lithography process should be ready a year later. Front-end modules are to be prepared by 1998, and back-end by 1999. Partners include the Dutch DIMES research center, the German Fraunhofer Institutes, the French GRESSI center, and chipmakers GEC-Plessey Philips, Siemens, and SGS-Thomson.

SGS-Thomson plans new fabs

SGS-Thomson will begin work on two new 200-mm wafer fabs in 1996, one in Italy and one in another country according to European press reports. Company executives said they expect to invest between $800 million and $1 billion in new facilities in 1996, about the same as 1995, and will also spend between $50 million and $100 million on eight factory upgrades. A formal announcement of the first fab is expected shortly, said the company.

Strong mask growth seen for European market

The European reticle/mask market will grow 10.2% in 1996, according to US firm The Information Network, Williamsburg, VA. The market is expected to reach $134

million this year, up from $122 million in 1995. Growth in the mask market will be driven by IC growth. The strong mask market showing in Europe is attributed to heavy investments by major semiconductor manufacturers Philips, SGS-Thomson, and Siemens; growth rates in excess of 90% among smaller European IC companies; Europe's lead in telecom and electronic components in automobiles; and strong consumption of masks by US companies in Europe.

Low-k dielectrics featured at 1996 DUMIC conference

As the world moves closer to using low dielectric constant (k) polymers for inter-metal dielectric (IMD) applications, engineers are being forced to consider all of the different materials properties they will need. This search was the focus of many of the 33 presentations at the second annual Dielectrics for VLSI/ULSI Multilevel Interconnection Conference (DUMIC), held in February in Santa Clara, Califomia. Some 500 attendees, up from 400 last year, heard reports on new materials and reexaminations of well-known dielectrics.

Researchers from Fujitsu presented a paper entitled, "Fluorocarbon Films Deposited by PECVD with High Thermal Resistance and Low Dielectric Constant". This work is the first time that low-k polymer films have been deposited by a process in which the reaction occurs on the wafer surface, and it opens up the possibility of entirely new processes for IMD. Films were deposited into 0.65-μm-deep quarter-μm gaps, with excellent results. Using C_2H_2 and C_4F_8 precursors, a k lower than 2.4 was achieved with thermal decomposition and glass transition temperatures higher than 400°C.

A last-minute substitution on the program was an exciting proof-of-concept paper on 2.4-k polymer foams. Since air has a k of 1.0, if some fraction of the polymer is converted into a gas, then the overall material would see a fractional reduction in k. Researchers at IBM-Almaden have worked out a two-step foam process where molecular phase segregation first produces a primary phase with a high glass transition temperature and a second phase that is burnt off during the second low-temperature step. There are two significant benefits of this two-step process. First, the burn-off can be done after metallization, which is advantageous for maintaining topography in vias. Second, there is very tight distribution of pore sizes between 10 and 100 nm.

Vacuum-deposited Parylene was the subject of two presentations. Specialty Coating Systems, of Indianapolis, IN, presented data showing excellent film qualities, including 2.28 k. Unfortunately, researchers from Rensselaer Polytechnic Institute presented data showing that it is difficult to achieve deposition rates above 200 Å/minute. The best conditions used a 500 V/cm electric field that reduced atomic oxygen incorporation and improved the deposition rate by 2 to 3.5 times.

The dielectric constant is not the only material property that is important for an IMD material. Just as the need for lower-k materials is driven by increasing interconnert speeds, there is a corresponding need for improved thermal conductivity to compensate for metal Joule heating. Researchers at Texas Instruments compared the characteristics of polyimide, methylsilsesquioxane spin-on polymer (SOP), and inorganic porous hydrogen silsesquioxane (HSQ) using ASTM electromigration test structures. The results quantify the 3 to 4 times reduction in thermal conductivity seen in these new low-k materials (see table). For a given current density, the reduced thermal conductivity will lead to a larger temperature increase, resulting in shorter electromigration lifetimes.

Results of TI study

Dielectric film	Thermal Conductivity (mW/cm °C)
PECVD	11.5
HDP-CVD oxide	12.0
Polymide	2.4
SOP	2.4
HSQ	3.7

The TI researchers showed through both simulation and experimental results that in a multilevel metal system, the inter-level dielectric (between metal layers) plays a more important role for thermal conduction than intra-level dielectrics (between metal lines within a given layer). Their report suggests that low-k materials be used only at the intra-level, where they will have the greatest impact for RC reduction and will not significantly reduce the thermal conductivity of the system.

This opinion was echoed by DUMIC luncheon speaker Betsy Weitzman, senior staff scientist in the Materials Research and Strategic Technologies organization within Motorola's Semiconductor Product sector. The process flow to create such a composite dielectric is identical to that currently used for spin-on glass (SOG) gap-fill, though the driver has changed from mechanical to electrical performance. Expect to start hearing about this process flow coming to a fab near you.

1-Gbit DRAM designs, exotic memories, highlight 1996 ISSCC

Attendance at the 43rd IEEE International Solid State Circuits Conference, held February 8-10 in San Francisco, jumped to 2800 from last year's 2200, with many sessions (including those concerning low-voltage devices and video cameras on a chip) filled to overflowing. Following are some of the highlights of the presented papers.

- This is the second year that 1-Gbit DRAM designs were presented. Mitsubishi has used x-ray lithography to define high-k barium-strontiumtitanate (BST) 0.29-square-micron gates, with 3 poly,1 tungsten, 2 copper, and 1 aluminum interconnect layers. Sam-

sung uses KrF optical lithography to define mid-k tantalumpentoxide 0.334-square-micron gates, with 3 poly,1 titanium-silicide, 2 tungsten, and 2 aluminum layers.

- Hitachi has developed an 8 x 8-bit "single-electron-memory" cell array using 3-nm-thick nanocrystalline silicon structures to control individual electrons by the Coulomb blockade effect. Data-line current changes were detected with the addition ("write") and the removal ("erase") of each of five separate electrons. Eventually, circuits based on this nonvolatile technology could achieve Giga- to Tera-bit densities. Write/erase times would be faster than conventional flash memories simply because the number of electrons moved would be dramatically lower.
- IBM researchers presented a 0.5-micron, triple-metal,1-Mbit, 100-MHz DRAM for cache memory that is intended for use as the second chip in a new microprocessor multichip module being designed by IBM. C4 flip-chip interconnects will handle approximately 1000 interconnects between chip and substrate. The device will also be available in a single-chip package compatible with the Intel Pentium bus.
- NEC showed a prototype 60 nano-second 1-Mbit nonvolatile ferroelectric memory chip. The 2000-Å-thick strontium-barium-tantalate (SBT) storage cell is formed by a sol-gel process, and has platinum contacts. The single 34.72 square-µm transistor and single 1-µm aluminum CMOS process yields a 90.9-sq-mm chip. Presenter Hiroki Koike of NEC said that second-generation chips could be in production in two to three years.
- Researchers from the Georgia Institute of Technology showed novel process and circuit designs to produce "adiabatic" MOS chips for gigascale integration. These energy-recovery logic circuits are called adiabatic because they rely on the relationship between entropy and heat in a closed system as described by the second law of thermodynamics. ARPA and the SRC sponsored this work, which could lead to high-speed chips that would consume much less power.
- Stanford's Center for Integrated Systems has developed a BiCMOS active substrate probe card fabricated using silicon MEMS process techlnology. Air pressure deflects micron-scale polyimide membranes to bring up to 1000 tungsten probe tips - in sets of two - into contact with test pads. Low-voltage current is forced between the two tips on each pad to break the oxide laver, allowing multiple probes without excess physical damage. Active circuitry on the card can be located just 1 cm from the probe tips to improve timing accuracy.

Članstvo v Eurolab Slovenija

Sredi leta 1992 je iniciativna skupina sedmih predstavnikov preskusnih laboratorijev, Urada za standardizacijo in meroslovje (USM) in Zveze inženirjev in tehnikov Slovenije (ZITS) ustanovila Sekcijo preskusnih laboratorijev pri ZITS, ki predstavlja nacionalno vejo Evropske organizacije za preskušanje (EUROLAB) in je bila na generalni skupščini Eurolab januarja 1993 sprejeta v članstvo kot opazovalka.

Slovenija kot opazovalka ni imela nikakršnih obveznosti, s tem pa tudi ne možnosti aktivnega delovanja. V Eurolab je Slovenijo zastopal direktor USM, pri čemer je USM, kolikor je bilo mogoče, tudi populariziral delo Eurolaba z objavami v Sporočilih in s spodbujanjem udeležbe na prireditvah Eurolaba, kot je bila npr. organizacija udeležbe na Simpoziju Eurolab aprila 1994.

Na zadnji skupščini, januarja 1996, pa je bil status Slovenije spremenjen v pridruženo članico. S tem se odpirajo povsem nove možnosti aktivnega sodelovanja, pa tudi seveda obveznost plačevanja članarine. Zato je napočil trenutek, da se Eurolab v Sloveniji vzpostavi kot širše interesno združenje preskusnih, analitskih in kalibracijskih laboratorijev v Sloveniji. O namenu in prednostih, ki jih prinaša članstvo v takšnem združenju, preberite v *Izhodiščih za delovanje slovenskega združenja preskusnih in kalibracijskih laboratorijev, Eurolab Slovenija*.

Če vas zanima sodelovanje pod navedenimi pogoji, odgovorite, prosimo, na vprašanja iz Vprašalnika za včlanitev v Eurolab Slovenija, ki je objavljen na zadnjih straneh Sporočil, in ga izpolnjenega vrnite na Urad za standardizacijo in meroslovje, z oznako "EUROLAB Slovenija".

V novembru 1996 (predvidoma 7. novembra 1996) nameravamo organizirati skupščino vseh laboratorijev, ki se 'elijo včlaniti v Eurolab. Skupaj s skupščino bo potekal tudi seminar z naslovom: *Zagotavljanje kakovosti v laboratorijih*, ki bo obravnaval praktične vidike uvajanja sistema kakovosti v preskusne, analitske in kalibracijske laboratorije.

Zoran Svetik, predsednik
pripravljalnega odbora EUROLAB Slovenije,
Slovenski institut za kakovost in meroslovje,
Tržaška c. 2, Ljubljana

KOLEDAR PRIREDITEV 1996

JULY

03.07.-05.07.1996
8th INTERNATIONAL CONFERENCE ON METERING AND TARIFFS FOR ENERGY SUPLY
Brighton, UK
INFO.: + 44 171 240 8830

08.07.-10.07.1996
2nd IEEE INTERNATIONAL ON-LINE TESTING WORKSHOP
Biarritz - Saint-Jean-de-Luz,FRANCE
Info.: + 33 76 57 46 19

21.07.-24.07.1996
29th ANNUAL CONVENTION "MICROSTRUCTURE:KEY TO ADVANCES IN MATERIALS"
Pittsburgh, Pennsylvania, USA
Info.: + 1 412 476 5883

AUGUST

05.08.-09.08.1996
9th INTERNATIONAL CONFERENCE ON MOLECULAR BEAM EPITAXY
Malibu,CA,USA
Info.: + 1 805 492 7072

31.08.-01.09.1996
7th INTERNATIONAL WORKSHOP ON COMPUTER ANIMATION AND SIMULATION
Poitiers,FRANCE
Info.: + 41 21 693 52 46

SEPTEMBER

02.09.-05.09.1996
22nd EUROMICRO CONFERENCE
Prague, Czech Republic
Info.: +44 1232 245 133

05.09.-06.09.1996
5th INTERNATIONAL WORKSHOP ON TIME VARYING IMAGE PROCESSING AND MOVING OBJECT RECOGNITION
Florence,ITALY
Info.: + 39 55 4796279

11.09.-13.09.1996
RTP'96 THERMAL PROCESSING CONFERENCE
Boise, Idaho, USA
Info.: +1 512 310 2884

25.09.-27.09.1996
2nd INTERNATIONAL CONFERENCE ON SATELLITE COMMUNICATIONS
Moscow, RUSSIA
Info.: + 7 95 203 4985

25.09.-27.09.1996
9th INTERNATIONAL SYMPOSIUM ON SYSTEM SYNTHESIS
La Jolla,CA,USA
Info.: +1 909 787 4710

25.09.-27.09.1996
INTERNATIONAL WORKSHOP ON THERMAL INVESTIGATIONS OF IC's AND MICROSTRUCTURES
Budapest, HUNGARY
Info.: E mail: Bernard.Courtois imag.fr

25.09.-27.09.1996
24th INTERNATIONAL CONFERENCE ON MICROELECTRONICS MIEL'96
AND 32nd SYMPOSIUM ON DEVICES AND MATERIALS, SD'96
Nova Gorica, SLOVENIJA
Info.: + 386 61 312 898

DRUŠTVO MIDEM IN KONFERENCA MIEL-SD NA INTERNETU

Dragi člani društva in bralci revije!

Ob pomoči Dejana Križaja s Fakultete za elektrotehniko, Ljubljana, laboratorij za elektronske elemente, smo koncem meseca aprila 1996 postavili dve MIDEM strani na INTERNETU in sicer:

1. Predstavitev društva MIDEM in revije "Informacije MIDEM" na naslovu
   http://pollux.fer.uni-lj-si/MIEL/MIDEM.htm
2. Predstavitev konference MIEL-SD'96 na naslovu
   http://pollux.fer.uni-lj-si/MIEL/miel96.htm
3. Elektronsko pošto lahko pošiljate na naslov:
   Iztok.Sorli@guest.arnes.si

Pri vpisu pazite na velike in male črke!!

MIDEM SOCIETY AND MIEL-SD CONFERENCE ON INTERNET

Dear readers and Society members!

With the help of Mr. Dejan Križaj, Faculty for Electrical Engineering, Ljubljana, Laboratory for Electron Devices, MIDEM Society has, since end of April 1996, two pages on INTERNET:

1. Presentation of MIDEM Society and Journal "Informacije MIDEM", address
   http://pollux.fer.uni-lj-si/MIEL/MIDEM.htm
2. Presentation of the Conference MIEL-SD'96, address
   http://pollux.fer.uni-lj-si/MIEL/miel96.htm
3. Email can be sent to:
   Iztok.Sorli@guest.arnes.si

When inputting the address, please type
lower and upper case letters as indicated.